Mechanistical and therapeutical aspects of preventing diabetes

Inaugural-Dissertation

zur Erlangung des Doktorgrades
der Mathematisch-Naturwissenschaftlichen Fakultät

der Heinrich-Heine-Universität Düsseldorf

vorgelegt von

Namir Shaabani

aus Aleppo

Düsseldorf, März 2014

aus dem Institut für Gastroenterologie, Hepatologie und Infektiologie

der Heinrich-Heine Universität Düsseldorf

Gedruckt mit der Genehmigung der
Mathematisch-Naturwissenschaftlichen Fakultät der

Heinrich-Heine-Universität Düsseldorf

Referent: Prof. Dr. Peter Proksch

Korreferent: Prof. Dr. Karl Sebastian Lang

Tag der mündlichen Prüfung: 04.11.2014

For Prophet Muhamad

Table of contents

Table of Figure

Summary

Diabetes mellitus type I is an autoimmune disease, which is associated with virus infections. Understanding different mechanisms involved in the induction of autoimmune diabetes can give new potential targets for therapy. In this thesis we investigated different immunological mechanisms, which can contribute to the induction of autoimmune diabetes.

We analyzed the role of the interferon-inhibitor Ubiquitine Specific Peptidase 18 *(Usp18)* in the induction of autoimmune diabetes. We found that expression of *Usp18* in bone marrow derived cells was essential to break immunological tolerance and to induce autoimmune diabetes. Expression of *Usp18* in antigen presenting cells enforced viral replication in those cell types which was essential to induce auto-reactive immune response. We showed that enforced viral replication is involved in breaking immunological tolerance and was essential to induce autoimmune diabetes. Using the vesicular stomatitis virus (VSV) as a virus model system, we found that *Usp18* dependent viral replication was associated with efficient, anatomically highly selective VSV replication. This replication was essential to activate an efficient antiviral immune response. Together these data clearly point to the importance of *Usp18* dependent enforced viral replication in the pathogenesis of diabetes.

In another series of experiments we analyzed the impact of the Wiskott-Aldrich syndrome protein (WASP) in the induction of autoimmune diabetes. We found that expression of WASP in bone marrow derived cells was efficient to induce diabetes. Lack of WASP was linked to a reduced ability of dendritic cells to produce type I interferon and to prime auto-reactive virus-specific $CD8^+$ T cells.

Moreover, we found that endoplasmic reticulum stress induced by Tunicamycin reduced the incidence of diabetes. Tunicamycin did not affect beta islet cells directly. However, activated beta-cell specific $CD8^+$ T cells were highly sensitive to Tunicamycin and underwent apoptosis upon activation. The exact mechanism of action remains to be determined. Furthermore, we analyzed the role of ATP receptor signaling and ER stress signaling in the role in the induction autoimmune diabetes. Therefore, we used a general inhibitor of ATP receptors oxidized ATP (oxATP) and the ER stress inducer Tunicamycin in the autoimmune diabetes model. We found that oxATP had a strong inhibitory effect on the IFN-γ production of auto-reactive $CD8^+$ T cells in vitro and *in vivo*. At higher concentrations oxATP induced apoptosis. *In vivo* oxATP suppressed activation of T cell responses and therefore suppressed T cell mediated autoimmune diabetes.

In conclusion we present several mechanisms, which participate in induction of autoimmune diabetes. In future work those mechanisms might be evaluated as targets for treating autoimmune diabetes in humans.

1. Chapter I: introduction

The human being is surrounded with a broad spectrum of infectious agents, such as a viruses, bacteria or prions. In order to defend the host against the invasion of these microorganisms, the human body has a well-organized, disciplined, developed and multiple mechanistic immune system. This system is also responsible for defense against tumors and supper active self-antigens [1]. The amazing character of immune system that, it can distinguish between self and none self-antigens [2]. Any breakdown in this mechanism can lead the immune system to attack the individual's own cells, which called autoimmune disease, and the reaction is called autoimmunity.

The immune system consists of two major sections: the first is called innate, which mediates the initial protection; and the second is called adaptive (acquired or specific), which develops slowly and mediates the protection in the late stages of infection [3,4].

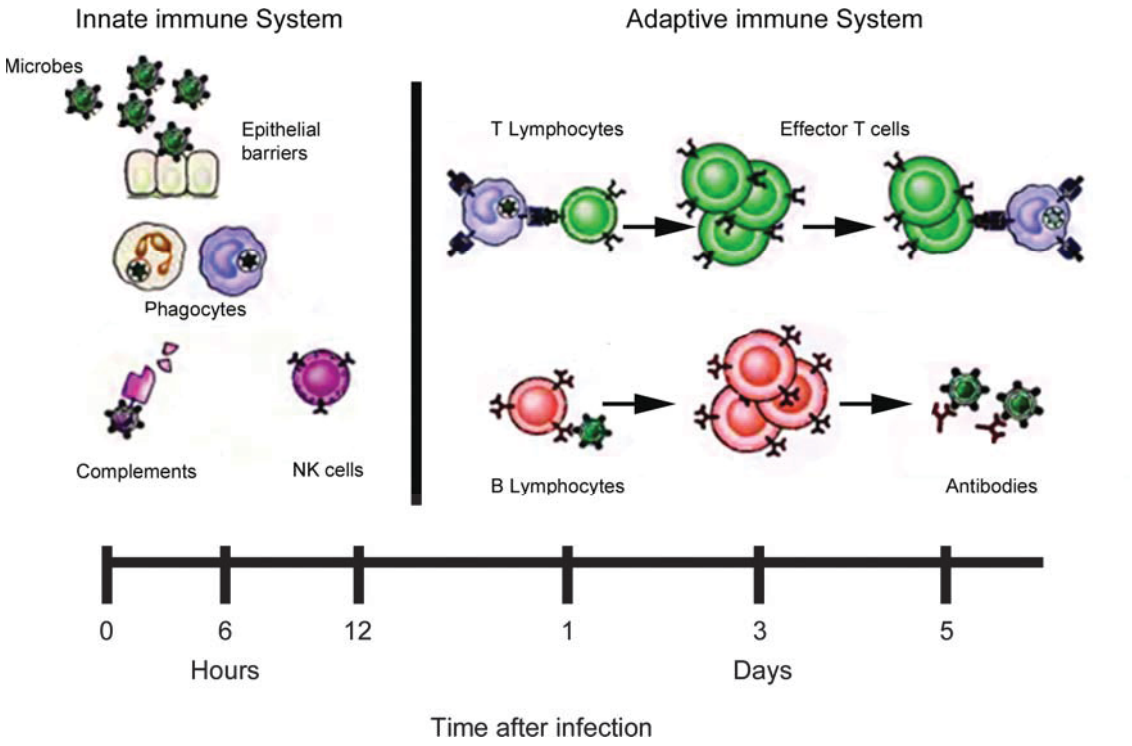

Figure 1-1 Innate and adaptive immune systems

Abbas AK & Lichtman AH (2004) *Basic immunology* (Elsevier)(modified)

The innate and adaptive immune systems take advantage of cell-surface and soluble receptors to sense potential threats. These receptors are generated in different ways, consequently provide a major discrimination between the two systems [3].

1.1. Innate immune system

The first line of defense in the innate immune system is provided by the skin which prevents the entrance of pathogenic organisms into the tissue or circulation. The mucus secreted by the membranes covers the inside surfaces of the body and acts as a protective barrier to block the adherence of foreign antigen to epithelial cells [3,4]. Besides the physical barrier, there are the innate immune cells, including dendritic cells, macrophages, monocytes, neutrophils, basophils, eosinophils and the platelets. In this study, we focused on dendritic cells and macrophages.

1.1.1. Dendritic cells (DCs)

Dendritic cells were discovered in 1973 by Ralph Steinman and Zanvil Cohn [5]. They derived their name from their forked branch out form, in tree mimicking shape "Dendron-Greek for tree". DCs are categorized under many subpopulations, each subpopulation has different function and receptor. For example, plasmacytoid dendritic cells (pDCs) produce the major amount of type I interferon [6,7], whereas follicular dendritic cells (FDCs) play an important role in supporting B cells in secondary lymph nodes and preventing autoimmune diseases [8]. Conventional dendritic cells (cDCs) are responsible for both the priming of adaptive immune responses and the induction of self-tolerance depending on the maturation of dendritic cells and the expression of costimulator receptors like CD40, CD80, CD83 and CD86 [9-11].

1.1.2. Macrophages

Macrophages were discovered initially by Ilja Metschikov in 1800, they acquire their name from Greek for "big eaters" due to their high ability to phagocyte, this potent capacity of phagocyting reflects their importance as first line in defending the body against foreign pathogens and dead cells [12].

Similar to dendritic cells, macrophages are categorized under many subpopulations dependent on their resident organ location [13]. For example:

Name	Location
Kupffer cells	Liver
Alveolar macrophages	Lung
Microglia	Neural tissue
Osteoclasts	Bone

All of these macrophages share the common feature of phagocytosing foreign antigens and further distinguishing charactertis are yet to be elucidated.

Additionally, there is a special subtype of macrophages, called metallophilic macrophages, which found to play an important role in capturing bacteria and viruses. Their location in the marginal zone in the spleen or in lymph nodes is essential in presenting the antigen and consequently the priming of adaptive immune cells [14], they are characterized by $CD169^+$ receptor and react differently to type I interferon than the other types of macrophages.

1.2. Adaptive immune system.

The most important two features of the adaptive immune system which distinguish it from the innate is the specificity against the antigen and the ability to memorize prior exposure to the antigen. The adaptive immune system includes two major groups, B cells and T cells. The antigen receptor of B cells can recognize a wide spectrum of macromolecules such as proteins, lipids, polysaccharides and nucleic acids [2]. On the other hand, T cells receptors can only recognize small residues of peptides presented with major histocompatibility complex 1 (MHCI) or major histocompatibility complex 2 (MHCII) [2]. Different types of antigen presenting cells (APCs) have distinct functions in T cell-dependent immune responses. Dendritic cells are considered as the most potent APCs for activating naive T lymphocytes and in addition they may also influence the nature of the response. There are two main subtypes of T cells: $CD8^+$ T cells which mediate the cytotoxic task of T cells (Cytotoxic T lymphocytes, CTL) and $CD4^+$ T cells which mediates the humoral task of T cells and help B cells to switch the antibody isotypes [3].

APCs can phagocyte pathogens and envelop them in an intracellular vesicles called endosomes which then fuse with lysosomes and digest the pathogen with proteolytic enzymes, afterwards, pathogen-derived peptides are loaded on MHCII and presented on the surface of APCs to $CD4^+$ T cells. In contrast, loading peptides on MHCI is restricted intracellular process, which means that the protein is derived from viruses which lives inside the host cells and not from phagocyted pathogen from the extracelluar environment [4].

However, an additional mechanism was described as an important process for APCs to present exogenous antigen to the CTLs, this mechanism is called cross presentation, by which APCs ingest infected cell (often damage) and load the microbal or viral antigen on MHCI. This mechanism can also explain how CTLs are primed in cases where the viruses can escape endogenous MHC I pathway like some members of Herpes virus family [15].

Dendritic cells (DCs) are considered the main cross-presenting cells comparing to the other antigen presenting cells [16]. Although pDCs are considered as weak APCs, they show cross presentation just *ex vivo* after stimulation of Toll like receptor, on the other hand, cDCs are divided also into different subtypes depending on the surface markers, $CD8^+$ DC are more efficient in cross presentation than $CD8^-$ DC, and the $CD103^+$ DC are the most efficient one [17].

In addition to the role of immune cells in defending the host against infection, cytokines play a major role in the clearance of the infection and development of immune cells. Cytokines are low molecular soluble proteins which are synthesized under a strict regulatory control of leukocytes and non-hematopoietic cells [2]. One of the most important and earliest discovered cytokine is the interferon.

1.3. Interferon (IFN)

Interferon was first described by Alick Issacs and Jean Lindenmann in 1957 [18]. Later on Nagata S et al. cloned and synthesized interferon through recombinant technology. And after it was proved for *in vivo* therapy, IFN is now considered as first line in therapeutic strategy of different diseases such as multiple sclerosis and chronic virus hepatitis [19,20].

IFN is a glycoprotein produced and released in response to invasion from pathogens like parasites, bacteria or viruses. However, tumor cells can stimulate also

the production of interferon. Its name came from the ability to interfere with the replication of the virus. Besides its antiviral effect, interferon activates the innate immune response and recruits the adaptive immune mediators. Three different types of interferons have been identified: IFN-α, IFN-ß and IFNγ, and each of them has many subtypes.

The IFN response is involved in the control and stimulation of a wide diversity of molecular and cellular responses. The mechanism of IFN signaling has been explained, and it suggests a main role of Janus activated kinase-signal transducer and activation of transcription (JAK-STAT) pathway. The interferon alpha receptor 1 subunit (IFNAR1) is associated with tyrosine kinase 2 (TYK2) activation, whereas the interferon alpha receptor 2 subunit (IFNAR2) is associated with JAK1 activation. After activation, the STAT 1 and STAT2 are phosphorylated and dimerized and translocated to the nucleus, where an IFN-stimulated response takes place [21].

Alternative signaling pathways have also been shown to be ivolved in IFN signaling, including the mitogen activated protein kinase (MAPK), the v-crk sarcoma virus CT10 oncogen homolog(avian)-like (CRKL) pathway,the Phosphoinositide 3-kinase (PI3K) and the classical or the alternative NF-kB cascade [22,23].

IFN type I stimulates different genes and amongs the most stimulated gene is *ISG15*, ISG15 was first described in 1979 by Farrell [24], it exists either as conjugated (ISGylation) or free form, the free form can act as cytokine to activate immune cells including NK cells, T cells and dendritic cells [25], its role as antiviral is very clear, *ISG15* knockout mice are unable to control many viruses [26,27]. However, ISG15 has no effect on vesicular stomatitis and lymphocytic choriomeningitis virus [28].

The signaling of Type I interferon has a feedback mechanism, which depends on Ubiquitin Binding Protein (UBP43). This protein is encoded by *USP18* and can split the ISG15 specifically and additionally inhibits IFN signaling [29,30], $Usp18^{-/-}$ mice are very susceptible and show high mortality after treatment with interferon stimulating agents including viruses or poly I:C treatment [29,30]. On the other hand, it has been shown that UBP43 can also inhibit IFN signaling independently from its ISG15 protease effect, but by interrupting IFNAR-JAK binding [31].

1.4. Wiskott-Aldrich syndrome protein

The Wiskott-Aldrich syndrome protein is the first actin cytoskeleton regulator identified in mammals and it has an important role in haematopoietic and immune cell functions [32]. Loss of this protein leads to x-linked disease associated with many complications including:

- Petechiae
- Bruising
- Thrombocytopenia
- Spontaneous nose bleeds and bloody diarrhea
- Eczema first month of life
- Recurrent bacterial infections develop by three months
- IgM levels are reduced, IgA and IgE are elevated, and IgG levels can be normal, reduced.

The importance of WASP is depending on the cell lineage and stage of maturation [33].

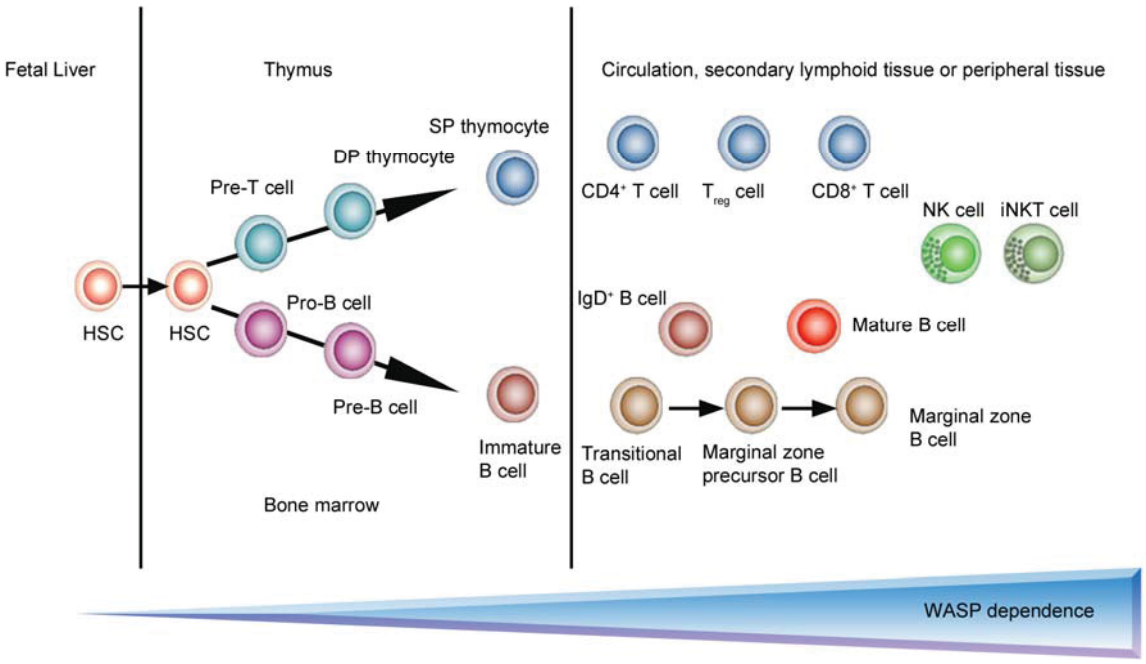

Figure 1-2 WASP and lymphocytes homeostasis

Adrian J. Trasher & Siohan O. Burns (2012) WASP: a key immunological multitasker (Nature reviews) (modified)

1.5. Autoimmune diseases

The immune system is able to react against a wide spectrum of antigens, while it has tendency to avoid attacking autoantigen. Any inappropriate response to autoantigen may lead to autoimmune disease.

A major concern of the immunologist is to understand the sophisticated mechanism behind self-non-self discrimination and by which autoimmune disease is prevented. In order to avoid the activation of the immune system against autoantigen, autoreactive lymphocytes are deleted by filtering them through central and peripheral tolerance processes [34,35].

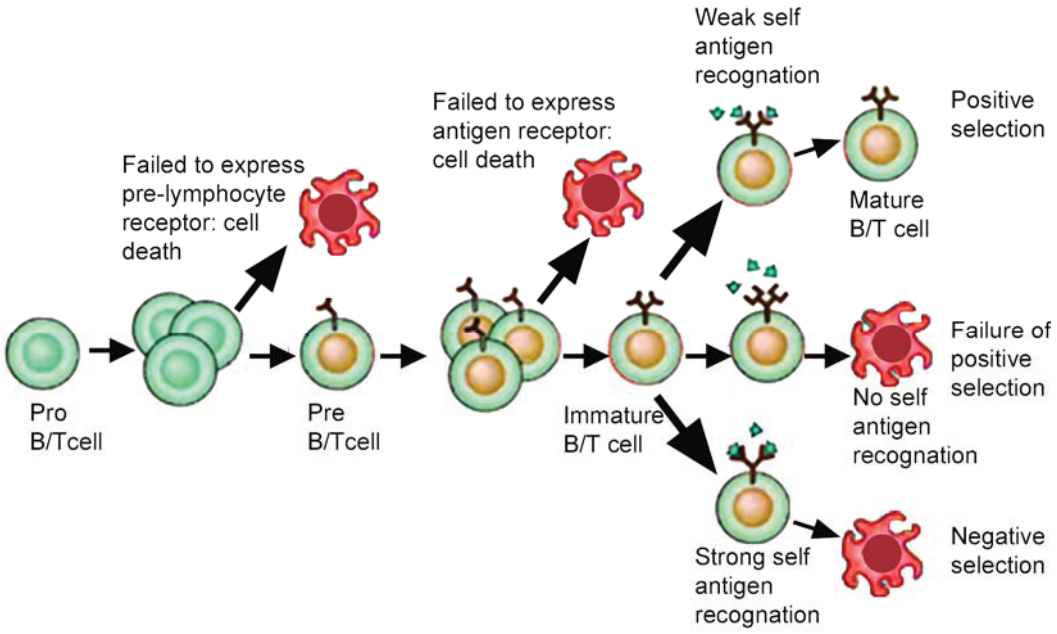

Figure 1-3 Central tolerance

Abbas AK & Lichtman AH (2004) Basic immunology (Elsevier) (modified)

During the development of lymphocytes, they are exposed to different antigens. If the lymphocytes have a high affinity for special antigen they will be deleted through apoptosis. This process, termed negative selection, is very important in eliminating the dangerous lymphocytes which can potentially react with self antigen and cause autoimmune disease. On the other hand, if lymphocytes do not recognize any antigen, they are also eliminated and failed to be positively selected. Only weak antigen recognizing lymphocytes are selected positively and migrate to the periphery as mature lymphocytes[36]. This process is called central tolerance and it is occurring in the thymus for T cells and in bone marrow for B cells [2].

However, some auto reactive lymphocytes may escape negative selection. Thus, additional mechanism, called peripheral tolerance, is necessary to overcome autoimmune disease, two key steps are occur during peripheral tolerance, the first step is called anergy and is happening when lymphocytes encounter auto-antigen without recieving adequate second signals from costimulation receptors, which leads to functional deactivation and death. The second step is happening by suppressing autoreactive lymphocytes by regulatory T cells [4].

Human autoimmune diseases are highly heterogeneous; accordingly they were classified under two main categories, systemic or organ-specific diseases [37].

Systemic autoimmune diseases	Organ-specific autoimmune diseases
Rheumatoid arthritis	Type I diabetes
Systemic lupus erythematosus	Multiple sclerosis

1.5.1. *Diabetes and autoimmunity*

The incidence of diabetes is increasing rapidly in Germany and worldwide. According to the International Diabetes Federation statistics (IDF) in 2010, 285 million people worldwide have diabetes, and the prevalence is expected to more than 438 by the year 2030.

Diabetes is classified as a metabolic disease, in which high concentration of glucose is diagnosed in the blood. The elevated concentration of glucose is due either to reduction of insulin production (insulin dependent diabetes) or to the non-response of insulin target cells to insulin itself (insulin independent diabetes) [38].

The untreated diabetic people suffer from specific symptoms including polydipsia, polyuria and polyphagia, where the neuropathy, nephropathy, and retinopathy are directly related to the extent of glycemic control.

Three main types of diabetes are described, Diabetes mellitus type 1 (DM type1) or formerly referred to as insulin–dependent diabetes mellitus (IDDM) , occurs if the body fails to produce insulin, mainly due to beta- islet cells destruction in the pancreas by T cells. In the presence of cross-reactive epitope to beta-islet cells, T cells will be activated and the peripheral tolerance will be broken. In this case, the

treatment depends mainly on the injection of insulin. Human insulin is produced by special strains of Escherichia coli or yeast that have been genetically modified to contain the gene for human insulin, the technique is called recombinant DNA technology. Different kinds of insulin are available through the modifications of the amino acid sequence of human insulin offering different pharmacokinetic properties.

Diabetes mellitus type 2 (DM type 2), also referred to as non insulin-dependent diabetes mellitus (NIDDM), results from the features of the cells to be resistance to the insulin. However, the specific defects resulting in insulin resistance are not known. The therapeutic strategy is mostly dependent on sulfonylureas, meglitinide analogs, biguanides, thiazolidinediones or glitazones, which increase generally the sensitivity of the cells to the insulin.

Diabetes mellitus form 3 (Gestational diabetes) occurs during pregnancy and may forego the development of DM type 2.

Many chemicals were suggested in order to suppress the immune response in cases of autoimmune diseases, the goal of this suppressor is to reduce the immune pathology and tissue damage, which results from the attacking of the immune cells to the own individual tissue.

1.6. Immune suppressors

In this study, we investigate the immune suppressive effects of tunicamycin and oxidized ATP.

1.6.1. *Tunicamycin*

Tunicamycin is produced by bacterium *Streptomyces lysosuperificus*, it has different mechanisms by which it can inhibit the highly proliferative cells. The main two mechanisms are the inhibition of glycolysation and arresting the mitosis process in G1 phase [39,40].

1.6.2. *Oxidized ATP (oxATP)*

oxATP is an antagonist of the ATP receptor P2rx7. ATP-sensitive cation channels have been shown to be important in T-cell activation. Activation of P2rx7 leads to ion

channel activity, which can depolarize the cell. This can lead to activation of several signaling cascades including PKC as well as the MAPK pathway.

In order to study the immunological mechanism of type I diabetes and clarify the role of specific cell or cytokine in the onset of diabetes, we used different kinds of transgenic mice.

1.7. Mouse models:

- RIP-GP / RIP-NP

RIP-GP model is a viral antigen-based model, where the glycoprotein GP (33-41) is expressed under the rat insulin promoter. In this model, LCMV specific $CD8^+$ T cells are not tolerized but not informed of the glycoprotein in the pancreas. After infection with lymphocytic choriomeningitis virus (LCMV), $CD8^+$ T cells are stimulated and infiltrate to the pancreas and destroy the ß-islet cells leading to type I diabetes [41].

Similar to RIP-GP mice, RIP-NP mice express the nucleoprotein of lymphocytic choriomeningitis virus (LCMV) under the rat insulin promoter. It differs from RIP-GP mice that the viral antigen is also expressed in the tymus. Consequently, the incidence of diabetes is delayed in this model [42].

- P14

These transgenic mice have specific $CD8^+$ T cells restricted to LCMV, and this model is used in order to study the conditional proliferation of LCMV specific $CD8^+$ T cell [43].

- *IFNAR*$^{-/-}$

In this model the receptor of interferon α/β is missing, excluding this receptor helps to study the effect of type I interferon during viral infection [44].

- *USP18*$^{-/-}$

This mouse model is lacking the ubiquitin specific peptidase 43 which is responsible for inhibition of interferon signaling through inhibiting the phosphorylation of the JAK binding site of the type I interferon receptor [45].

- CD169-DTR and CD11c- DTR

These transgenic mice have the diphtheria toxin receptor under the promoter of CD169 or CD11c, respectively. By administration of diphtheria toxin into these mice we can deplete $CD169^+$ macrophages in the CD169-DTR mice and $CD11c^+$ cells in the CD11c-DTR [46].

- Aly/aly

The mice in this model have a mutation in the alymphoplasia gene "aly", the aly/aly mice are deficient in both humoral and cell–mediated immune functions, and are very susceptible to infections and they do not have lymph nodes but do have a spleen [47].

- DEE

In this model, the glycoprotein of lymphocytic choriomeningitis virus is expressed under the actin promoter [48].

- *CHOP*$^{-/-}$

These mice are missing the unfolded protein response UPR-induced transcription factor C/EBP homologous protein [49].

- *WASP*$^{-/-}$

The mice lack the Wiskott-Aldrich syndrome protein.

1.8. Viruses

In order to study the immune response during the incidence of diabetes mellitus type I, we used two different viruses, depending on the immune response which we wanted to achieve.

1.8.1. *Lymphocytic choriomeningitis virus (LCMV)*

The first virus we employed in our studies is lymphocytic choriomeningitis virus (LCMV). This virus has a single strand genome, and it belongs to Arenaviridae family. LCMV was discovered by Armstrong and Lillie in 1933, and it causes meningitis in rodents and humans. The virus is not cytopathic itself, and it replicates in the cells without destroying them. The virus can be detected in the infected animals within urine and feces.

Kinetics of viral infection are mainly dependent on the strain of the virus, four strains are described; two are neurotropic: Armstrong (mild) and Clone13 (aggressive), and two are hepatotropic: WE (mild) and Docile (aggressive) [50,51]. When C57Bl/6 mice are infected with LCMV, virus infects the marginal zone macrophages and dendritic cells [52], which in turn present the virus to $CD8^+$ T cells. $CD8^+$ T cells are very essential in controlling LCMV, as $CD8^+$ T cell deficient mice or depletion of $CD8^+$ T cells leads to persistence of the virus.

1.8.2. *Vesicular stomatitis virus (VSV)*

The second virus which we used in our studie is the vesicular stomatitis virus (VSV). This virus has also a single strand RNA genome from the Rhabdoviridae family, which belongs to the same family of the famous rabies virus. Its hosts are insects, horses, pigs and cattle. It is used in the laboratory to study the rhabdovirus structure and replication and the immune response to this family, especially the response of B cells to viral infection. VSV triggers the production of neutralizing antibodies after four days of infection, while LCMV neutralizing antibodies can be detected after around 60 days of infection [53].

In some experiments, we wanted to study the role of viral replication mechanisms on the immune response, and to distinguish that from the role of non replicating-antigen, we used Ribavirin. Ribavirin is an antiviral drug against wide spectrum of viruses (RNA and DNA) [54]. Recently, it has been used in combination with interferon alpha as a therapeutic strategy for the treatment of hepatitis C [55,56].

Ribavirin is a prodrug, its mode of action is considered on three levels; first, it is converted to guanosine analogue which explain its effects on the RNA viruses. Secondly, Ribavirin 5'-monophosphate inhibits cellular inosine monophosphate dehydrogenase, which explains it effects on the DNA viruses and also its toxicity. Third, it helps the host-T cell to switch from type 2 to type 1.

In addition to Ribavirin, we used the immune stimulator Polyinosinic:polycytidylic acid (poly I:C), Poly I:C has similar structure as double strain RNA. Due to that it can interact with Toll like receptor 3 which is expressed on different type of cells including B cells and dendritic cells as well as macrophages [44].

In this thesis we showed different genes and mechanisms which can be targeted in future to invent new drugs to treat IDDM.

2. Chapter II: "Enforced virus replication" activates adaptive immunity and is essential to control cytopathic virus

Nadine Honke, Namir Shaabani, Giuseppe Cadeddu, Ursula R. Sorg, Dong-Er Zhang, Mirko Trilling, Karin Klingel, Martina Sauter, Reinhard Kandolf, Nicole Gailus, Nico van Rooijen, Christoph Burkart, Stephan E. Baldus, Melanie Grusdat, Max Löhning, Hartmut Hengel, Klaus Pfeffer, Masato Tanaka, Dieter Häussinger, Mike Recher, Philipp A. Lang and Karl S. Lang

2.1. Abstract

The innate immune system limits virus replication by interferon type I and also induces presentation of viral antigens to adaptive immune cells. Using vesicular stomatitis virus infection in mice, we analyzed how the innate immune system inhibits virus propagation but still allows the presentation of antigen to adaptive immune cells. We found that the expression of *Usp18* in metallophilic macrophages reduces their type I IFN responsiveness, thereby allowing locally restricted replication of virus. This was essential for the induction of adaptive antiviral immune responses and, therefore, for preventing fatal outcome of infection. In conclusion, we found that "enforced virus replication" within marginal zone macrophages is an immunological mechanism that ensures the production of sufficient antigen for effective adaptive immune activation.

2.2. Introduction

The innate immune system limits virus replication during systemic infection by production of type I interferon. Consistently, the lack of type I interferon receptor (IFNAR) promotes viral replication and results in viral persistence and the death of virus-infected animals [57,58]. Macrophages are key players during type I IFN–mediated virus suppression [59-62]. With their potent phagocytic capacity, macrophages act as a first line of defense against pathogens entering tissues. Splenic red pulp, marginal zone macrophages and Kupffer cells are associated with the endothelium and can capture antigens from the blood vessel lumen [61,63,64]. They clear the blood from immune complexes, high molecular and complex particles including virus particles [63-65]. Virus phagocytosis is followed by suppression of their replication in a type I IFN–dependent manner [60,61]. This mechanism suppresses the spread of virus but obviously limits the amount of antigen that is available for priming the adaptive immune response.

Binding of type I IFN leads to IFNAR dimerization, which phosphorylates and activates receptor-associated tyrosine kinase 2 (Tyk2) and Janus kinase 1 (Jak1). These kinases recruit signal transducer and activator of transcription 1 (STAT1) and STAT2. The STATs form homodimers and heterodimers that can translocate to the nucleus and initiate the transcription of type I IFN–stimulated genes (ISG) [22]. More than 300 genes are regulated by IFN-α or IFN-β [66]. Examples of genes that exert antiviral activity are *Isg15* (IFN-stimulated gene 15), *Mx1* (myxovirus resistance 1), *Oas1* (2′5′-oligoadenylate synthetase 1), *Eif2ak2* (protein kinase R), and *Rnasel* [58]. One potent inhibitor of this signaling cascade is *Usp18* (UBP43) [30], which binds to the Jak1 binding site of the interferon alpha receptor and inhibits its phosphorylation [30,31]. Accordingly *Usp18* deficiency in mice increases type I IFN sensitivity and results in limited virus replication after viral infection [30]. However, it remains unclear how *Usp18* expression in various cell types influences the overall immune response.

In addition to controlling viral replication, innate immune cells initiate priming of adaptive immune cells. Priming usually occurs in secondary lymphoid organs, such as lymph nodes and spleen. Antigens from the lymph can be captured by the cells in the subcapsular zone of the lymph node, whereas antigens from the blood are filtered in the spleen by macrophages from the red pulp and the marginal zone [67].

Metallophilic macrophages in the marginal zone are characterized by the expression of the C-type lectin CD169 (Siglec-1) [68]. $CD169^+$ macrophages present captured virus antigen directly to B cells [69]. Fibroblastic reticular cells (FRCs) form FRC conduits together with type I and type III collagen [70]. These channels reach into the marginal zone of the spleen and can distribute antigens from metallophilic macrophages through the splenic white pulp [71]. Resident dendritic cells (DCs) take up these antigens and present them to T cells [71].

The amount of presented antigen limits the adaptive immune response [72-76]. *In vitro* studies have shown that at least 10 peptide-major histocompatibility complex (pMHC) complexes are required to form an immunological synapse between DCs and T cells [77]. *In vivo* induction of T cell proliferation in the lymph node requires DCs with at least 2×10^4 pMHC complexes [78]. Low-affinity T cell receptors (TCRs) require a larger antigen dose than high-affinity TCRs [79]. These findings suggest that a larger antigen dose improves T cell immunity. Consistently, low-dose application of inactivated, replication-incompetent virus results in limited induction of neutralizing antibodies, whereas replicating virus leads to a strong antibody response [80]. However, the existence of a specific compartment that would promote virus replication and increase the presented antigen in order to improve the adaptive immune response remains unknown.

In this study, using the murine vesicular stomatitis virus (VSV), we demonstrate that $CD169^+$ macrophages in the marginal zone of the spleen form a compartment of "enforced virus replication". Early after infection, red pulp macrophages in the spleen and Kupffer cells in the liver captured virus and effectively suppressed virus replication in a type I IFN-dependent manner. In contrast, $CD169^+$ macrophages captured virus but did not respond to type I IFN and thus allowed anatomically restricted virus replication in the splenic marginal zone. Enhanced replication in $CD169^+$ macrophages was linked to overexpression of *Usp18*. $Usp18^{-/-}$ mice exhibited little virus replication in $CD169^+$ macrophages. The lack of either $CD169^+$ cells or *Usp18* resulted in impaired and delayed adaptive immunity to VSV. The delayed induction of antibodies in $Usp18^{-/-}$ mice led to distribution of virus to neuronal tissue and to death of mice. Taken together, our findings suggest that "enforced virus replication" in $CD169^+$ macrophages promotes the adaptive immune response and guarantees survival after infection with a prototypic cytopathic virus.

2.3. Results

2.3.1. *CD169^{+} metallophilic macrophages allow virus replication*

To determine how the reticuloendothelial system inhibits the spread of systemic virus while presenting sufficient amounts of antigen to adaptive immune cells, we first analyzed the virus-capturing capability of macrophages after intravenous infection. We treated mice with clodronate liposomes to deplete macrophages before VSV infection [69]. Replicating virus remained detectable in the blood for a prolonged period of time in the absence of macrophages (**Fig. 1a**). This observation suggests that macrophages play a crucial role in virus uptake. In mice lacking spleen and lymph nodes (splenectomized aly/aly mice) [47], virus inoculate was still taken up efficiently (**Fig. 1a**) suggesting that, in the absence of macrophages in the spleen, macrophages from other tissues, most likely liver Kupffer cells, sufficiently take up virus. This indicates that macrophages in lymphoid and non-lymphoid compartments participate to systemic virus clearance.

We next analyzed viral production after uptake by macrophages. Replicating virus was detected 1 and 7 hours after infection in the spleen, while no virus was detectable in other tissues (**Fig. 1b**). To analyze viral replication in the absence of macrophages after intravenous infection we depleted macrophages by injecting clodronate liposomes and noticed enhanced replication of VSV in several organs (**Fig. 1c**). Accordingly, macrophage-depleted mice were highly susceptible to VSV infection (**Fig. 1d**). These observations uncover that macrophages are crucial for the control of VSV replication in non-lymphoid tissue. To test the hypothesis that type I IFN suppresses VSV replication in macrophages, we infected mice lacking the interferon alpha receptor (*Ifnar*$^{-/-}$ mice) with VSV intravenously. *Ifnar*$^{-/-}$ mice exhibited excessive VSV replication in the liver, lung, kidney, spleen, thymus and brain, whereas wild-type mice exhibited infectious VSV only in the spleen (**Fig. 1e**). These results show that macrophages in non-lymphoid tissues capture the virus and suppress its replication in a type I IFN-dependent manner. In macrophage-competent wild-type mice, infectious virus particles were detectable only in the spleen but not in other organs (**Fig. 1b**). This suggests that type I IFN-dependent suppression of viral replication in macrophages was limited in the spleen compared to other organs.

To determine the mechanism of enhanced virus replication in the spleen we next determined virus protein expression by immunohistological analysis of spleen and liver 7 hours after VSV infection. VSV glycoprotein was readily detectable in the spleen but not in the liver (**Fig. 1f**). Immunohistological analysis showed that $CD169^+$ metallophilic macrophages allowed VSV protein expression (**Fig. 1g**). Upon administration of ultraviolet light (UV)-inactivated VSV, glycoprotein expression was undetectable in $CD169^+$ cells (**Fig. 1h**), supporting the hypothesis that VSV actively replicates in these cells. To address the contribution of $CD169^+$ macrophages to VSV replication, we used mice that express the diphtheria toxin receptor under the CD169 promoter (CD169-DTR mice) [81]. Treatment with diphtheria toxin depletes $CD169^+$ macrophages in these mice. We generated bone marrow chimeras by transferring bone marrow from control wild-type or CD169-DTR mice into irradiated wild-type recipients. After reconstitution we treated chimeric mice with diphtheria toxin and infected them with VSV intravenously. Administration of diphtheria toxin depleted $CD169^+$ macrophages in the spleen (**Fig. 1i**). Immunohistological VSV staining in the marginal zone was not detectable in $CD169^+$ macrophage-depleted mice but was detectable in control mice (**Fig. 1i**), suggesting that $CD169^+$ macrophages within the marginal zone enforced virus replication, whereas conventional macrophages in the red pulp suppressed virus propagation. Spleen sections showed VSV replication in $F4/80^+$ red pulp macrophages and in $CD169^+$ macrophages from *Ifnar*$^{-/-}$ mice, but only in $CD169^+$ macrophages from wild-type mice (**Fig. 1j**). In line with this result, IFNAR–deficient Kupffer cells expressed VSV glycoprotein (VSV-GP) in the liver (**Fig. 1j**). These findings suggest that in wild-type mice, Kupffer cells and red pulp macrophages suppress virus replication in a type I IFN–dependent manner, whereas $CD169^+$ macrophages are resistant to the effects of type I IFN. We conclude that early uptake of virus by macrophages followed by type I IFN-mediated suppression of replication is essential for the control of VSV infection and the survival of mice. $CD169^+$ macrophages however allow virus replication in the presence of type I IFN.

2.3.2. *Expression of Usp18 in CD169$^+$ macrophages enhances virus replication*

We next investigated the mechanism underlying the enforced virus replication in $CD169^+$ macrophages. Because *Usp18* is an inhibitor of the type I IFN signaling

pathway competing with Jak1 [30,31], we hypothesized that *Usp18* expression might allow VSV replication in CD169$^+$ macrophages. We performed *in situ* hybridization of *Usp18* during VSV infection. *Usp18* was upregulated during infection within the lymph follicle and the marginal zone but not in the red pulp (**Supplementary Fig. 1**). To directly compare the expression of *Usp18* between CD169$^+$ macrophages and F4/80$^+$ macrophages, we sorted F4/80$^+$ macrophages and CD169$^+$ macrophages by magnetic activated cell sorting (MACS) and fluorescence activated cell sorting (FACS) (**Supplementary Fig. 2**) and performed quantitative real-time polymerase chain reaction (qRT-PCR) for *Usp18* mRNA expression. The expression of *Usp18* was significantly higher in CD169$^+$ cells than in CD169$^-$ F4/80$^+$ macrophages (**Fig. 2a**). To further confirm enhanced *Usp18* expression in CD169$^+$ macrophages we performed laser capture microdissection of cells from the marginal zone and red pulp (**Supplementary Fig. 3**). Cells isolated from the marginal zone expressed higher levels of *Usp18* than cells from the red pulp (**Fig. 2b**). To analyze whether differences in *Usp18* expression can directly affect VSV replication, we transfected HeLa cells with increasing concentrations of *Usp18* expression plasmids [31].In addition we used treatment with IFN-α2 because HeLa cells respond well to this interferon subtype. In the presence of IFN-α2, *Usp18* expression enhanced VSV replication in a dose-dependent manner (**Fig. 2c**). To further determine whether the expression of *Usp18* in CD169$^+$ macrophages is responsible for enhanced VSV replication *in vivo*, we infected *Usp18*$^{-/-}$ mice with VSV intravenously. Immunohistological analysis demonstrated that the distribution of CD169$^+$ macrophages was similar in *Usp18*$^{-/-}$ mice and in wild-type mice. However, we hardly detected any viral protein expression in CD169$^+$ macrophages from *Usp18*$^{-/-}$ mice (**Fig. 2d**). VSV replication in the spleen of *Usp18*$^{-/-}$ mice was significantly lower than in wild-type mice (**Fig. 2e**). Together, these results indicate that expression of *Usp18* in CD169$^+$ macrophages within the lymph follicle is essential for the enforced replication of VSV.

2.3.3. *VSV replication in CD169$^+$ macrophages promotes adaptive immunity*

Next we analyzed the physiological role of VSV replication in metallophilic macrophages. Intravenous immunization with inactive (UV-light inactivated) virus results in a limited adaptive immune response[80,82]. We hypothesized that enforced

virus replication in $CD169^+$ macrophages could promote adaptive immunity. Inactivation of VSV replication by UV-light limited the virus-specific $CD8^+$ T-cell response (**Fig. 3a**). Lack of replicating VSV blunted the induction of total neutralizing Ig (IgM and IgG) and of neutralizing IgG (**Fig. 3b**). Next we addressed the involvement of $CD169^+$ metallophilic macrophages during adaptive immune activation. The antiviral B cell response in C57BL/6 mice that had received CD169-DTR bone marrow transplants and had been treated with diphtheria toxin before intravenous VSV infection was delayed and reduced compared to C57BL/6 mice that had received WT bone marrow transplants and had been treated with diphtheria toxin (**Fig. 3c**). To explore the role of *Usp18* in adaptive immune activation, we analyzed adaptive immune responses in $Usp18^{-/-}$ mice after intravenous VSV infection. *Usp18*-deficient mice exhibited a highly impaired VSV-specific $CD8^+$ T cell response compared to wild-type mice (**Fig. 3d**). Additionally, the $CD4^+$ T cell response was lower in $Usp18^{-/-}$ mice than in wild-type mice (**Fig. 3e**).

Next we analyzed whether the observed reduction in the numbers of VSV-specific $CD4^+$ T cells was dependent on defective antigen presentation early after infection. We transferred splenocytes from transgenic mice that express a VSV-specific T-cell receptor (VSV-TCR, L7 mice) into VSV-infected wild-type and $Usp18^{-/-}$ mice[83]. The expansion of adoptively transferred $CD4^+$ T cells was significantly reduced in $Usp18^{-/-}$ mice compared to wild-type mice (**Fig. 3f**). This suggests that *Usp18* deficiency in antigen-presenting cells, but not in T cells, is responsible for the reduced expansion of VSV-specific $CD4^+$ T-cells in $Usp18^{-/-}$ mice *in vivo*. Next we analyzed B cell responses. $Usp18^{-/-}$ mice exhibited a delayed VSV-neutralizing IgM response and a delayed formation of VSV-neutralizing IgG antibodies after infection with live VSV (**Fig. 3g**). To assess whether the delayed antibody induction in $Usp18^{-/-}$ mice was due to reduced replication of VSV, we immunized wild-type and $Usp18^{-/-}$ mice with non-replicating UV-inactivated VSV. To induce measurable antibody titers we used 100-times the dose of UV-inactivated VSV. Immunization with replication-deficient UV-inactivated VSV did not produce any difference in the induction of VSV-specific B-cell responses between wild-type and $Usp18^{-/-}$ mice (**Fig. 3h**). This suggests that the differential replication activity of VSV was responsible for the differences in antibody induction. Together these

findings indicate that the replication of VSV in metallophilic macrophages is essential for the induction of an efficient adaptive immune response.

2.3.4. *Usp18 expression in DCs allows live virus-derived antigen presentation*

Dendritic cells are professional antigen-presenting cells and are therefore likely to contribute to the activation of the adaptive immune response during VSV infection. Some DCs expressed VSV glycoprotein at later time points of infection (**Supplementary Fig. 4**). We asked whether replication of VSV in DCs might contribute to adaptive immune activation. It was reported that active virus replication in DCs correlates with T cell priming [84]. *In vitro* generated wild-type and *Usp18*$^{-/-}$ DCs were infected with VSV and two hours later transgenic CD4^{+} T cells were added. We observed reduced T cell proliferation in co-cultures with virus-infected *Usp18*$^{-/-}$ DCs compared to WT DCs (**Supplementary Fig. 4**). Next we analyzed the activation capacity of *Usp18*$^{-/-}$ DCs in the presence of non-replicating virus. Co-culture of DCs with 100-times more UV-inactivated VSV particles showed enhanced activation of T cells in the absence of *Usp18*. Peptide-labeled DCs induced proliferation in peptide-specific CD8^{+} T cells independent of *Usp18* expression (**Supplementary Fig. 4**). Taken together, these findings indicate that *Usp18* expression in DCs enhances the presentation of replicating antigen.

2.3.5. *Enforced VSV replication promotes survival*

We found that replication of VSV in the spleen was necessary for neutralizing antibody production. Such neutralizing antibodies are essential for control of VSV[85]. Next we asked whether *Usp18*-mediated virus replication in lymph follicles would be beneficial for survival during VSV infection. Following intravenous VSV infection, *Usp18*$^{-/-}$ mice showed typical VSV-mediated paralysis and died one week after infection, while wild-type mice survived VSV infection (**Fig. 4a**). Paralysis and death of *Usp18*$^{-/-}$ mice could be explained by spread of VSV into the spinal cord or the brain (**Fig. 4b**). In summary, we conclude that *Usp18*-mediated enforced VSV replication in CD169^{+} macrophages promotes adaptive immunity, to guarantee fast neutralization of infectious VSV and survival of the infected host.

Next we analyzed whether enforced virus replication in lymph follicles and spleen would be beneficial for survival of peripheral VSV infection. Intranasal administration of VSV leads to fast spread of VSV to the CNS[86]. In light of our data we speculated that during this infection route, virus replication in lymphoid tissue is limited and this would reduce the adaptive immune response against VSV. To directly determine whether enforced replication of virus in the spleen could prevent spread of VSV from peripheral sites to CNS, we infected mice with VSV intranasally. In addition, we infected the mice by intravenous injection with 2×10^6 plaque-forming units (PFU) of either replication-competent VSV or UV-inactivated VSV. Mice receiving intravenous live virus in addition to intranasal VSV infection exhibited enhanced neutralizing antibody titers (**Fig. 5a**) and survived the infection (**Fig. 5b**). Mice receiving UV-inactivated VSV exhibited lower antibody titers and died of intranasal VSV infection (**Fig. 5a, b**). Thus, intravenous infection with live VSV induces protective adaptive immunity and protects from lethal intranasal VSV infection.

2.3.6. *Lymphotoxin-β receptor mediates enforced virus replication*

Lymphotoxins are important for the development and function of several innate immune cells, including DCs and $CD169^+$ macrophages[87,88]. We speculated that lymphotoxins are involved in the process of "enforced virus replication". VSV glycoprotein expression was strongly impaired in the spleen of *Ltbr*-deficient mice ($Ltbr^{-/-}$ mice), correlating with a reduced number of $CD169^+$ metallophilic macrophages (**Supplementary Fig. 5**). Accordingly, early virus titers in the spleen were significantly reduced in $Ltbr^{-/-}$ mice after VSV infection (**Supplementary Fig. 5**), suggesting that lymphotoxins are involved in the process of "enforced virus replication". $CD8^+$ T cell responses were impaired in $Ltbr^{-/-}$ mice (**Supplementary Fig. 5**). In line with these results, the VSV-specific B cell response was delayed in $Ltbr^{-/-}$ mice (**Supplementary Fig. 5**). $Ltbr^{-/-}$ mice exhibited typical VSV-mediated paralysis and died 7 days after infection (**Supplementary Fig. 5**). The death of $Ltbr^{-/-}$ mice could be explained by VSV propagation in the brain, the spinal cord, or both (**Supplementary Fig. 5**). These data show that lymphotoxins influenced early virus replication and this might partially contribute to immunodeficiency in these mice.

2.4. Discussion

In this study we found that CD169$^+$ metallophilic macrophages allow virus replication to promote adaptive immunity. Macrophages of the spleen and the liver captured virus particles after systemic virus infection. Although red pulp macrophages and Kupffer cells suppressed virus replication in a type I IFN–dependent manner, CD169$^+$ macrophages exhibited enhanced expression of *Usp18*, and the subsequent type I IFN resistance enforced virus replication. Either the lack of CD169$^+$ macrophages or a deficiency in *Usp18* led to limited virus replication in the spleen. Low virus titers in the spleen resulted in impaired priming of the adaptive immune system. Lack of neutralizing antibodies in *Usp18*$^{-/-}$ mice allowed the spread of virus from low-level replication at peripheral sites to neuronal tissue, thus leading to paralysis and death of the animals.

The innate immune response is a double-edged sword. Type I IFN production inhibits virus replication, and this inhibition is crucial to prevent virus distribution [57]. In addition, type I IFN enhances proteasomal degradation and cross-priming [89,90], up-regulates co-stimulatory molecules on DCs [91], and increases the proliferative capability of activated T cells [92] and B cells [93]. Our findings confirm recent studies indicating that macrophages capture virus particles and suppress virus replication in the red pulp of the spleen and the liver [61]. However, the inhibition of virus replication decreases the amount of antigen that can be presented to the adaptive immune system. It has been shown that the amount of antigen is positively correlated with the degree of adaptive immune stimulation [78,79]. Our findings suggest that virus replication is required for the promotion of T cell priming and the production of neutralizing antibodies.

CD169$^+$ macrophages are ideally situated to promote such virus replication. They reach into the marginal sinus and filter pathogens from the bloodstream [62]. Their anatomical location in the spleen allows antigen presentation to B cells [67,69,87]. Additionally, CD169$^+$ cells connect to FRC conduits, which can transport antigen to DCs in the T cell zone [71]. CD169$^+$ cells are important for the presentation of virus to plasmacytoid DCs and therefore are essential for innate immune activation [94]. In subcutaneous VSV infection, the induction of protective type I IFN was reported only in the presence of VSV replication in the lymph node[94]. This observation could

suggest that "enforced virus replication" is important not only for adaptive immune activation but perhaps also for innate immune activation.

Several signaling molecules influence the responsiveness of cells to type I IFN[95]. Therefore, enhanced expression of suppressors of cytokine signaling (SOCS) could contribute to the type I IFN-unresponsiveness of $CD169^+$ macrophages [22,58,95]. Indeed, we found enhanced basal expression of *Socs1, Socs3*, but not of *Oas1* or *Isg15* in $CD169^+$ macrophages (data not shown). Therefore, in addition to *Usp18, Socs1* and *Socs3* may act synergistically to allow VSV replication in $CD169^+$ macrophages. In this study we focused on the role of *Usp18* and its influence on VSV replication.

Lack of *Usp18* led to VSV replication in the brain and spinal cord, early paralysis, and death after systemic infection with 2×10^6 PFU VSV. A previous study has shown that *Usp18*-deficiency prevented death after intracranial infection with 10 PFU VSV [30]. Control of virus replication during infection *via* an intracranial route depends only on innate immune responses. In contrast, the adaptive immune response is essential for preventing lethal VSV infection during systemic intravenous infection with 2×10^6 PFU VSV [85,96]. Therefore, the expression of *Usp18*, even though it may locally augment VSV replication in the spleen, is of overall benefit for the host during systemic infection.

It remains to be investigated how the mechanism of enforced viral replication contributes to adaptive immune response against other viruses and to vaccination strategies against human pathogenic viruses. Using the non-cytopathic lymphocytic choriomeningitis virus (LCMV), we found that "enforced virus replication" also contributed to the adaptive immune response against this virus (data not shown). Earlier studies indicate that, in the case of human pathogenic viruses, replicating viruses elicit a stronger neutralizing antibody response than inactivated virus particles [80,82]. A number of live attenuated vaccines provide sufficient protection, whereas inactivated vaccines fail to induce a protective antibody response (e.g., rubella, measles, mumps, yellow fever, varicella, chicken pox). Vaccination with active rubella virus or poliovirus induces long-term protective IgG responses and also induces the production of IgA [97,98]. IgA can very efficiently neutralize poliovirus in the gut, therefore immunization with active virus would not only provide longer

protection but also be beneficial in disrupting the chain of infection. We would speculate that *Usp18* expression in the splenic marginal zone may enforce poliovirus replication and induce rapid protective neutralizing antibodies. Indeed, although type I IFN suppresses poliovirus in several cell types, in type I IFN-competent mice virus still replicates in the marginal zone[99]. Whether this replication is dependent on *Usp18* expression and whether it is essential for the induction of IgA remains to be determined.

We found that the absence of *Usp18* in dendritic cells was important for the activation of $CD4^+$ T cells during immunization with live virus. This finding could imply that immune activation at later stages of VSV infection depends on *Usp18* expression and virus replication in dendritic cells. During influenza virus infection it was shown that active virus replication in DCs increases antiviral T cell responses[84]. If "enforced virus replication" contributes to the strong co-stimulatory ability of DCs remains to be addressed.

$CD169^+$ macrophages may enhance the amount of foreign virus antigen through "enforced virus replication", so that immunological ignorance is converted to immune activation. In the RIP-GP model, a model of virus-induced autoimmune diabetes, limited virus replication or soluble antigen can hardly induce diabetes[100-102]. This finding is mainly explained by limited co-stimulation and limited inflammatory signals within the β-islet cells [101,102]. In light of our findings, the lack of antigen amplification in $CD169^+$ macrophages may participate in the lack of diabetes during immunization with soluble non-replicating antigen.

In conclusion, "enforced virus replication" is triggered by *Usp18* expression in $CD169^+$ metallophilic macrophages and leads to anatomically restricted virus replication and to rapid production of virus-neutralizing antibodies, thereby preventing fatal disease.

2.5. Acknowledgments

We thank K.Schättel for technical support. K. Lang was funded by the Sofja Kovalevskaja Award 2008 by the Alexander von Humboldt Foundation. P. Lang was supported by the Sofja Kovalevskaja award 2010 by the Alexander von Humboldt

Foundation. Further support came from the Sonderforschungsbereich SFB575, Experimentelle Hepatologie (Sprecher: Prof. D. Häussinger), DFG grant LA1419/3-1, FOR729 to K.P., DFG-grant SFB-TR19 (K. Klingel. R. Kandolf),Transregio TTR60 (Sprecher: Prof. M. Roggendorf) and the MOI Manchot Graduate school (Jürgen Manchot Foundation). M. Recher was supported by grant PASMP3-127678/1 from the Swiss National Science Foundation (SNF/SSMBS). *Usp18*-related work in D. Zhang lab is supported by the NIH, USA (R01 HL091549).

2.6. Author contribution statement:

N. H. planned and performed most experiments, N. S. planned and performed several experiments, G. C. and S.E.B. performed laser capture dissection, U. R. S. contributed to *Ltbr*$^{-/-}$ mice experiments, D.E.Z. contributed to experiments regarding *Usp18*, M. T. and C.B. contributed to transfection experiments, K. K., M.S. and R.K. performed and interpreted in situ hybridization, N. G. performed in vitro experiments, N. vR. contributed to macrophage depletion experiments, M. G. performed in vitro stimulation with DCs, M. L., H.H., K.P. M.T. D.H. and M.R. discussed and interpreted data and helped writing the manuscript, P. A. L. and K. S. L. initiated and designed the study and wrote most of the manuscript.

2.7. Figure Legends

2.7.1. *Figure 1: CD169^{+} metallophilic macrophages, but not red pulp macrophages and Kupffer cells, allow virus replication in the spleen*

(a) Blood titers of VSV in splenectomized alymphoplasia (aly/aly) mice, macrophage-depleted C57BL/6 mice (WT + clodronate) and control C57BL/6 mice (WT) injected intravenously with 2×10^6 PFU of VSV determined post infection (*n = 4* pooled from two experiments). **(b)** VSV titers of C57BL/6 mice infected intravenously with 2×10^6 PFU VSV determined post infection (*n = 5* pooled from two experiments). **(c, d)** Virus replication measured after 16 hours **(c)** and survival **(d)** of clodronate (macrophage-depleted) and empty-liposomes injected (control) mice, infected 1 day later with 2×10^7 PFU of VSV intravenously (**c**, *n = 5*; **d**, *n = 4 – 6;* pooled from two experiments). **(e)** Virus titers of wild-type (WT) and IFNAR-deficient (*Ifnar*$^{-/-}$) mice infected with 2×10^6 PFU of VSV intravenously determined 16 hours post infection (*n = 2*; one of two experiments is shown). **(f)**

Immunofluorescence in spleen and liver sections from C57BL/6 mice infected intravenously with 2×10^6 PFU or 2×10^8 PFU and stained for VSV glycoprotein (VSV-GP; green) 7 hours after infection (*n = 3*). **(g)** Immunofluorescence of spleen sections from C57BL/6 mice infected with 2×10^8 PFU VSV intravenously and stained for VSV-GP (green), B220 (B cells, blue) ,CD90.2 (T cells, lilac), F4/80 (macrophages, red), and CD169 (metallophilic macrophages, red) 7 hours after infection (*n = 3*). **(h)** Immunofluorescence of spleen sections from C57BL/6 mice infected intravenously with either 2×10^8 PFU active VSV or 2×10^8 PFU of ultraviolet light (UV)-inactivated VSV and stained for VSV-GP (green) and CD169 (red) 7 hours post infection (*n = 3*). **(i)** Immunofluorescence of spleen sections from C57BL/6 bone marrow chimeras reconstituted with CD169-DTR or WT bone marrow cells as control, treated intraperitoneally with diphtheria toxin and infected intravenously 3 days later with 2×10^8 PFU of VSV and stained with immunofluorescence antibody for VSV-GP (green) and CD169 (red) 7 hours post infection (*n = 4*). **(j)** Immunofluorescence of spleen and liver sections from WT and *Ifnar*$^{-/-}$ mice infected intravenously with 2×10^6 PFU of VSV and stained for F4/80 (red), CD169 (red) and VSV-GP (green) 16 hours post infection (*n = 3*) ***P < 0.01* Scale bar, 100 µm; Scale bar insert 20 µm.

2.7.2. *Figure 2: Expression of Usp18 in CD169$^+$ cells is responsible for enhanced virus replication*

(a) Expression of *Usp18* mRNA in CD169$^+$ macrophages and F4/80$^+$ macrophages sorted from naïve C57BL/6 mice (*n = 4 – 5,* pooled from two experiments). **(b)** Expression of *Usp18* mRNA in marginal zone tissue and red pulp tissue isolated from spleen sections from naïve C57BL/6 mice using laser capture microdissection (*n = 4,* pooled from two experiments). **(c)** VSV titers in supernatant derived from HeLa cells, transfected with various concentrations of *Usp18*-expressing plasmid, infected with VSV (MOI 0.01) and treated with the indicated concentrations of recombinant IFN-α2 24 hours later determined 24 hours post infection (*n = 6,* pooled from three experiments). **(d)** Immunofluorescence of spleen sections from *Usp18*$^{-/-}$ mice or WT mice, infected intravenously with 2×10^8 PFU of VSV and stained for VSV-GP (green), CD169 (red) and B220 (blue) 7 hours post infection (*n = 3*). **(e)** Spleen virus titers from *Usp18*$^{-/-}$ mice and WT mice infected intravenously with 2×10^6 PFU of

VSV determined 7 hours post infection (*n = 5,* pooled from two experiments). * *p < 0.05,* ** *p < 0.01;* Scale bar, 100 µm.

2.7.3. *Figure 3: Vesicular stomatitis virus replication in the spleen is required for efficient T-cell and B-cell response*

(a, b) Intracellular IFN-γ staining of splenocytes derived from C57BL/6 mice 7 days after immunization and 6 hours after restimulation with VSV-derived MHC-I restricted p52 peptide **(a)** and VSV-neutralizing antibodies **(b)** from C57BL/6 mice immunized intravenously with either replicating (2×10^6 PFU) or UV-inactivated (2×10^6 PFU) VSV (a, *n = 3*; b, *n = 3 – 4*, one of two experiments is shown). **(c)** VSV-neutralizing antibodies from C57BL/6 bone marrow chimeras reconstituted with CD169-DTR or wild-type (WT) cells as control, treated intraperitoneally with diphtheria toxin and infected intravenously 3 days later with 2×10^6 PFU of VSV (*n = 5 – 6,* pooled from two experiments). **(d, e)** Intracellular IFN-γ staining of splenocytes derived from WT or *Usp18*$^{-/-}$ mice infected intravenously with 2×10^6 PFU VSV and restimulated with p52 peptide **(d)** or with the VSV-derived MHC-II restricted p8 peptide **(e)**(d, *n = 5; e, n = 3;* pooled from two experiments). **(f)** Expansion of $CD4^+$ T-cells carrying a VSV-specific receptor as a transgene (L7 mice) after transfer into WT and corresponding *Usp18*$^{-/-}$ mice and intravenous infection with 2×10^6 PFU VSV 1 day later determined 3 days post infection (numbers of expanded L7 splenocytes in WT mice was set to 100 percent, *n = 4,* pooled from 2 experiments). **(g, h)** VSV-neutralizing antibodies from WT mice and *Usp18*$^{-/-}$ mice infected intravenously with 2×10^6 PFU VSV **(g)** or immunized with 2×10^8 PFU UV-inactivated VSV **(h)**(g, *n = 3 – 6;* h, *n = 7 – 8,* pooled from 3 experiments). * *p < 0.05,* ** *p < 0.01,* *** *p < 0.001*

2.7.4. *Figure 4: Defective induction of adaptive immune response leads to spread of vesicular stomatitis virus into brain*

Survival (**a**) and virus titers in brain and/or spinal cord 7-8 days post infection (**b**) determined in wild-type mice and *Usp18*$^{-/-}$ mice after intravenous infection with 2×10^6 PFU VSV (**a**, *n = 7 – 11;* **b**, *n = 4 – 5,* pooled from 3 experiments). * *p < 0.05,* ** *p < 0.01*

2.7.5. *Figure 5: Replication of VSV in the spleen protects from lethal intranasal infection*

VSV-neutralizing antibodies (**a**) and survival (**b**) of WT mice intranasally infected with 5×10^5 PFU of live VSV and injected intravenously with either 2×10^6 PFU of live VSV or 2×10^6 PFU of UV-inactivated VSV (**a**, $n = 6 – 7$; **b**, $n = 6 – 7$, pooled from 2 experiments). $*p < 0.05$, $**p < 0.01$

2.7.6. *Supplementary Figure 1: Usp18 is up-regulated in the lymph follicle during VSV infection*

Usp18 in situ hybridization of spleen sections from C57BL/6 mice after intravenous infection with 2×10^6 PFU of VSV at 0, 7 and 15 hours post infection. One of $n = 3$ representative stains is shown. Sense-control staining was negative. White dots indicate the border between red and white pulp (WP, lymph follicle). Scale bar 100 µm; scale bar of insert, 20 µm.

2.7.7. *Supplementary Figure 2: Detection of VSV in CD169$^+$ macrophages by FACS*

(a) FACS staining of splenocytes from C57BL/6 bone marrow chimeras reconstituted with CD169-DTR or wild-type bone marrow cells as control, treated intraperitoneally with diphtheria toxin (30µg/kg body weight) and infected intravenously 3 days later with 2×10^8 PFU of VSV and stained with immunofluorescence antibodies for CD169, F4/80, and CD11b 7 hours post infection (One of two stainings is shown). **(b)** FACS staining of splenocytes from C57BL/6 mice infected intravenously with 2×10^8 PFU of VSV and stained for VSV-GP, CD169 and F4/80 7 hours post infection. Shown are cells gated on CD169 or F4/80. Grey area represents isotype control. Back line shows staining with anti-VSV glycoprotein (VSV-GP). One of two representative stains is shown.

2.7.8. *Supplementary Figure 3: Visualization of micro-dissected areas*

Histology of snap-frozen tissue from spleen sections stained for CD169 and dissected using laser capture technique. Slides show tissue before microdissection, tissue after microdissection, and captured micro-dissected cells.

2.7.9. *Supplementary Figure 4: Enhanced antigen presentation of live virus in Usp18 competent dendritic cells*

(a) Immunofluorescence in spleen sections from C57BL/6 mice infected intravenously with 2×10^8 PFU and stained with antibodies for VSV glycoprotein (VSV-GP; green) and dendritic cell marker (CD11c; red) 7, 16 and 36 hours after infection. Various magnifications are shown. One of three representative slides is shown. Scale bar, 50 µm. **(b)** Proliferation of T cells in cocultures of CFSE-labeled T cells from mice carrying a VSV-specific T-cell receptor as a transgene (L7 mice) and DCs generated from WT and *Usp18*$^{-/-}$ bone marrow and incubated with live VSV (MOI 1) or with UV-inactivated VSV (MOI 100) together with IFN-α4 (50 U/mL) two hours before T cells were added, analyzed 60 hours post infection (One of 3 representative stainings is shown). **(c)** Proliferation of T cells in cocultures of CFSE-labeled purified T cells from a mouse carrying a LCMV-GP33-specific $CD8^+$ T-cell receptor as a transgene (P14 mice) and DCs generated from WT and *Usp18*$^{-/-}$ bone marrow and labeled with MHC-I restricted epitope GP33 in the presence of IFN-α4 (50 U/mL) two hours before T cells were added, analyzed 60 hours post labeling (One of 3 representative stainings is shown).

2.7.10. *Supplementary Figure 5: Lymphotoxin-β receptor is essential for replication of VSV in the spleen, for activation of adaptive immune cells and for survival of VSV infection*

(a) Immunofluorescence in spleen sections from WT and *Ltbr*$^{-/-}$ mice infected intravenously with 2×10^8 PFU and stained with antibodies for VSV glycoprotein (VSV-GP; green), CD169 (red) and B220 (blue) 7 hours after infection (One of three representative slides is shown). Scale bar, 100µm. **(b)** Virus titers from WT and *Ltbr*$^{-/-}$ mice infected intravenously with 2×10^6 PFU determined 7 hours post infection ($n = 5$, pooled from two experiments). **(c)** Intracellular IFN-γ staining of splenocytes derived from WT or *Ltbr*$^{-/-}$ mice infected intravenously with 2×10^6 PFU VSV and restimulated for 6 hours with the VSV-derived MHC-I restricted p52-peptide analyzed 7 days post infection ($n = 5$). **(d, e)** VSV-neutralizing antibodies (**d**) and survival (**e**) from WT or *Ltbr*$^{-/-}$ mice infected intravenously with 2×10^6 PFU VSV (**d**, $n = 4$ - 6,

pooled from three experiments **e**, *n = 11*, pooled from three experiments). **(f, g)** Virus titers (**f**) and immunofluorescence of brain sections stained for VSV-GP (green) and DAPI (blue) (**g**) from WT or *Ltbr*$^{-/-}$ mice infected intravenously with 2×10^6 PFU VSV 7 days after infection (**f**, *n = 4;* **g**, *n = 3;* pooled from two experiments). Scale bar, 20 μm; *$P < 0.05$, **$P < 0.01$, ***$P < 0.001$

2.8. Online Methods

2.8.1. Mice

Usp18$^{-/-}$ mice were bred heterozygously on a Sv129 × C57BL/6 background F4. *Usp18*$^{-/-}$ mice were directly compared to littermate controls. All other mice used in this study were maintained on a C57BL/6 background. During survival experiments, the health status of the mice was checked twice daily. Upon the appearance of clinical signs of VSV replication in the central nervous system (CNS), such as paralysis, mice were removed from the experiment and counted as dead. Animal experiments were carried out with the authorization of the Veterinäramt of Nordrhein Westfalen, Germany, and in accordance with the German law for animal protection, the institutional guidelines of the Ontario Cancer Institute, or both.

2.8.2. Bone marrow chimeras

For generation of bone marrow chimeras, C57BL/6 mice were irradiated with 1050 rad. After 24 hours, mice were reconstituted intravenously with 10^7 bone marrow cells. Fifteen days later, all mice were treated with 200 μL clodronate liposomes to guarantee donor-derived origin of marginal zone macrophages. Thirty-five days after reconstitution, mice were used for experiments.

2.8.3. Depletion of macrophages

For depletion of CD169$^+$ macrophages, 30 μg/kg body weight diphtheria toxin was injected into each mouse intraperitoneally (Sigma Aldrich). For depletion of complete macrophages, 200 μL clodronate liposomes were injected intravenously. Control animals were injected with empty liposomes.

2.8.4. *Generation of dendritic cells*

Bone marrow cells from C57BL/6 and *Usp18*$^{-/-}$ mice were cultured with murine GM-CSF (4 ng/ml) (Pan Biotech GmbH) for 9 days.

2.8.5. *Virus*

VSV, Indiana strain (VSV-IND, Mudd-Summers isolate), was originally obtained from Prof. D. Kolakofsky (University of Geneva, Switzerland). Virus was propagated on BHK-21 cells at a multiplicity of infection (MOI) of 0.01 and was then plaqued onto Vero cells. VSV was inactivated in UV light for 10 minutes. Peptides were derived from Polypeptide group (Strasbourg, France).

2.8.6. *Neutralizing antibody assay*

Serum was prediluted (1:40). Complement system was inactivated (56°C for 30 min). To obtain IgG kinetics, we treated diluted samples with β-mercaptoethanol (0.1 M) to remove IgM. Serum was titrated 1:2 over 12 steps and incubated with 1000 PFU of VSV. After 90 minutes of incubation, the virus-serum mixture was plaqued on Vero cells. Overlay was added after one hour. Plaques were counted 24 hours later by crystal violet staining.

2.8.7. *Histology*

Histological analyses were performed on snap-frozen tissue by using self-made anti-VSV-GP monoclonal antibody (clone Vi10). CD45R (B220) and CD90.2 were purchased from eBioscience (San Diego, CA). Red pulp macrophages were stained with F4/80 (eBiosciences) and dendritic cells with CD11c (eBiosciences). CD169 antibody was obtained from Abcam (Moma-1, Cambridge, MA), and the SIGN-R1/CD209b antibody was obtained from BMA Biomedicals (Augst, Switzerland).

2.8.8. *In situ hybridization*

For the localization of *Usp18*, mRNA was examined by using the clone pBK-CMV-mUBP43 containing the full-length murine UBP46 cDNA. 5-µm tissue sections were dewaxed and hybridized basically as described. Hybridization mixture contained either the ^{35}S-labeled RNA antisense or sense control probes obtained from full-length mUBP46 (500 ng/mL) in 10 mM Tris HCl, pH 7.4/50% (vol/vol) deionized formamide/600 mM NaCl/1 mM EDTA/0.02% polyvinylpyrrolidone/0.02% Ficoll/0.05% bovine serum albumin/10% dextrane sulfate/10 mM

dithiothreitol/denatured sonicated salmon sperm DNA at 200 µg/mL rabbit liver tRNA at 100 µg/mL. Hybridization with RNA probes proceeded at 42°C for 18 hr. Slides were then washed as described followed by 1 hr at 55°C in 2× standard saline citrate. Non-hybridized single-stranded RNA probes were digested by RNase A (20 µg/mL) in 10 mM Tris HCl, pH 8.0/0.5 M NaCl for 30 min at 37°C. Tissue slide preparations were autoradiographed for 3 weeks and stained with hematoxylin/eosin.

2.8.9. *Laser capture microdissection (LCM)*

Frozen tissue sections (10 µm thick) were cut under RNase-free conditions. On the day of microdissection, the sections were either stained for CD169-biotin and streptavidin-peroxidase or with the HistoGene Frozen Section Staining Kit (Applied Biosystems, Darmstadt, Germany) according to the manufacturer`s protocol. For dehydration, slides were placed consecutively in 75%, 95%, and 100% ethanol for 30 s and then in Xylene for 5 min. After the dehydration procedure, the sections were air-dried for 12 min. Samples of spleen tissue were captured from the stained slides on Capsure HS LCM caps by using a PixCell II laser capture microscope (Applied Biosystems) with the laser pulse power set at 75 mW and a threshold voltage of 200 mV.

2.8.10. *Total RNA extraction, cDNA synthesis, and quantitative real-time polymerase chain reaction (qRT-PCR)*

Total RNA was extracted from cells on the caps with the PicoPure RNA isolation kit (Arcturus, Applied Biosystems) according to the manufacturer's protocol. The RNA of the sorted cells was isolated with the RNA Mini Kit (Qiagen, Hilden, Germany). The RNA was reverse-transcribed to cDNA with the Quantitect Reverse Transcription kit (Qiagen, Hilden, Germany). Gene expression analysis *Gapdh, Usp18* was used from Applied Biosystems. Expression levels were normalized against *Gapdh* and compared between study groups.

2.8.11. *Flow cytometry*

Lymphocytes were stained with anti-CD8, anti-CD4, and anti-IFN-γ (BD Biosciences, San Jose, CA) after six hours of restimulation with VSV antigen p8-peptide or p52-peptide. For staining of $CD169^{+}$ macrophages, 36 µg anti-CD169-biotin (Abcam) was injected intravenously. After 15 min, spleens were digested with

Liberase and DNAse. $CD169^+$ macrophages were stained with streptavidin-PE (eBiosciences) in combination with CD11b or F4/80 (eBiosciences).

2.8.12. *Sorting of macrophages and T cells*

We injected 36 µg anti-CD169-biotin (Abcam) into C57BL/6 mice. After 10 min, splenocytes were digested with Liberase DNAse (Roche, Basel, Switzerland) and stained with anti-biotin microbeads (Miltenyi, Bergisch Gladbach, Germany) and streptavidin-PE (eBiosciences, San Diego, CA) or with F4/80-PE (eBiosciences) and anti-PE microbeads (Miltenyi). After 30 min incubation, splenocytes were sorted by MACS. $CD169^+$ cells were additionally sorted by FACS. T cells were sorted by using the MACS untouched kit.

2.8.13. *Transfection with Usp18 plasmid*

For transcription of *Usp18*, the construct pcDNA3-hUSP18 (Burkart et al, manuscript submitted) was used. 10^6 HeLa cells were transfected using Superfect-Kit (Qiagen, Hilden, Germany) with 4 µg DNA derived from *Usp18*-expressing plasmid and empty vector at different ratios. IFN-α2 was derived from RDI.

2.8.14. *Statistical analysis*

Data are expressed as means ± S.E.M. Student's *t*-test was used to detect statistically significant differences between two groups. The level of statistical significance was set at $P < 0.05$

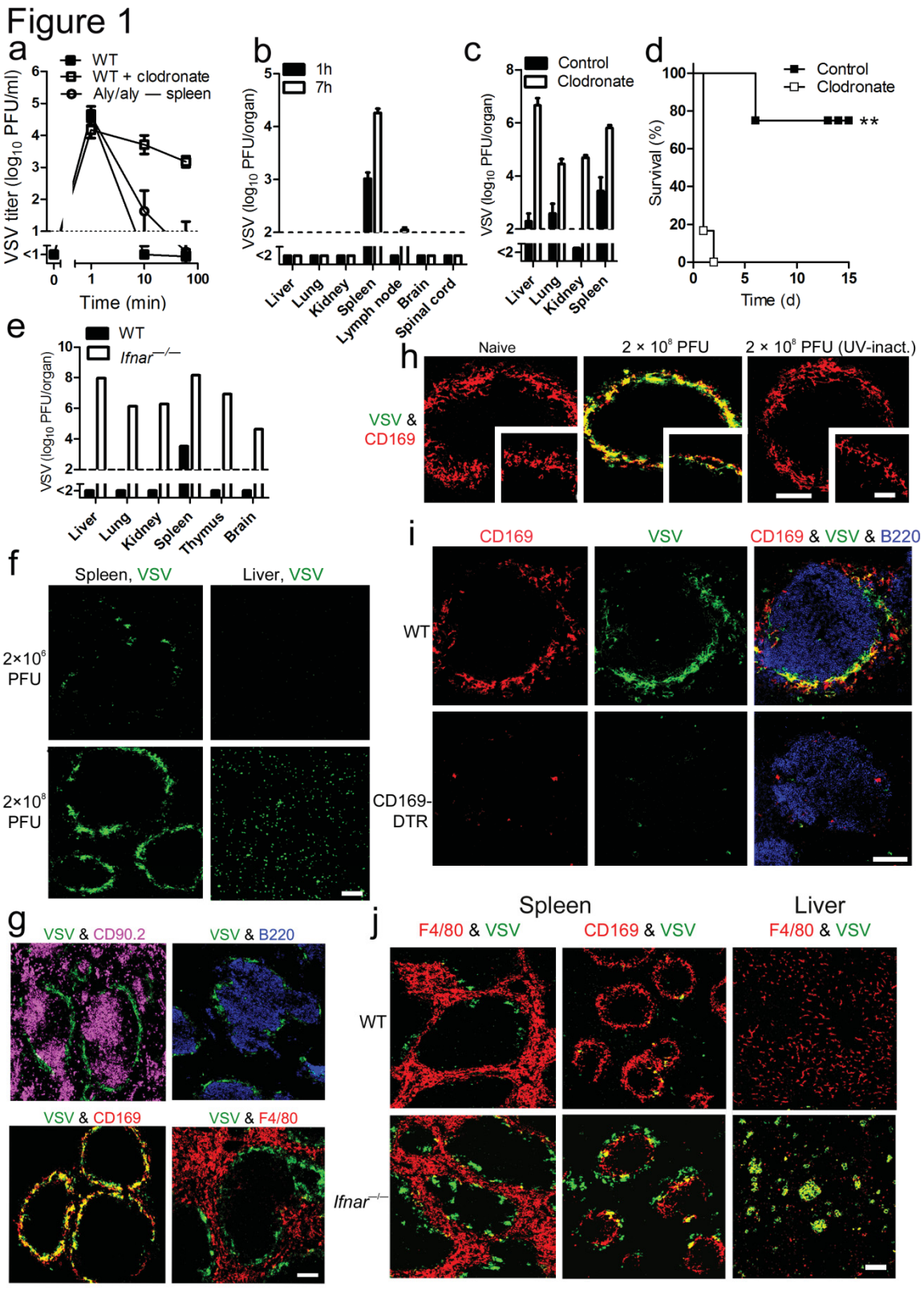

Figure 2-1 CD169^{+} metallophilic macrophages allow viral replication in the spleen, but red pulp macrophages and Kupffer cells do not.

Figure 2

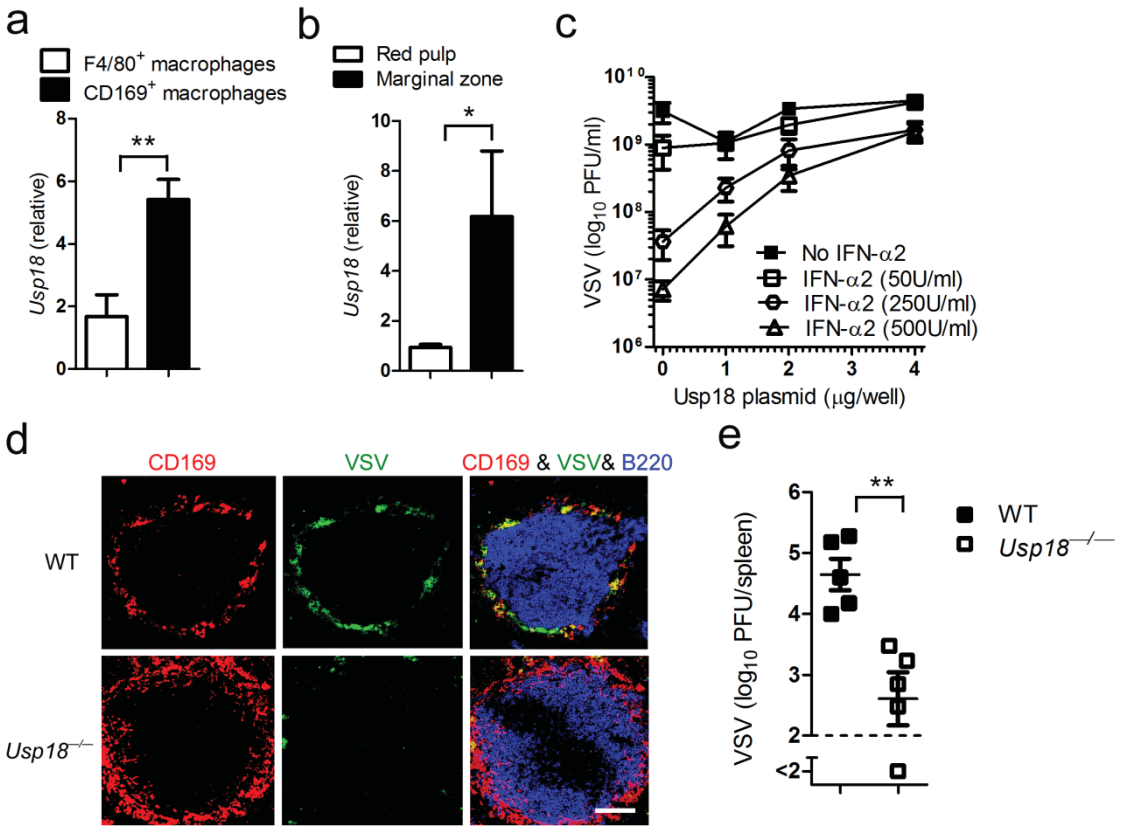

Figure 2-2 Expression of *Usp18* in CD169$^+$ cells in responsible for enhanced viral replication

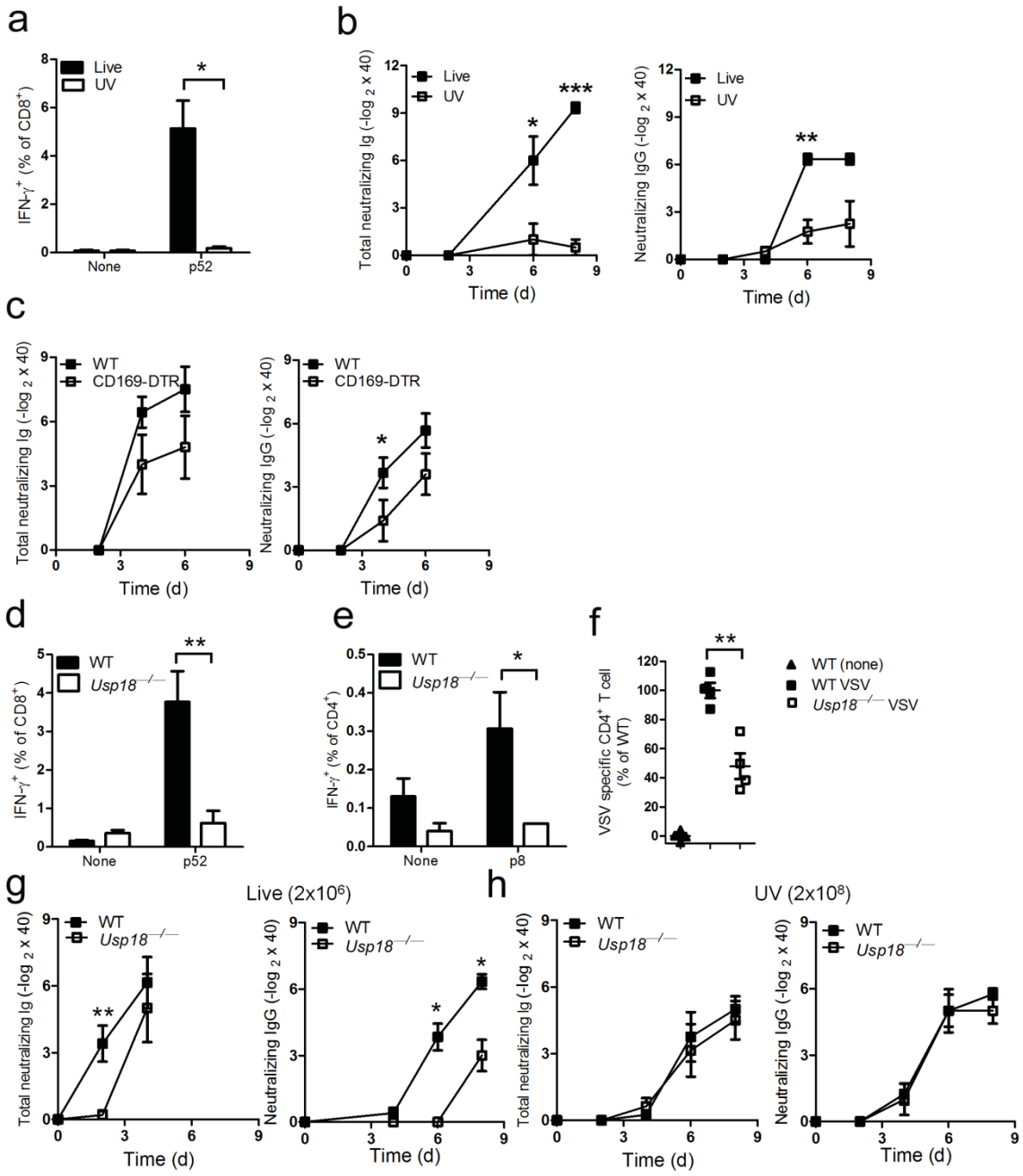

Figure 2-3 VSV replication in the spleen is required for efficient T cell and B cell responses

Figure 4

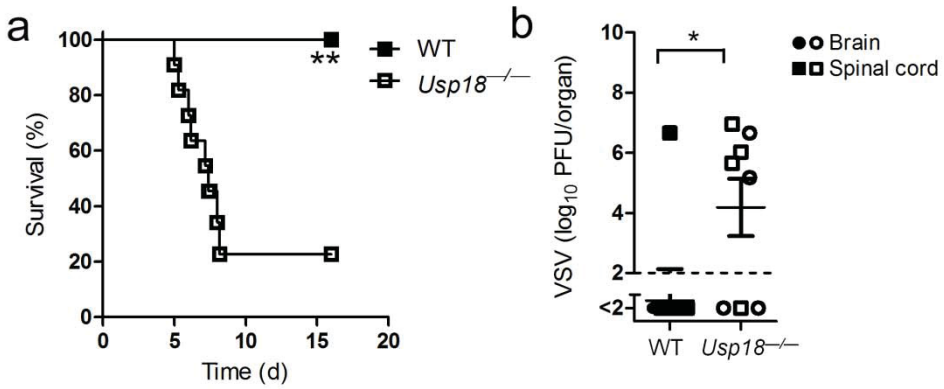

Figure 2-4 Defective induction of adaptive immune response leads to the spread of VSV into the brain

Figure 5

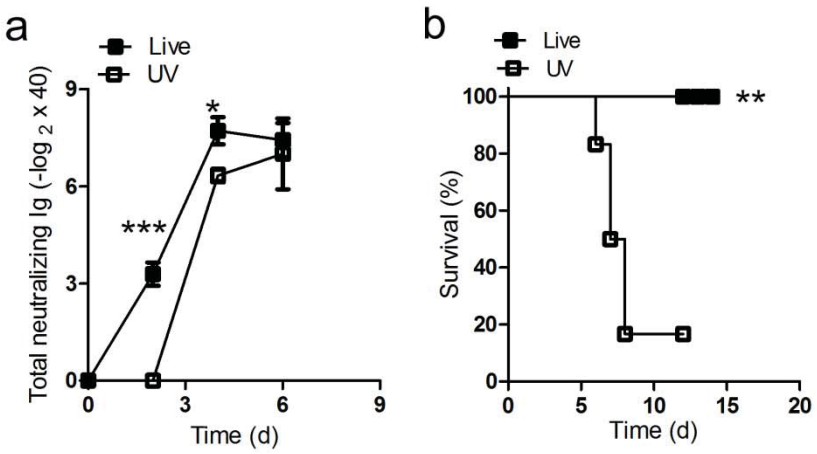

Figure 2-5 Replication of VSV in the spleen protects mice from lethal intranasal infection

Supplementary Figure 1

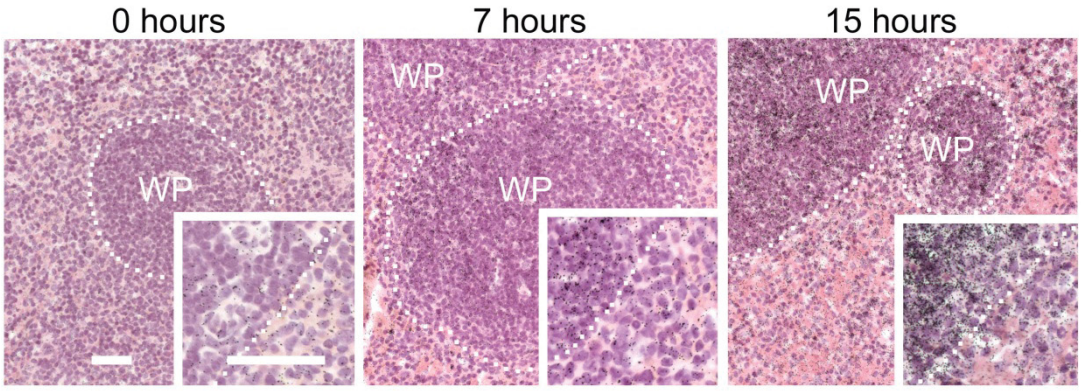

Supplementary Figure 2-1 *Usp18* is up-regulated in the lymph follicle during VSV infection

Supplementary Figure 2

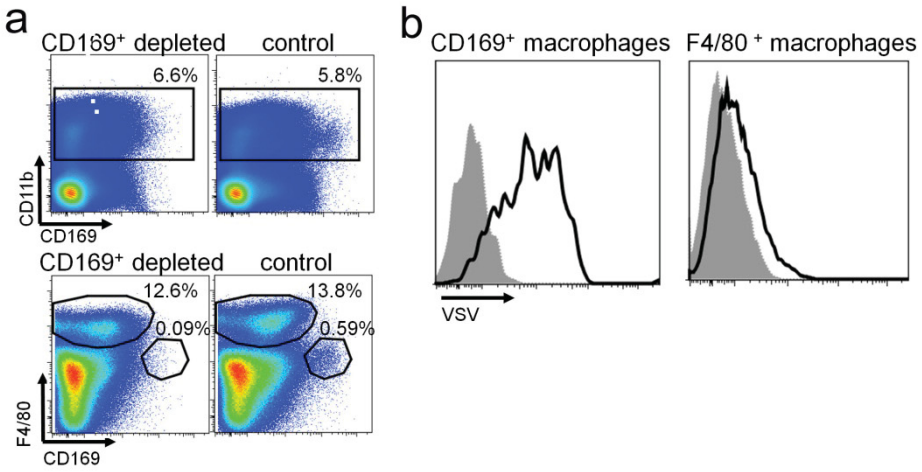

Supplementary Figure 2-2 Detection of VSV in CD169^{+} macrophages by FACS

Supplementary Figure 3

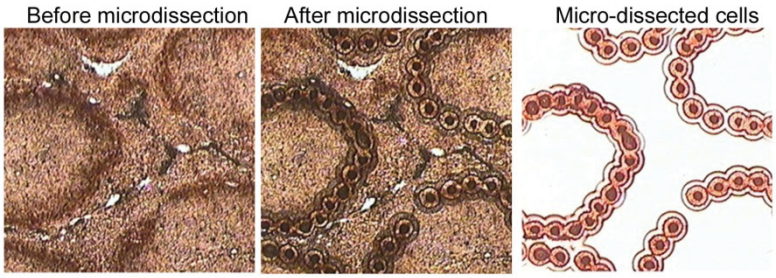

Supplementary Figure 2-3 Visualization of micro-dissected areas

Supplementary Figure 4

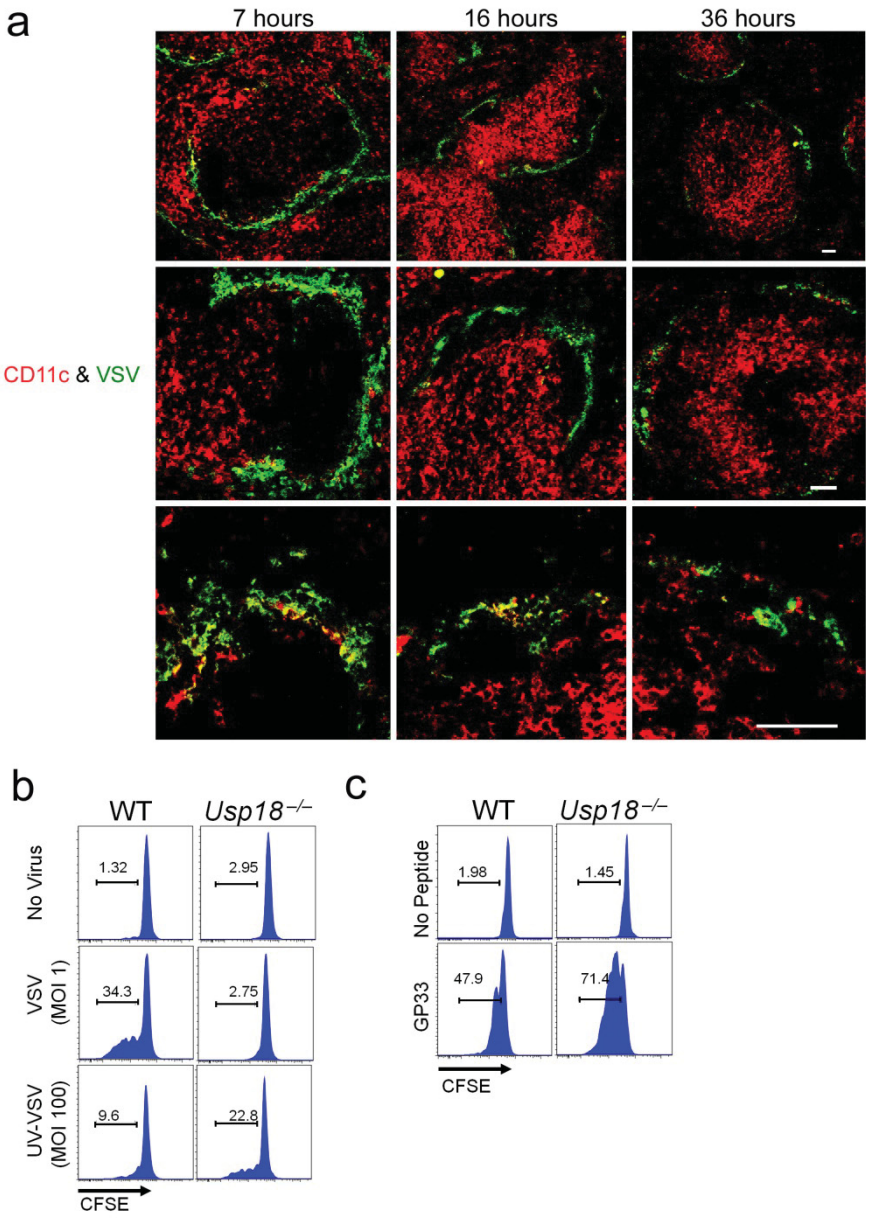

Supplementary Figure 2-4 Enhanced antigen presentation of live virus in *Usp18* competent dendritic cells

Supplementary Figure 5

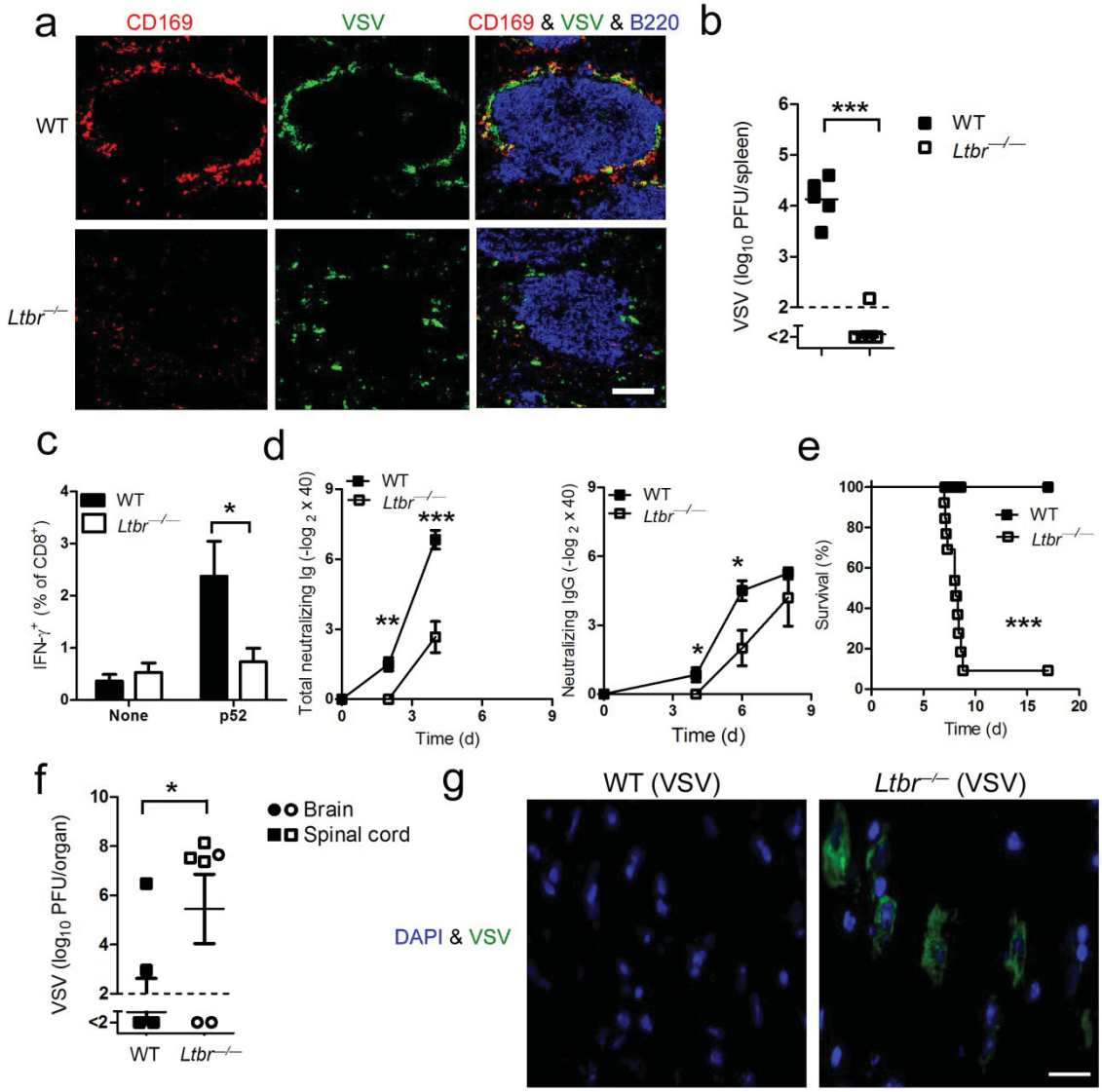

Supplementary Figure 2-5 Lymphotoxin-β receptor is essential for replication of VSV in the spleen, for activation of adaptive immune cells and for survival of VSV infection

Anteilserklärung

1. Publikation:

Honke N, Shaabani N, Cadeddu G, Sorg UR, Zhang DE, Trilling M, Klingel K, Sauter M, Kandolf R, Gailus N, van Rooijen N, Burkart C, Baldus SE, Grusdat M, Löhning M, Hengel H, Pfeffer K, Tanaka M, Häussinger D, Recher M, Lang PA, Lang KS

Enforced viral replication activates adaptive immunity and is essential for the control of a cytopathic virus.

Nat Immunol 2012; 13(1):51-7

Name des Journals:	*Nature Immunology*
Impact factor (Stand 2013):	26,199
Anteil an Experimenten in dieser Arbeit (%):	20 %
Autor:	Co-Autor
Beitrag an dieser Arbeit:	Herr Namir Shaabani führte einen großen Teil der praktischen Experimente und Auswertungen der Versuche durch. Außerdem war er am experimentellen Design beteiligt.

Namir Shaabani

Prof. Dr. Karl Lang

3. Chapter III: Usp18 driven enforced virus replication in dendritic cells contributes to break of immunological tolerance in autoimmune diabetes

Nadine Honke*, Namir Shaabani*, Dong-Er Zhang, George Iliakis, Haifeng C Xu, Dieter Häussinger, Mike Recher, Max Löhning, Philipp A. Lang* and Karl S. Lang*

3.1. Abstract:

Infection with viruses carrying cross-reactive antigens is associated with break of immunological tolerance and induction of autoimmune disease. Dendritic cells play an important role in this process. However, it remains unclear why autoimmune-tolerance is broken during virus infection, but usually not during exposure to non-replicating cross-reactive antigens.

Here we show that antigen derived from replicating virus but not from non-replicating sources undergoes a multiplication process in dendritic cells in spleen and lymph nodes. This enforced viral replication was dependent on *Usp18* and was essential for expansion of autoreactive $CD8^+$ T cells. Preventing enforced viral replication by depletion of $CD11c^+$ cells, genetically deleting *Usp18*, or pharmacologically inhibiting of viral replication blunted the expansion of autoreactive $CD8^+$ T cells and prevented autoimmune diabetes. In conclusion, *Usp18*-driven enforced viral replication in dendritic cells can break immunological tolerance and critically influences induction of autoimmunity.

3.2. Author summary

Autoimmune diabetes in humans is linked to viral infection, which carry cross-reactive antigens. Virus derived cross-reactive antigens break immunological tolerance to pancreatic islets, which initiates disease. Several other none-viral sources of cross-reactive antigens are known, however they usually fail to induce diabetes. Here we found that viral antigen underwent an *Usp18* dependent replication in dendritic cells. This mechanism was essential to generate sufficient amount and quality of cross-reactive antigen and to expand auto-reactive $CD8^+$ T cells. Blocking of virus replication by either depletion of dendritic cells, genetic depletion of *Usp18* or pharmacological inhibition of replication blunted expansion of auto-reactive $CD8^+$ T cells and prevented diabetes. In conclusion we found that enforced virus replication broke the tolerance to self-antigen, which partially explains the strong association of autoimmune diseases with virus infections.

3.3. Introduction

Autoimmune diabetes in humans is characterized by immunological destruction of beta islet cells in the pancreas; this cellular destruction leads to hyperglycemia [103]. T cells specific for beta islet cell antigens play an important role in the development of the disease and have been found to arise after exposure to viruses that contain cross-reactive epitopes [104-106]. Viruses known to contain cross-reactive epitopes are enterovirus, rubella virus, and rotavirus. Infection with these viruses are often found during the onset of diabetes [107-109]. Recent evidence of the ability of viruses to induce diabetes comes from epidemiological and genetic analyses, which have shown that functional polymorphisms in interferon-regulating genes are strongly associated with autoimmune diabetes [110-112]. Thus, viral infection is associated with the onset of autoimmune diabetes in humans, and molecular mimicry is an obvious explanation for the immunological destruction of pancreatic beta cells. Besides viruses, several other pathogens and environmental proteins, such as bovine serum albumin (BSA) and beta-casein, carry cross-reactive epitopes to beta islet cells [113-115]. Because both substances are found in cow milk, many people are exposed to those antigens. However, this exposure is not strongly linked to the induction of autoreactive T cells or to the occurrence of autoimmune diabetes [116,117]. Several bacterial species (e.g. Escherichia coli, Pseudomonas species, and Campylobacter) are known to carry epitopes that are cross-reactive to beta islet cells [118,119]. Although infection with these opportunistic pathogens will lead to presentation of cross-reactive beta islet antigens in combination with high amounts of bacterial Toll-like receptor (TLR) ligands, the contribution of these bacteria to the incidence of diabetes remains uncertain [120]. Thus, cross-reactive viruses, but not other exposures to cross-reactive antigens, are very efficient in breaking immunologic tolerance.

During the onset of autoimmune diabetes, antigen presenting cells (APCs) in secondary lymphoid organs (SLO) are key players in regulating immunologic tolerance and immune activation [103]. With their ability to express costimulatory molecules, APCs like dendritic cells (DCs) or macrophages efficiently prime antigen-specific $CD8^+$ T cells [103,121]. DCs express costimulatory molecules after antigen uptake in combination with pattern recognition receptor ligation. Therefore activation of pattern recognition receptors by pathogen-derived patterns is an important mechanism by which DCs can differentiate between self-antigen and foreign antigen.

In addition to costimulatory molecules, the amount of antigen presented is important in determining whether tolerance induction or immune activation will occur [75,76]. A low amount of presented antigen on DCs induces immunological tolerance against this antigen, even if it is presented in parallel with costimulatory signals [122,123]. In contrast, DCs loaded with high amounts of antigen may induce immune activation even in the absence of costimulatory molecule expression [122,124,125]. Thus, the amount of presented antigen is another independent factor that determines tolerance induction or immune activation. We recently reported that $CD169^+$ macrophages enforce virus replication, which enhances adaptive immune response [126]. If dendritic cells participate in antigen amplification and how this affects immunological tolerance remains unknown. To examine the importance of enforced viral replication in the context of autoimmune diabetes, we studied the induction of autoimmune diabetes in the RIP-GP mouse model [41]. In this model the glycoprotein (GP) of lymphocytic choriomeningitis virus (LCMV) is expressed as a transgene under the control of the rat insulin promoter (RIP). Following LCMV infection, LCMV-GP specific $CD8^+$ T cells are primed and destroy the LCMV-GP expressing insulin producing pancreatic islet cells leading to autoimmune diabetes.

3.4. Results

3.4.1. *Depletion of dendritic cells blunted early virus replication and prevented autoimmune diabetes.*

To analyze the contribution of dendritic cells in LCMV replication, we used CD11c-DTR mice. Treatment of CD11c-DTR mice with diphtheria toxin depletes dendritic cells [46]. Lack of dendritic cells completely blunted early LCMV replication in spleen and lymph nodes (Figure 1A). Reduced LCMV replication in the $CD11c^+$ compartment impaired viral antigen expressed within the spleen as assessed by immune-histology (Figure 1B). This reduction of replicating antigen in the spleen correlated with the lack of induced interferon-alpha (Figure 1C). Subsequently, the LCMV-specific $CD8^+$ T cell response against LCMV-GP was blunted in the absence of dendritic cells (Figure 1D) and CD8+ T cell-mediated autoimmune diabetes was prevented (Figure 1E). In the absence of DCs virus could not be controlled and persisted in the blood (Figure 1F). This secondary virus propagation was most likely due to the lack of innate and adaptive immune response [127,128].

3.4.2. *Pharmacologic reduction of viral replication inhibits onset of autoimmune diabetes.*

Besides enhancing early LCMV replication, dendritic cells are known to initiate the immune response by potent expression of co-stimulatory molecules (Figure S1). To see whether virus replication, and not other dendritic cell functions were essential to initiate autoimmune diabetes we treated mice with the anti-viral drug Ribavirin, which can efficiently suppress LCMV replication [129]. Indeed Ribavirin treatment was associated with significantly suppressed early LCMV replication (Figure 2A). In line with that innate antiviral IFN-α production was reduced in Ribavirin treated mice (Figure 2B). Reduced early virus replication blunted LCMV-specific $CD8^+$ T cell priming and prevented onset of diabetes (Figure 2C and D).These data imply that indeed early virus replication in dendritic cells is essential to break immunological tolerance.

3.4.3. *Expression of* Usp18 *in dendritic cells contributes to early virus replication and onset of diabetes.*

We found that LCMV replicated in dendritic cells in spleen and lymph nodes. In other organs no virus replication was detected, due to suppression of virus replication by IFN-I (Figure 3A). Therefore we wondered whether expression of endogenous inhibitors of IFN-I signaling in dendritic cells contributed to LCMV replication in dendritic cells. *Usp18* (UBP43) binds to the Jak1 binding site of the type I interferon receptor and inhibits its phosphorylation [31]. Therefore *Usp*18 is a very efficient IFN-I inhibitor. First we analyzed expression of UBP43 in dendritic cells. Naïve dendritic cells, but not bone marrow–derived macrophages or fibroblasts, exhibited high expression of UBP43 (Figure 3B). Absence of UBP43 in *Usp18*$^{-/-}$ mice [30] reduced LCMV replication in DCs in vitro (Figure 3C) and was associated with reduced LCMV replication in spleen and lymph nodes in vivo (Figure 3D). These findings demonstrate that LCMV replication is enforced in dendritic cells as a consequence of *Usp*18 expression. To test the role of *Usp18* in priming virus specific $CD8^+$ T cells we infected WT and *Usp18*$^{-/-}$ mice with 200PFU LCMV. The absence of *Usp18* strongly impaired expansion of antiviral CD8+ T-cells in the spleen till day 7 (Figure 3E).

Reduced frequencies of virus specific CD8+ T cells was in line with reduced numbers of IFN-γ producing $CD8^+$ T cells after restimulation (Figure 3F). In the blood *Usp18*$^{-/-}$ mice showed limited frequencies of virus-specific $CD8^+$ T cells (Figure 3G). Although CD8+ T cells were reduced virus could be controlled in *Usp18*$^{-/-}$ mice (Figure S2). Next we generated bone marrow chimeras by transferring *Usp18*$^{-/-}$ bone marrow into irradiated RIP-GP mice to analyze the role of *Usp18* on virus induced auto-reactive $CD8^+$ T cells. Lack of *Usp18* on bone marrow derived cells blunted auto-reactive $CD8^+$ T cell response (Figure 3H). To underline the role of *Usp18* in CD11c expressing cells we generated mixed bone marrow chimeras by using *Usp18*$^{-/-}$ bone marrow mixed 1:1 with bone marrow from CD11c-DTR mice in C57BL/6 wild-type mice. Diphtheria toxin treatment of these chimeric mice will deplete *Usp18*-competent DCs derived from CD11c-DTR mice but not *Usp18*-deficient DCs. Control mice were given a 1:1 mixture of WT and CD11c-DTR bone marrow. Thirty days later, mice were treated with diphtheria toxin. After infecting these mice with LCMV we observed reduced expansion of islet-specific $CD8^+$ T cells, implying that *Usp18* affects virus replication in DCs intrinsically (Figure 3I). Next we infected irradiated RIP-GP mice that had been reconstituted with bone marrow from *Usp18*$^{-/-}$ or WT mice with LCMV. The absence of auto-reactive $CD8^+$ T cells in *Usp18* deficient mice reduced the incidence of autoimmune diabetes, although mice still could control LCMV infection (Figure 3J). In conclusion, lack of *Usp18* in $CD11c^+$ cells reduced priming of islet-specific $CD8^+$ T cells and prevented induction of diabetes.

3.4.4. *Only replicating autoantigen is efficient in inducing autoimmune diabetes*

We speculated that infection with replicating virus might be associated with the production of much higher amounts of autoantigen than treatment with soluble autoantigen. Western blot analysis showed that the initial virus inoculate did not contain measurable LCMV-GP as assessed by western blotting while 0.1µg purified glycoprotein (GP) was clearly detectable (Figure 4A). In contrast, LCMV-GP was detected in increasing amounts in spleen lysates for up to 7 days following LCMV infection (Figure 4A). In contrast, immunization with 2µg soluble LCMV-GP was associated with detectable LCMV-GP in the spleen for only 24 hours (Figure 4A). This finding indicated that the amount of antigen expressed in the spleen correlates

with active replication of LCMV. Infecting RIP-GP mice with LCMV led to expansion of LCMV-specific $CD8^+$ T cells associated with induction of autoimmune diabetes to 100% of the mice, as demonstrated by elevated serum glucose concentrations (Figure 4B) [41]. To compare the immunogenicity of replicating virus with soluble antigen, we immunized RIP-GP mice with soluble LCMV-glycoprotein (LCMV-GP) together with the TLR ligand polyinosinic-polycytidylic acid (poly I:C) at concentrations known to induce potent innate immune responses [44]. In contrast to replicating virus, soluble LCMV-GP failed to induce measurable numbers of GP33-specific $CD8^+$ T cells in peripheral blood, and diabetes was not induced (Figure 4C). Transferring CFSE-labeled LCMV-specific transgenic $CD8^+$ T cells (derived from P14 mice [43]) into mice immunized with soluble LCMV-GP and poly I:C revealed that nonreplicating LCMV-GP induced detectable but limited $CD8^+$ T cell proliferation in vivo (Figure 4D). To determine whether self-antigen released during the damage of beta islet cells in conjunction with poly I:C treatment could activate LCMV-specific $CD8^+$ T cells, we treated RIP-GP mice with Streptozotocin, which is directly toxic to beta islet cells [130]. Streptozotocin treatment in combination with poly I:C as a innate immune activator induced diabetes in RIP-GP mice (Figure 4E). However, induction of diabetes was most likely due to the direct toxic effects of Streptozotocin, since GP33-specific $CD8^+$ T cells were not detected in peripheral blood after Streptozotocin treatment (Figure 4E). To analyze the ability of the released LCMV-GP in this experimental setting to activate autoreactive $CD8^+$ T cells, we transferred CFSE labeled GP33-specific $CD8^+$ T cells into RIP-GP mice and then treated them with Streptozotocin plus poly I:C. CFSE-labeled LCMV-specific $CD8^+$ T cells showed detectable but limited proliferation (Figure 4F). This finding suggested that even massive destruction of pancreatic islet cells was not sufficient to break the immunological tolerance of GP33-specific $CD8^+$ T cells even in the presence of an inflammatory environment induced by poly I:C treatment. Next, we administered RIP-GP mouse–derived pancreatic homogenates to naïve RIP-GP mice, again in combination with poly I:C to stimulate innate immunity. This treatment led to very limited expansion of GP33-specific $CD8^+$ T cells and was not associated with induction of autoimmune diabetes (Figure 4G). Similarly, administration of liver homogenates derived from DEE mice [131] which express the LCMV-GP under the actin promoter in combination with poly I:C to RIP-GP mice only led to limited expansion of LCMV-specific $CD8^+$ T cells and did not induce autoimmune diabetes

(Figure 4H). Autoimmune diabetes was also not induced in RIP-GP mice infected with listeria expressing the glycoprotein of LCMV (Listeria-GP) again correlated with limited expansion of LCMV-specific $CD8^+$ T cells (Figure 4I). In summary, we found that non- or poorly-replicating antigen, even in combination with innate immune activation, is very inefficient in inducing the priming of autoantigen-specific $CD8^+$ T cells. Only virus infection, supported by the *Usp18* driven enforced replication process in $CD11c^+$ APCs is efficient in breaking immunologic tolerance to pancreatic islet cells in our model.

3.4.5. *Lack of early virus replication limits break of tolerance in RIP-NP diabetes model*

The LCMV RIP-GP model is a model of acute onset of diabetes. The concurrent activation of the adaptive and innate immune response is essential to induce diabetes in this model [44]. In humans diabetes is often induced over a long period of time or in two or more events [132]. We found that enforced virus replication is activating both innate and adaptive immune response. Therefore it remains questionable if early virus replication can impact on diabetes in a model which is almost independent of innate immune activation. To get insights we infected RIP-NP mice with 200 PFU LCMV-WE. RIP-NP mice show partial expression of LCMV-NP in the thymus and therefore typically show a delayed onset of diabetes [42,133]. Similar to our previous results, induction of antiviral LCMV-GP-specific $CD8^+$ T cells was reduced by Ribavirin treatment in the RIP-NP mice (Figure 5). Induction of auto-reactive LCMV-NP-specific $CD8^+$ T cells was in addition limited in the absence of enforced virus replication (Figure 5). In line with these results mice treated with Ribavirin showed enhanced beta islet function compared to than control mice (Figure 5).

3.5. Discussion

In this study we examined why replicating self-antigen is much more efficient in breaking autoimmune tolerance than the exposure to non-replicating self-antigen. Our findings emphasize that the development of autoimmune diabetes requires active autoantigen replication in specialized APCs that are characterized by the expression of *Usp18*, a known inhibitor of type I interferon signaling [31]. Since *Usp18* expressing

APCs are not responsive to the antiviral actions of type I interferons, they act as endogenous "replicators" of auto-antigen.

Recently we found that expression of *Usp18* in $CD169^+$ macrophages is important for initiating neutralizing antibodies against vesicular stomatitis virus [126]. In light of our data here we suggest that this mechanism is also of importance in dendritic cells for initiating innate and adaptive immune response against LCMV. In addition to LCMV replication, high expression of *Usp18* in DCs could explain the long-known phenomenon that DCs can be easily infected with several viruses [134]. Administration of autoantigen in various non-replicating forms only led to very limited activation and expansion of autoimmune $CD8^+$ T cells, suggesting that the mechanism of enforced virus replication could be an essential factor allowing the immune system to differentiate between foreign and self-antigen.

In addition to (auto)antigen amplification, *Usp18* may have other functions in DCs. Indeed, lack of *Usp18* expression reduces the number of $CD11b^+$ dendritic cells by 50% [135]. We found that after treatment with poly I:C, expression of MHC I and the costimulatory molecule CD80 was enhanced in $Usp18^{-/-}$ DCs compared to WT DCs (data not shown), implying that there is no general activation defect in *Usp18*-deficient DCs. In fact, the absence of IFN signaling (as in WT DCs), rather than enhanced interferon signaling (as in $Usp18^{-/-}$ DCs), impairs DC functions such as proteasomal degradation, cross-priming [90,136], and costimulation [91]. Therefore, we hypothesize that lack of antigen amplification is the major defect in $Usp18^{-/-}$ DCs.

Immunohistological costainings revealed that LCMV replicates in the spleen mainly in $CD169^+$ macrophages and $CD11c^+$ cells (data not shown). Depletion of both cell types in CD11c-DTR mice completely blunted early LCMV replication in the spleen, while depletion of $CD169^+$ macrophages in CD169-DTR mice showed no reduction in early LCMV titers (data not shown). This suggests that contribution of LCMV replication in $CD169^+$ macrophages to total splenic LCMV replication is minor.

The results of several studies suggest that viral infection may be linked to the onset of human autoimmune diabetes. Using mouse models, we and others have demonstrated that this association can be explained by the activation of pattern recognition receptors during disease onset [44,137]. Especially IFN-I enhances antigen presentation and

induces an inflammatory status in beta islet cells [44]. Recent genetic analyses have indeed found that genes regulating the interferon response are important contributors to onset of diabetes [110,111,138,139]. In particular, enhancement of the activity of the pattern recognition receptor RIG I is linked to a high risk of diabetes onset [138]. Therefore enhanced activity of *Usp18* in beta islet cells would limit IFN-I signaling in these cells and could prevent diabetes during exposure to IFN-I [140]. We found here that lack of *Usp18* in dendritic cells prevented enforced virus replication and would therefore limit induction of auto-reactive $CD8^+$ T cells, but also induction of IFN-I production. Therefore we would suggest that *Usp18* expression in dendritic cells could drive autoimmune diabetes by promoting activation of cross-reactive $CD8^+$ T cells, but also by induction of high levels of IFN-I. Whether indeed the expression of interferon inhibitors such as *Usp18* in certain cell types contributes to the risk of human diabetes remains to be tested.

It still remains to be explained how bacteria, that express cross-reactive antigen might contribute to autoimmune diabetes induction. In humans there is no clear link between certain bacterial infection and onset of diabetes [120]. We found, using recombinant LCMV-GP33 expressing facultative intracellular Listeria monocytogenes that indeed low doses of systemic bacterial infection did not induce diabetes in RIP-GP mice. While this suggests that amplification of virus antigen was more efficient to break immunological tolerance, the contribution of intracellular bacterial amplification to the overall autoimmune activation remains to be studied.

We demonstrate here a *Usp18* driven mechanism which allows replicating virus, but not non-replicating autoantigen to break immunologic tolerance. Blocking *Usp18* may be a potential target for pharmacological interference in the early pathogenic steps leading to the induction of autoimmune diabetes in humans.

3.6. Methods

3.6.1. Mice:

All experiments were performed with the animals housed in single ventilated cages, with the authorization of Veterinäramt Nordrhein Westfalen (Düsseldorf, Germany), and in accordance with the German law for animal protection. Project was licensed under identification number (84-02.04.2011, A246). Rat insulin promoter-glycoprotein (RIP-GP) or promoter-nucleoprotein (RIP-NP) mice [41,42], which express the LCMV glycoprotein or LCMV nucleoprotein respectively as a transgene under the rat insulin promoter, were used for the analysis of autoimmune diabetes and were maintained on a C57BL/6 background. P14 mice expressing a LCMV-GP33-41 specific TCR as a transgene were used for adoptive transfer experiments and were also maintained on a C57BL/6 background [43]. Mice expressing CD45.1 were used to track cells in adoptive transfer experiments. DEE mice express LCMV-GP under the actin promoter [131]. *Ifnar*$^{-/-}$ mice [44] and CD11c-DTR mice [46,47] were maintained on C57BL/6 background. *Usp18*$^{-/-}$ mice were generated in the Zhang lab and bred heterozygously on a Sv129 × C57BL/6 background F4 and directly compared with littermate control animals.

3.6.2. Lymphocyte transfer

Splenocytes from P14 mice expressing CD45.1 were labeled with carboxyfluorescein succinimidyl ester (CFSE, 1µM, Invitrogen) and were injected intravenously into RIP-GP or C57BL/6 mice. One day later, mice were infected with LCMV-WE (200 PFU or 2×106 PFU) or with purified LCMV glycoprotein or were treated with Streptozotocin (5 mg). Five days after LCMV infection, the proliferation of P14 T cells was assessed in the spleen by CFSE dilution and flow cytometry.

3.6.3. Bone marrow chimeras

For the generation of bone marrow chimeras, recipient mice were irradiated with 9.5 Gy (320 kV X-rays, 3 Gy/min, 0.35 mm copper + 1.5 mm aluminium filter; Pantak-Seifert, Ahrensburg, Germany) on day -1. On the next day, 10^7 bone marrow cells were transferred. After 15 days Clodronate-Liposomes were administered to ensure macrophages exchange in *Usp18*$^{-/-}$>RIP-GP, WT>RIP-GP, CD11c-DTR>RIP-GP, WT>RIP-GP, WT/CD11c-DTR>WT and *Usp18*$^{-/-}$/CD11c-DTR>WT chimeras. Infections with LCMV were performed after 30 days.

3.6.4. *Cell culture, generation of murine primary cells:*

To generate primary macrophages, we isolated bone marrow from femurs and tibias of mice and eliminated erythrocytes. Bone marrow cells were cultured in very low endotoxin Dulbecco's Modified Eagle Medium (VLE-DMEM) supplemented with 10% (v/v) fetal calf serum (FCS) and 0.1% (v/v) ß-mercaptoethanol (ß-ME) and 20% (v/v) macrophage colony-stimulating factor (M-CSF). On day 9 or 10 of differentiation, cells were harvested for use in subsequent experiments. To generate primary fibroblasts, we removed the lungs of mice and digested them with DNase and Liberase for 60 min at 37°C. After being flushed through a strainer, cells were cultivated in DMEM supplemented with 10% (v/v) FCS and penicillin-streptomycin glutamine (PSG). On day 3, adherent cells were rinsed with fresh growth medium. After 3 more days of cultivation, differentiated fibroblasts were split. On day 10, fibroblasts were used for experiments. To generate conventional dendritic cells (cDCs) we isolated bone marrow taken from femurs and tibias of mice. Erythrocytes were eliminated. We cultured bone marrow cells in very low endotoxin Dulbecco's Modified Eagle Medium (VLE-DMEM) supplemented with 10% fetal calf serum (FCS) and 0.1 % ß-mercaptoethanol (ß-ME) in the presence of granulocyte macrophage colony-stimulating factor (GM-CSF). On day 3 of differentiation, an equal volume of growth medium was added. Growth medium was exchanged on day 6 of differentiation. On day 9 or 10 of differentiation, cells were harvested for use in subsequent experiments.

3.6.5. *Virus and plaque assay*

LCMV strain WE was originally obtained from F. Lehmann-Grube (Heinrich Pette Institute, Hamburg, Germany) and was propagated in L929 cells. Mice were infected intravenously with LCMV at the indicated doses. Viral titers were measured in a plaque-forming assay using MC57 cells as previously described [128].

3.6.6. *Bacteria*

Listeria monocytogenes (L.m.) expressing the LCMV-GP33 as transgen was grown overnight in brain–heart infusion broth or thawed from frozen aliquots, washed two times in phosphate-buffered saline (PBS), and injected intravenously in 200 µl into the tail vein. 10^3-CFU of *L.m.* intravenously was used as low-dose infection.

3.6.7. *Pharmaceutical compounds*

Ribavirin (Essexpharma, Belgium) was administered intraperitoneally (5 mg daily) starting on day -3 before LCMV infection. Streptozotocin was administrated (5 mg) intraperitoneally once on day 0. Twelve hours later, 400 µL of glucose solution (20% in PBS) was injected intraperitoneally to prevent severe hypoglycemia. Diphtheria toxin was injected intraperitoneally at a dose of 30 µg/kg or 10 µg/kg as indicated. For immune activation, 100 µg poly (I:C) (Amersham) was given intravenously per mouse.

3.6.8. *Immunization with LCMV-GP*

HEK-GP cells, which express the LCMV glycoprotein (GP), were cultured in 40 mL DMEM + 10% FCS and Hygromycin B (300 µg/mL) in a 150-cm^2 tissue culture flask. After approximately 80% of the cells were confluent, cells were washed twice with PBS and cultured in 8 mL DMEM with no supplements. After 48 hours the supernatant was harvested, and the LCMV-GP that was released by the cells into the supernatant was purified with sepharose PD-10 desalting columns (GE Healthcare) [141]. Liver tissue derived from DEE mice was smashed in 1ml PBS using tissue lyser (Qiagen). Mice were immunized intraperitoneally with 100 mg in 200 µl PBS. Pancreas tissue derived from RIP-GP mice was smashed in 1ml PBS using tissue lyser (Qiagen). Mice were immunized intraperitoneally with 40 mg in 200 µl PBS.

3.6.9. *Flow cytometry*

Tetramers were provided by the National Institutes of Health (NIH) Tetramer Facility. 20 µl blood was stained with allophycocyanin (APC)-labeled GP33 MHC class I tetramers (GP33/H-2Db) for 15 minutes at 37°C. After incubation, the samples were stained with anti-CD8 peridinin-chlorophyll-protein-complex (PerCP; BD Biosciences, Franklin Lakes, NJ) for 30 minutes at 4°C. Erythrocytes were then lysed using 1ml BD lysing solution (BD Biosciences); washed 1x and analyzed with flow cytometer. Absolut numbers of GP33-specific $CD8^+$ T cells/µl blood were calculated from FACS analysis using fluorescing beads (BD Biosciences).

3.6.10. *Blood glucose measurement, glucose tolerance test*

Serum glucose concentrations were measured with a contour meter (Bayer, Leverkusen). Mice were considered diabetic if the glucose concentration was higher than 200 mg/dl. For glucose tolerance test, mice were fasted for 15 hours and then

received a single intraperitoneally injection of 2 mg/g body weight glucose (Merck). Blood glucose was measured immediately before injection and then at 15, 30, 60, 90 and 120 minutes after injection.

3.6.11. *ELISA*

IFN-α ELISA was performed according to the protocol of the manufacturers (PBL Interferon source).

3.6.12. *Histology*

Conventional histology was performed as previously described [142]. Briefly, snap-frozen tissue was stained with rat anti-mouse polyclonal antibody to LCMV nucleoprotein (VL4; made in-house). Polyclonal anti-rat biotin antibody (eBioscience) and anti-biotin streptavidin peroxidase (Thermo Scientific) were then used before visualization with a 2-solution DAB staining kit (Invitrogen).

3.6.13. *Western blot*

Proteins were isolated with trizol and solubilised with 10 M urea/ 50 mM DTT. Protein lysates were normalized for total protein (Bio-Rad). Proteins were analyzed by electrophoresis under denaturating conditions using 4–20% SDS ClearPAGE and blotted onto nitrocellulose membranes (Whatman). LCMV-GP was stained with KL25 antibody (made in-house) or UBP43 (Santa Cruz 98431)

3.6.14. *Statistical analysis*

If not differently stated data are expressed as means and S.E.M. Student's *t*-test was used to detect statistically significant differences between groups, or Log-rank(Mantel-Cox) test to detect statistically significant differences of incidence of diabetes. Significant differences between several groups were detected by two-way analysis of variance (ANOVA). The level of statistical significance was set at $P < 0.05$.

3.7. Acknowledgments

We gratefully thank Konstanze Schättel and Patricia Spieker for technical support. We thank Wolfgang-Ulrich Müller for his help with generating bone marrow chimeras. National Institutes of Health (NIH, USA) Tetramer Core Facility provided the tetramers.

3.8. Figure Legends

3.8.1. *Figure 1: Depletion of dendritic cells blunted early viral replication and prevented autoimmune diabetes.*

(**A**) CD11c-DTR mice and C57BL/6 mice were treated intraperitoneally with diphtheria toxin (30 µg/kg) on day -3. Mice were infected with LCMV (200 PFU) or LCMV (2×10^6 PFU) on day 0. Viral titers were analyzed at the indicated time points in different organs (200 PFU n = 6 and $2x10^6$ PFU, n = 3). (**B***)* C57BL/6 and CD11c-DTR mice were treated intraperitoneally with diphtheria toxin (30 µg/kg) on day -3 and then infected with LCMV (2×10^6 PFU) on day 0. After one day, immunohistologic staining for LCMV-NP was performed on spleen sections (n = 3, scale bar main images 500 µm, inlets 100 µm). (**C**) CD11c-DTR mice and control WT mice were treated with 30 µg/kg diphtheria toxin on day -3. On day 0 mice were infected with $2x10^6$ PFU LCMV. After two days IFN-α was measured in the serum by ELISA (n = 6). (**D-F***)* RIP-GP mice were lethally irradiated and one day later were reconstituted with 10^7 bone marrow cells from either CD11c-DTR mice or C57BL/6 mice as control animals. Thirty days later, mice were treated intraperitoneally with diphtheria toxin (10 µg/kg) on days -1, 2, 5, and 8 and were infected intravenously with 200 PFU LCMV-WE on day 0. A representative dot plot and the quantification of virus specific $GP33^+$ $CD8^+$ T cells analyzed on day 8 in the blood with FACS analysis is shown (n = 10-14, D). The incidence of diabetes was determined by measuring serum glucose concentrations after LCMV infection (n = 7-11, E). Virus titers were analyzed in the blood at different time points after infection by plaque assay (n = 5-11, F). *** $P < 0.001$ (Student's *t*-test) (**C** and **D**), Log-rank (Mantel-Cox) (**E**) two-way analysis of variance (ANOVA)(**F**).

3.8.2. *Figure 2: Pharmacologic inhibition of viral replication inhibits onset of autoimmune diabetes.*

(A-B) C57BL/6 mice were treated intraperitoneally with Ribavirin (5 mg daily), starting on day -3. On day 0, mice were infected with 200 PFU LCMV. LCMV titers in the spleen were measured by plaque assay on days 1 and 2 after infection (n = 5 – 7, A). Levels of IFN-α was measured in the serum by ELISA (n = 4-5, B). (C-D) RIP-

GP mice were treated intraperitoneally with Ribavirin (5 mg daily), starting on day -3. On day 0, mice were infected with 200 PFU of LCMV-WE. Numbers of islet-specific $CD8^+$ T cells were determined by tetramer staining and flow cytometry (C, n = 4). The onset of diabetes was assessed by measuring serum glucose concentrations at the indicated time points (D, n = 9). *** $P < 0.001$ (Student's t-test) (A and B), two-way analysis of variance (ANOVA)(C) or Log-rank (Mantel-Cox)(D).

3.8.3. *Figure 3: Expression of Usp18 in dendritic cells guarantees early viral replication and onset of autoimmune diabetes*

(**A**) WT and *Ifnar*$^{-/-}$ mice were infected with 200 PFU of LCMV-WE. Viral titers were analyzed in various organs by plaque assay on day 4 (n = 4). (**B**) Expression of UBP43 (protein encoded by *Usp18*) was assessed by Western blot in bone marrow–derived dendritic cells, macrophages, and fibroblasts (n = 3). Dendritic cells from *Usp18*$^{-/-}$ mice served as a control for antibody specificity. (**C**) Bone marrow–derived dendritic cells from WT or *Usp18*$^{-/-}$ mice were infected with LCMV *in vitro* (MOI=1) or left uninfected. In addition, cells were treated with recombinant IFN-α (50 U/mL) or left untreated. After 48 hours, LCMV titers were measured in the culture supernatants by plaque assay (n = 9). (**D**) WT and *Usp18*$^{-/-}$ mice were infected with LCMV 2×10^6 PFU. After one day viral titers were measured in the spleen and lymph nodes by plaque assay (n = 3). (**E**) FACS analysis of $GP33^+$ $CD8^+$ T cells measured in splenocytes from WT or *Usp18*$^{-/-}$ mice on day7 after infection with 200 PFU LCMV-WE (One of three is shown). (**F**) FACS analysis of IFN-γ^+ $GP33^+$ /and $NP396^+$ $CD8^+$ T cells measured in splenocytes from WT or *Usp18*$^{-/-}$ mice on day7 after infection with 200 PFU LCMV-WE six hours after restimulation with GP33-peptide (n = 3-4). (**G**) FACS analysis of $GP33^+$ $CD8^+$ T cells measured in blood from WT or *Usp18*$^{-/-}$ mice at different time points after infection with 200 PFU LCMV-WE (n = 4-6, G). (**H**) RIP-GP mice were lethally irradiated and one day later were reconstituted with 10^7 bone marrow from either *Usp18*$^{-/-}$ mice or WT littermate control mice. Thirty days later, mice were infected with 200 PFU LCMV. GP33-specific $CD8^+$ T cells in the blood were counted by flow cytometry at the indicated time points after LCMV infection (n = 4). (**I**) C57BL/6 mice were lethally irradiated and one day later were reconstituted with a 1:1 mixture of bone marrow derived from *Usp18*$^{-/-}$ and CD11c-DTR mice or from WT and CD11c-DTR mice as control animals. Thirty days later,

mice were treated intraperitoneally with diphtheria toxin (10 µg/kg) on days -1, 2, 5, and 8 and were infected intravenously with 2×10^6 PFU LCMV-WE on day 0 (n = 4). GP33-specific $CD8^+$ T cells were assessed in peripheral blood 8 days after LCMV infection by tetramer staining and flowcytometric analysis. Results of 2 experiments are pooled. (**J**) RIP-GP mice were lethally irradiated and one day later were reconstituted with 10^7 bone marrow cells from either *Usp18*$^{-/-}$ mice or WT littermate control mice and were infected with 200 PFU of LCMV 30 days later. The incidence of autoimmune diabetes was determined by measuring serum glucose concentrations at the indicated time points (n = 7-10). * $P < 0.05$, ** $P < 0.01$ and *** $P < 0.001$ (Student's *t*-test) (**C**, **D,F** and **I**), two-way analysis of variance (ANOVA) (**G and H**) or Log-rank (Mantel-Cox) (**J**).

3.8.4. *Figure 4: Only replicating antigen is efficient in breaking autoimmune tolerance*

(**A**) Initial LCMV inoculate (2×10^6 PFU and 200 PFU) and purified LCMV glycoprotein (GP) (0.01, 0.1, 1 µg) were stained for LCMV-GP by Western blot analysis. After immunization of C57BL/6 mice with live LCMV (200 PFU, i.v.) and purified LCMV glycoprotein (GP, 2µg, i.v.), spleen lysates were analyzed by Western blot for LCMV-GP expression at the indicated time points. (**B**) RIP-GP mice were infected intravenously with 200 PFU of LCMV-WE. The number of GP33-specific $CD8^+$ T cells was determined by tetramer staining and flow cytometry, and serum glucose concentration was determined at the indicated time points (n = 4-11). (**C**) RIP-GP mice were immunized intravenously with 2 µg purified LCMV-GP in combination with poly I:C (100 µg). The number of autoreactive $CD8^+$ T cells was determined by tetramer staining and flow cytometry, and serum glucose concentration was determined at the indicated time points (n = 4). (**D**) 10^7 Splenocytes from P14/CD45.1 mice were labeled with CFSE and adoptively transferred into C57BL/6 mice. After 24 hours, C57BL/6 mice were left uninfected (both histogram blots, dotted line) or infected with 200 PFU LCMV-WE (left histogram blot, filled area) or immunized with 2 µg LCMV-GP (n = 3, right histogram blot, filled area). Proliferation of $CD45.1^+CD8^+$ T cells was assessed by CFSE dilution in spleen 6 days after transfer. Histograms show cells gated on $CD45.1^+$ $CD8^+$ T cells. One representative set of data is shown. (**E**) RIP-GP mice were treated intraperitoneally

with Streptozotocin (5 mg) and intravenously with poly I:C (100 µg). The number of islet-specific $CD8^+$ T cells was determined by tetramer staining and flow cytometry, and serum glucose concentration was determined at the indicated time points (n = 3). (**F**) 10^7 Splenocytes from P14/CD45.1 mice were labeled with CFSE and transferred into RIP-GP mice or C57BL/6 mice. After 24 hours, RIP-GP mice were treated either left untreated (right histogram blot, dotted line) or were treated intraperitoneally with 5 mg Streptozotocin and intravenously with poly I:C (100 µg, right histogram blot, filled area). C57BL/6 mice were either left untreated (left histogram blot, dotted line) or infected with 2×10^6 PFU LCMV (left histogram blot, filled area). Proliferation of $CD45.1^+CD8^+$ T cells was assessed by CFSE dilution in the spleen 6 days after transfer (n = 3). Blots show cells gated on $CD45.1^+$ $CD8^+$ T cells. One representative set of data is shown. (**G**) RIP-GP mice were immunized intraperitoneally with homogenized pancreas (40 mg) from RIP-GP mice and intravenously with poly I:C (100 µg). The number of islet-specific $CD8^+$ T cells was determined by tetramer staining and flow cytometry, and serum glucose concentrations were determined at the indicated time points (n = 4). (**H**) RIP-GP mice were immunized intraperitoneally with homogenized liver derived from DEE mice (100 mg) and immunized intravenously with poly I:C (100 µg). The number of islet-specific $CD8^+$ T cells was determined by tetramer staining and flow cytometry, and serum glucose concentration was determined at the indicated time points (n = 4). (**I**) RIP-GP mice were infected with 10^3 CFU of Listeria-GP33 intravenously. Number of islet-specific $CD8^+$ T cells was determined by tetramer staining and flow cytometry, and serum glucose concentration was measured at the indicated time points (n = 4-7).

3.8.1. *Figure 5: Ribavirin blunts auto-reactivity in RIP-NP diabetes model*

RIP-NP mice were treated intraperitonealy with Ribavirin (5 mg daily), starting on day -3. On day 0, mice were infected with 200 PFU of LCMV-WE. (A) Numbers of virus-specific Tet-$GP33^+$ $CD8^+$ T cells were determined by tetramer staining and flow cytometry (n = 5-6). (B) Numbers of auto-reactive Tet-$NP396^+$ $CD8^+$ T cells were determined by tetramer staining and flow cytometry (n = 5-6). (C) On day 50 glucose tolerance test was performed (n = 5-6). * $P < 0.05$ and *** $P < 0.001$ two-way analysis of variance (ANOVA).

3.8.2. *Figure S1: Dendritic cells are activated during LCMV infection*

C57/BL6 mice were infected with 2×10^6 PFU of LCMV. Expression of MHC-I and CD86 on splenic dendritic cells was analyzed at the indicated time points. Dotted line indicates staining with isotype antibody.

3.8.3. *Figure S2: Usp18$^{-/-}$ mice can coupe with LCMV infection*

Virus blood titers of WT or *Usp18*$^{-/-}$ mice measured on day 5 and 30 after infection with 200 PFU LCMV-WE using in plaque assay (n = 4) *** $P < 0.001$ (Student's *t*-test).

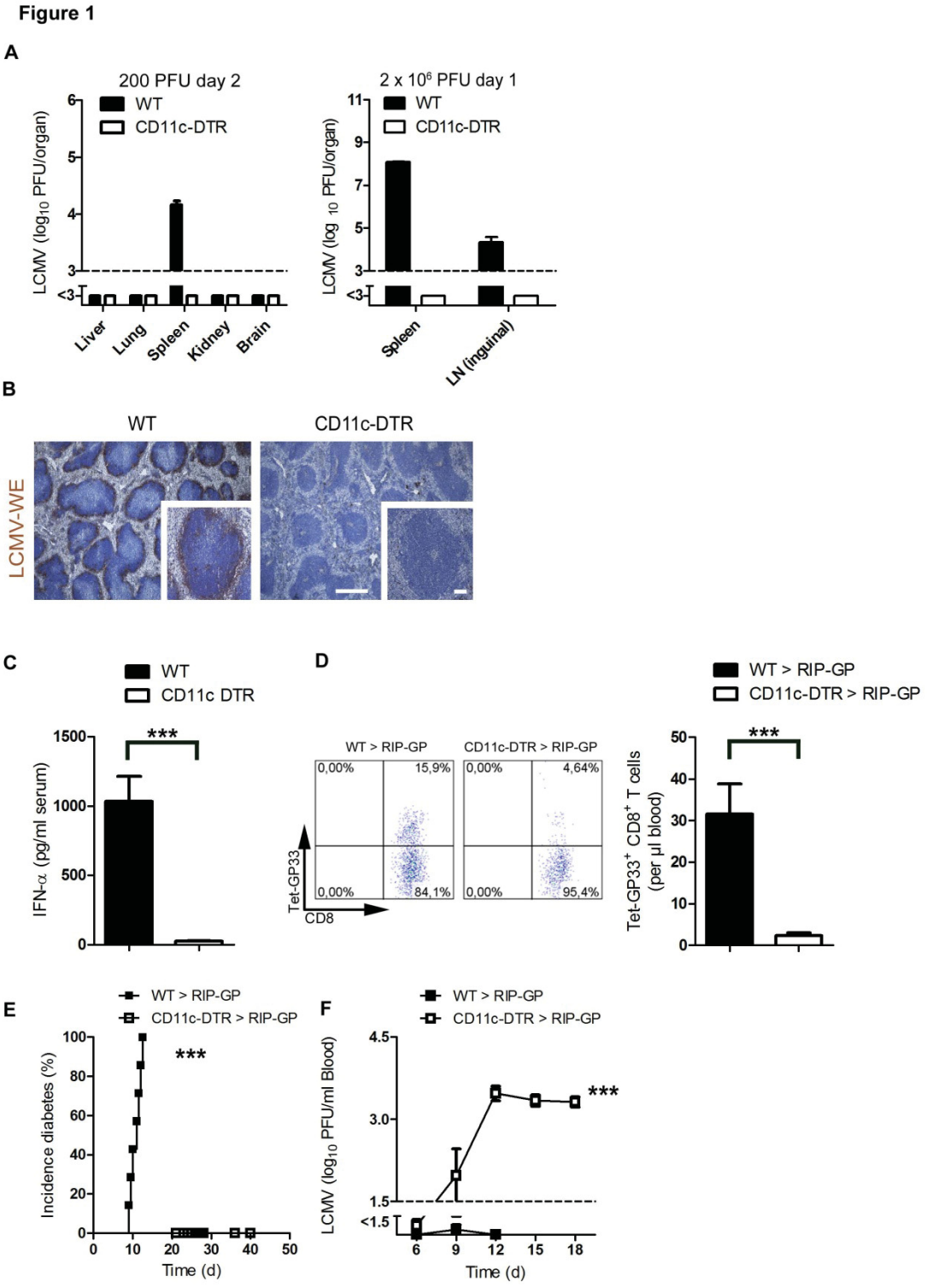

Figure 3-1 Depletion of dendritic cells blunted early viral replication and prevented autoimmune diabetes

Figure 2

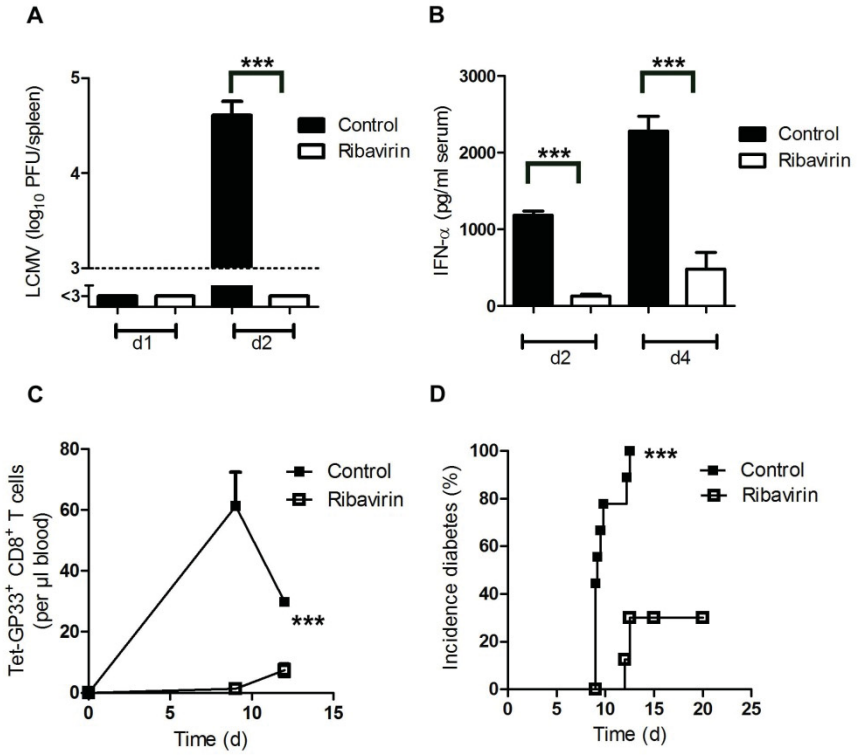

Figure 3-2 Pharmacologic inhibition of viral replication inhibits onset of autoimmune diabetes

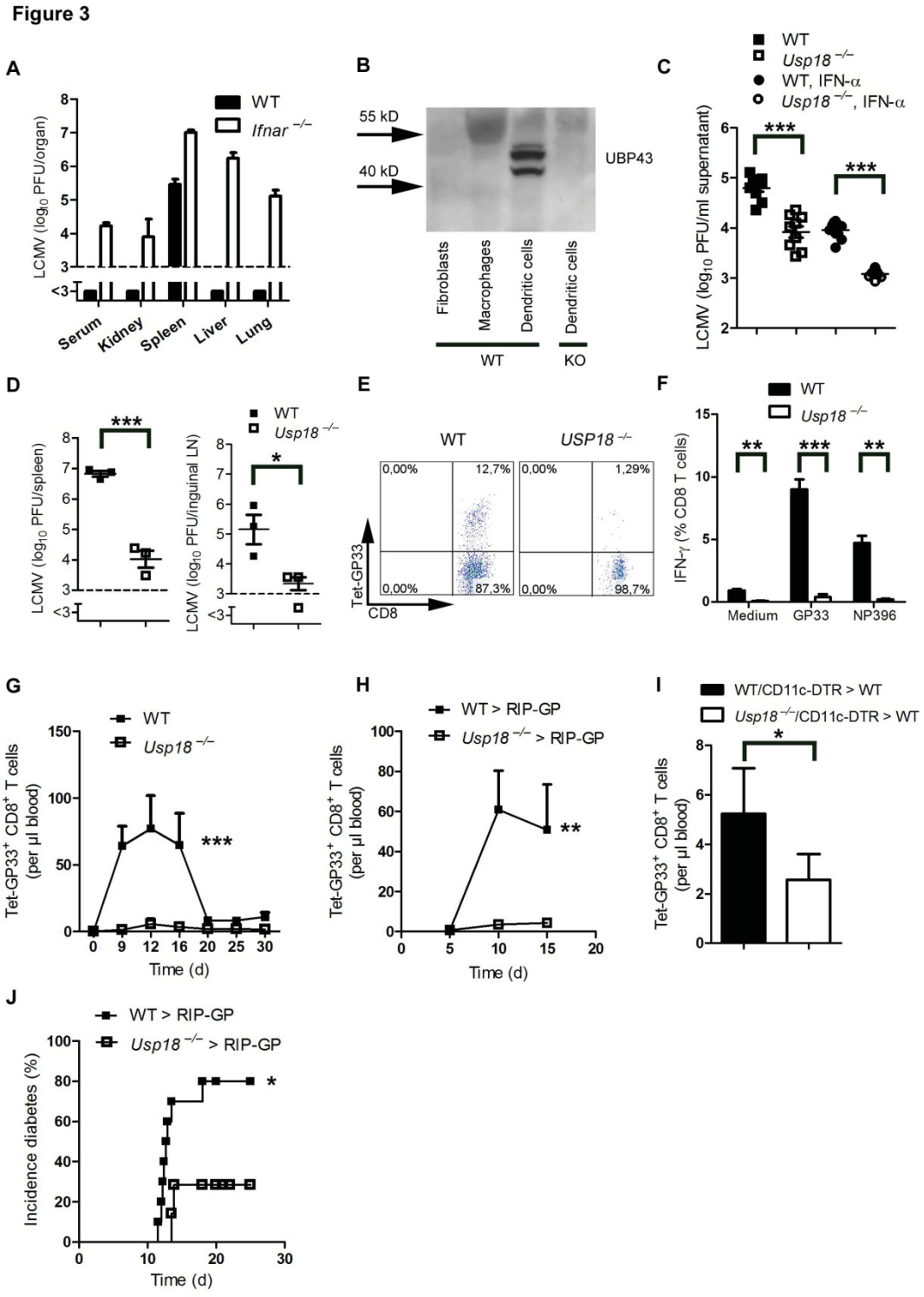

Figure 3-3 Expression of *Usp18* in dendritic cells guarantees early viral replication and onset of autoimmune diabetes

Figure 4

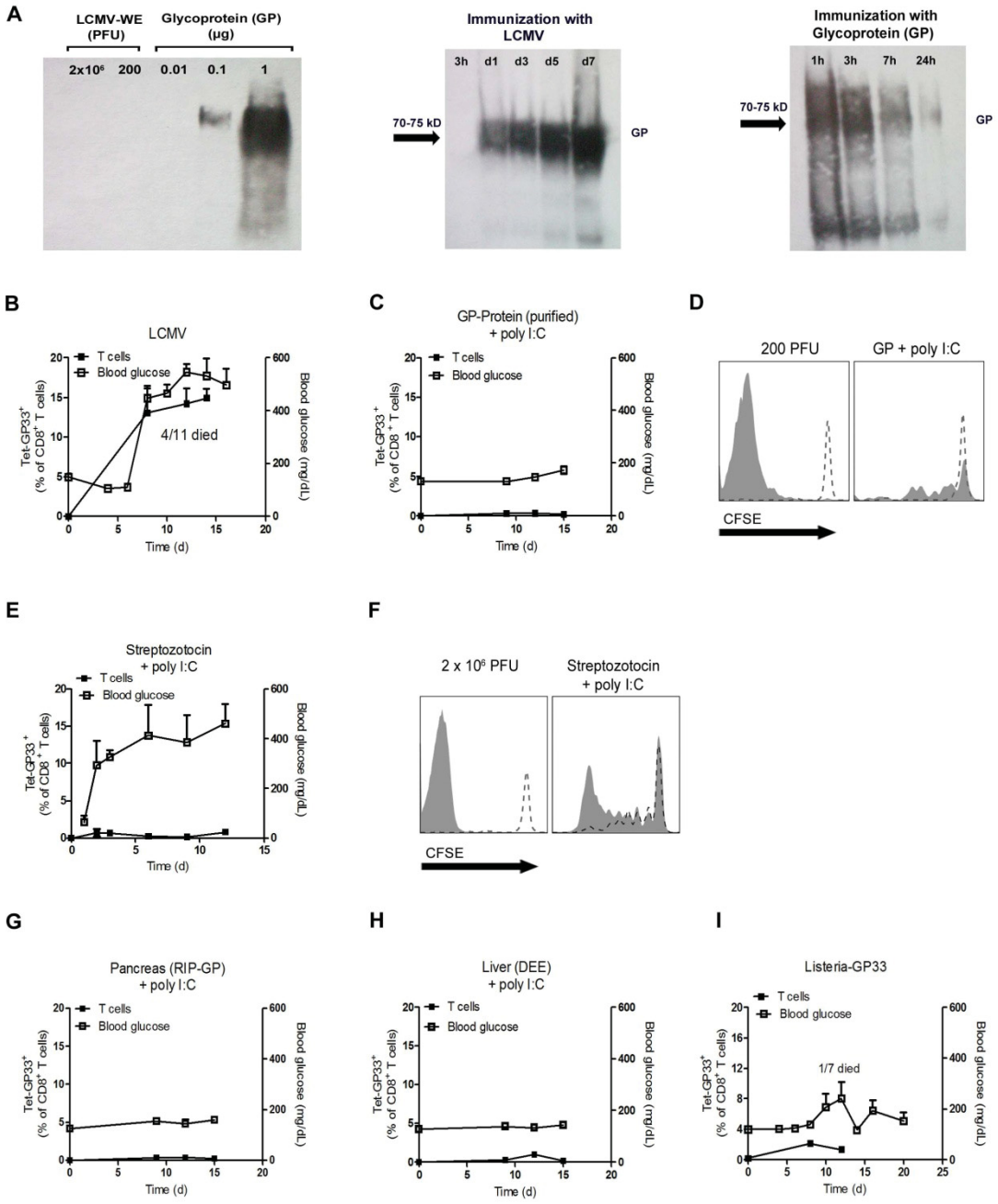

Figure 3-4 Only replicating antigen is efficient in breaking autoimmune tolerance

Figure 5

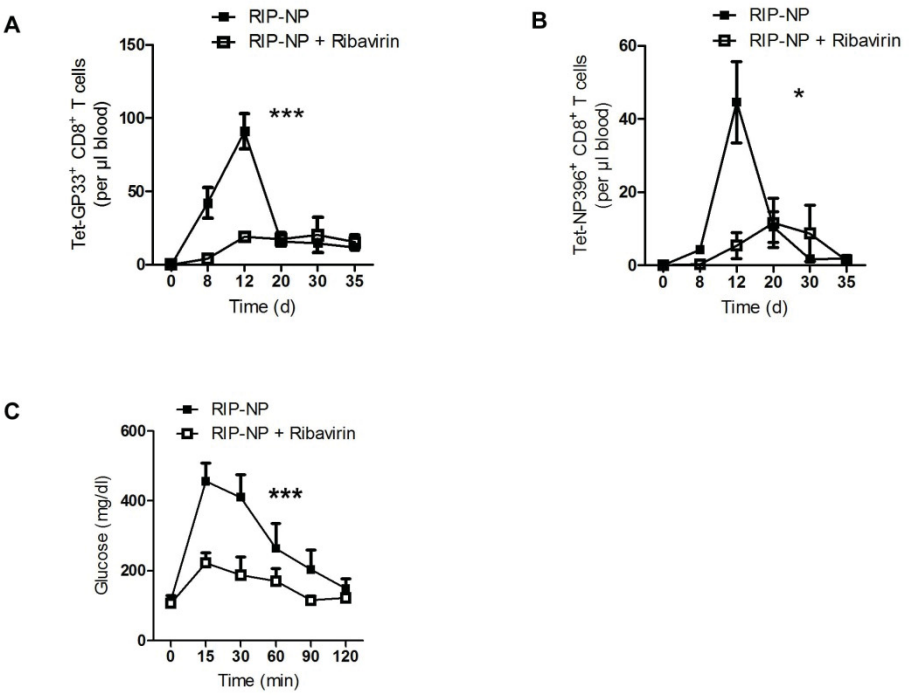

Figure 3-5 blunts auto-reactivity in RIP-NP diabetes model

Figure S1

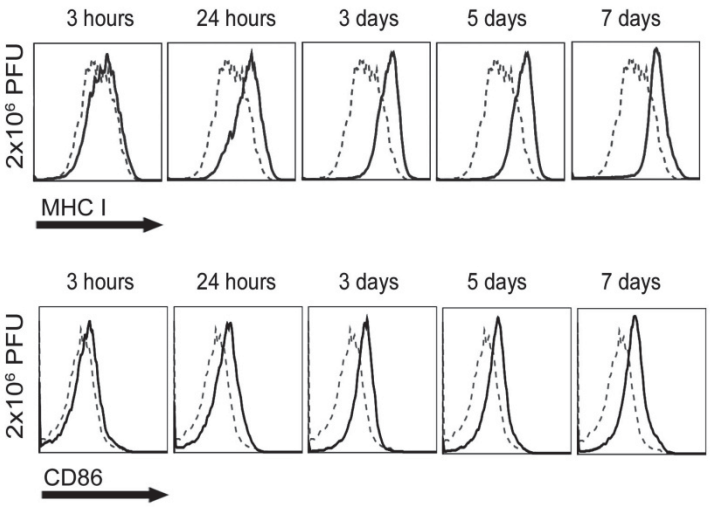

Supplementary Figure 3-1 Dendritic cells are activated during LCMV infection

Figure S2

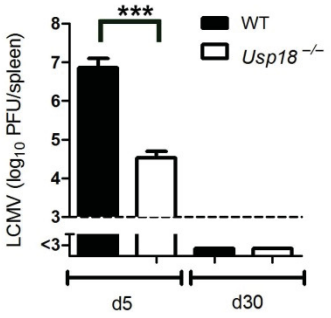

Supplementary Figure 3-2 *Usp18*$^{-/-}$ mice can cope with LCMV infection

Anteilserklärung

2. Publikation:

Honke N*, **Shaabani N***, Zhang DE, Tanaka M, Häussinger D, Recher M, Lang PA, Lang KS

Usp18 driven enforced viral replication in dendritic cells contributes to break of immunological tolerance in autoimmune diabetes

PLoS Pathog. 2013 Oct;9(10):e1003650.

Name des Journals:	*PlosPathogen*
Impact factor (Stand 2013):	8,136
Anteil an Experimenten in dieser Arbeit (%):	48 %
Autor:	Erstautor (* geteilte Erstautorschaft)
Beitrag an dieser Arbeit:	Herr Namir Shaabani führte einen großen Teil der praktischen Experimente und Auswertungen der Versuche durch. Außerdem war er am experimentellen Design und entscheidend an der Manuskripterstellung beteiligt.

Namir Shaabani

Prof. Dr. Karl Lang

4. Chapter IV: Reduced type I interferon production by dendritic cells and weakened antiviral immunity in Wiskott-Aldrich syndrome protein deficiency

Philipp A. Lang*, Namir Shaabani*, Stephanie Borkens, Nadine Honke, Stefanie Scheu, Sarah Booth, Dirk Brenner, Andreas Meryk, Carmen Barthuber, Mike Recher, Tak W. Mak, Pamela S. Ohashi, Dieter Häussinger, Gillian M. Griffiths, Adrian J. Thrasher, Gerben Bouma,,* and Karl S. Lang*

4.1. Abstract

Background: The Wiskott Aldrich syndrome (WAS) is a rare X-linked primary immunodeficiency caused by absence of WAS protein (WASP) expression resulting in defective function of many immune cell lineages and susceptibility to severe bacterial, viral and fungal infections. Despite a significant proportion of WAS patients developing recurrent viral infections, surprisingly little is known about the effects of WASP deficiency on antiviral immunity.

Objective: To evaluate the antiviral immune response in WASP deficiency *in vivo*.

Methods: Viral clearance and associate immunopathology was measured following infection of WASP deficient (WAS KO) mice with lymphocytic choriomeningitis virus (LCMV). Induction of antiviral $CD8^+$ T cell immunity and cytotoxicity was documented in WAS KO by temporal enumeration of total and antigen-specific T cell numbers. Type I interferon (IFN-I) production was measured in serum in response to LCMV challenge and characterized *in vivo* using IFN-I reporter mice crossed with WAS KO mice.

Results: WAS KO mice showed reduced viral clearance and enhanced immunopathology during LCMV infection. This was attributed to both an intrinsic $CD8^+$ T cell defect as well as defective priming of $CD8^+$ T cells by dendritic cells. IFN-I production by WAS KO dendritic cells was reduced both *in vivo* and *in vitro*.

Conclusions: These studies use a well-characterized model of persistence-prone viral infection to reveal a critical deficiency of $CD8^+$ T cell responses in murine WASP deficiency, in which abrogated production of IFN-I by dendritic cells may play an important contributory role. These findings may help to understand the immunodeficiency of the WAS.

Key messages

- WASP deficient mice show reduced viral clearance and enhanced virus induced immunopathology
- Priming and effector function of $CD8^+$ T cells is impaired in WASP deficiency
- Type I interferon production by dendritic cells is reduced in the absence of WASP

4.2. Introduction

The Wiskott Aldrich syndrome (WAS) is a rare X-linked genetic human disease associated with thrombocytopenia, eczema and life-threatening immunodeficiency [33,143]. Patients often also suffer from increased incidence of autoimmune disease and malignancies [144,145]. WAS is caused by mutations in the gene encoding the Wiskott Aldrich syndrome protein (WASP), which is a member of a family of proteins that are required for the transduction of signals from the cell surface to the actin cytoskeleton [146]. As expression of WASP is restricted to cells of the hematopoietic lineage, the absence of WASP results in defective function of many immune cell lineages, leading to a combined cellular and humoral immune defect. Defective immune cell function resulting from WASP deficiency is multifactorial, including global defects of migration of lymphoid and myeloid lineages [147-151], as well as impaired cell-specific effector function. For instance, in the absence of WASP function, uptake of particulate antigen by macrophages by means of phagocytosis is defective [147-153], podosome formation and T cell priming ability of dendritic cells (DC) is impaired [147,154-156], B and T cell proliferation in response to B or T cell receptor ligation is reduced [157-161] and homeostasis of mature B cell populations [162,163] as well as homeostasis and function of regulatory T cells is disturbed [164-167]. Therefore, the severe immunodeficiency resulting from WASP deficiency is thought to be the result of a complex combination of cellular immune defects.

While many studies have focused on characterizing the role of WASP in individual immune cell lineages, still much is unknown about the role of WASP for antiviral immunity despite a significant proportion of WAS patients developing recurrent infections, most commonly involving members of the herpes virus family [144,145]. Previous reports have indicated susceptibility of WAS KO mouse models to influenza infection, which seemed more pronounced after secondary viral challenge, reflecting impaired memory function[168,169]. Recently, WASP deficient $CD8^+$ cells derived from patients have been shown to polarize lytic granules poorly, and to exhibit diminished cytotoxicity [170]. Acute and chronic infection with persistence-prone viruses often results in organ specific immunopathology [171-173]. In this setting, virus-specific T cells are a major determinant of immunopathology as they contribute to organ infiltration and are directly cytotoxic to virus-infected target cells [51]. Mechanisms of virus control and virus induced immunopathology have been studied

in mice using the non cytopathic RNA virus Lymphocytic choriomeningitis virus (LCMV) where immunopathology is predominantly mediated by $CD8^+$ T cell-mediated cytotoxicity against virus infected cells. Complete lack of $CD8^+$ T cells strongly reduces immunopathology even though virus replication is enhanced.[34] In contrast, delayed innate or adaptive immune response also enhances virus replication in the target organ, leading to exaggerated immunopathology [51,174,175]. As well as $CD8^+$ T cells, type I interferons (IFN-I) are crucial for the control of viral replication [57], and are induced at early time-points following viral infection. Host production of IFN-I is elicited by the ligation of host pattern recognition receptors by viral molecules, generally activating the transcription factor IRF7, which then translocates to the nucleus and promotes IFN-I production [176].

Here we have used models of virus-induced immunopathology to analyze antiviral immunity in WASP deficiency. We found that WASP deficiency results in impaired viral clearance and enhanced immunopathology. This was associated with an impaired CD8+ T cell response, and reduced production of IFN-I by DC.

4.3. Methods

4.3.1. *Mice and viruses*

WAS KO, RIP-GP and $IFN\beta^{mob/mob}$ were bred in our own facilities. Control C57BL/6 were purchased from the Jackson Laboratory. For some experiments, WAS KO mice were crossed with $IFN\beta^{mob/mob}$ (both C57BL/6 background). WAS KO were also crossed to RIP-GP mice (C57BL/6 background). For generation of WAS KO bone marrow chimeras in RIP-GP mice (both C57BL/6 background), recipient mice were irradiated with 1050 rad on day -1. On day 0, 10^7 bone marrow cells were transferred i.v. and mice were used for experiments 7 weeks later. All experiments were performed in single ventilated cages. Animal experiments were carried out either with authorization of the Veterinäramt of the Kanton Zurich and in accordance with the Swiss law for animal protection or with the approval of and according to UK Home Office Animal Welfare legislation. Further animal experiments were carried out with the authorization of the Landesamt für Natur, Umwelt und Verbraucherschutz of Nordrhein-Westfalen, Germany, and in accordance with the

German law for animal protection, the institutional guidelines of the Ontario Cancer Institute, or both.

LCMV strain WE was originally obtained from F. Lehmann-Grube (Heinrich Pette Institute, Hamburg, Germany) and was propagated in L929 cells. Virus titers were measured using a plaque forming assay as described [177]. Mice were infected with 200 plaque forming units (pfu) LCMV-WE unless stated otherwise. Vesicular stomatitis virus (VSV), Indiana strain (VSV-IND, Mudd-Summers isolate), was originally obtained from Prof. D. Kolakofsky (University of Geneva, Switzerland). Virus was propagated on BHK-21 cells at a multiplicity of infection (MOI) of 0.01 and was then plaqued onto Vero cells.

4.3.2. *Immunohistochemistry*

Cryostat sections of 7 µm thickness were cut onto poly-L-lysine coated slides (VWR, Leuven, Belgium), fixed for 20 min in 1% paraformaldehyde (BDH, Poole,UK) and rinsed in PBS. Slides were blocked with 2% normal mouse serum (Dako Cytomation), then followed by incubation for at least one hour with primary antibodies specific for CD4 (eBiosciences), CD8 (BD Biosciences) or MHC I (Biolegend). After washing, slides were incubated 30-45 min with alkaline phosphatase conjugated anti-rat secondary antibody (Dako). Naphthol red was used as substrate (Sigma) and hematoxylin (Merck, Darmstadt, Germany) used for counterstaining.

4.3.3. *Assessment of diabetes*

Blood glucose concentrations were analyzed from a drop of blood using a Glucometer Elite (Bayer). When animals showed blood glucose levels higher than 14mM on two consecutive days they were considered diabetic.

4.3.4. *FACS analysis*

Tetramer production and FACS analysis was performed as described previously [124]. Briefly, splenocytes or peripheral blood lymphocytes were stained using PE-labeled GP33 MHC class I tetramers (GP33/H-2D^b) for 15 minutes at 37°C, followed by staining with anti-CD8 (BD Biosciences) for 30 minutes at 4°C. For determination of LCMV specific CD4$^+$ T cells lymphocytes were stained with anti-CD4 and anti Thy1.1 (CD90.1, BD Biosciences). For determination of their activation status, lymphocytes were stained with anti-CD25, anti-CD69, anti-GITR, anti-CD62L, anti-

CD44 and anti IL-7Rα (BD Biosciences) for 30 minutes at 4°C. Cells were fixed with 1% Formalin and permeabilized with saponin. Cells were stained for intracellular IFN-γ, IL-10, IL-4 (BD Biosciences) and intracellular Granzyme B (CALTAG, Burlingame, CA). IFN-α production by dendritic cells was assessed by intracellular FACS after culture of bone marrow cells for ten days with Flt3L (100 ng/ml; Peprotech). For identification of dendritic cells CD11c (BD Biosciences) was used and CD8α, CD11b and B220 or pDCA1 (BD Biosciences) used to distinguish between $CD8^+$, conventional and plasmacytoid dendritic cells, respectively. Cells were analyzed using a FACS Calibur or FACS Canto II (BD Biosciences).

4.3.5. *T cell priming*

DC were cultured from bone marrow cells in the presence of GM-CSF (20 ng/ml; Invitrogen) for 7 days and pulsed overnight with ovalbumin (100 µg/ml; Sigma) and LPS (100 ng/ml; Sigma). DC ($2x10^6$) were injected s.c. in the tail base of wild type C57BL/6 mice and spleen and draining lymph nodes (inguinal) harvested at the indicated time points. Single cells suspensions of lymph node and spleen were co-cultured with SIINFEKL peptide (2 µM; Proimmune) and RMA-S cells (kindly provided by Dr. Anne-Marie McNicol) in the presence of brefeldin A (5 µg/ml; Sigma). The RMA-S cells were incubated overnight at 26ºC prior to the experiment to establish expression of empty MHC class I molecules on the cell surface, which during the culture with lymph node or spleen cells will present the SIINFEKL peptide. After 4 hours the cells were stained with FITC-conjugated CD3 and PerCP-conjugated CD8, then permeabilized (BD Perm/Wash; BD Pharmingen) and stained with PE-conjugated IFN-γ (Ebioscience, San Diego, CA). The cells were analyzed on a Cyan flow cytometer.

4.3.6. *IFN-α ELISA*

Mice were infected with LCMV, VSV or injected with Poly (I:C) and blood obtained at the indicated time points. Serum IFN-α was determined by ELISA according to the manufacturers' specifications (Research Diagnostics RDI).

4.3.7. *Cytotoxicity assay*

EL4 target cells were loaded with 51Cr and pulsed with or without GP33 or NP396. Splenocytes of immunized mice were incubated directly *ex vivo* (Primary) or after re-stimulation with GP33 or NP396 for 5 d (Secondary) with the target cells.

Supernatant was assessed after 8 h. For killing of allogeneic BALB/c splenocytes, a Cytotox 96 nonradioactive kit (Promega) was used following the instructions provided. Ficoll-purified T cells were plated at the effector/target ratios shown using 10^4 BALB/c splenocytes (target) cells. Lactate dehydrogenase release was assayed after 4 h incubation at 37°C. Percentage cytotoxicity = (experimental effector spontaneous − target spontaneous / target maximum − target spontaneous) × 100.

4.3.8. *Statistical analysis*

Data are expressed as mean ± SEM. When comparing data expressed as curves, linear regression was used. When curves did not follow linear pattern, the area under curve (AUC) or peak values were determined and compared using Students t-test. When comparing two groups, Students t-test was used. Survival data was analyzed using log rank test. All statistical tests were performed using Prims 5 (GraphPad). P values < 0.05 were considered as statistically significant.

4.4. Results

4.4.1. *Reduced viral clearance in WAS KO mice*

To investigate the ability of WAS KO mice to mount a protective immune response against viral infection and to investigate immunopathology, we challenged mice with LCMV (WE strain). The levels of serum alanine-aminotransferase (ALT) and total bilirubin were used as a direct measurement of virus induced hepatic immunopathology [51]. WAS KO mice showed a similar, albeit slightly earlier, ALT response, but exhibited elevated bilirubin levels after viral challenge (Fig 1, *A-B*). Furthermore, WAS KO mice showed persistence of viral replication and a hepatic T cell infiltrate 15 days after infection, while by that time wild type C57BL/6 animals had cleared viral infection and showed no sign of T cell infiltration (Fig 1, *C-D*). These finding indicate that WAS KO mice are compromised in their ability to clear LCMV despite the presence of an inflammatory T cell infiltrate.

4.4.2. *Defective induction of $CD8^+$ T cell response*

We used the RIP-GP model of autoimmune diabetes to study the induction of an effective antiviral $CD8^+$ T cell response *in vivo*. These mice express the LCMV glycoprotein under regulatory control of the rat insulin promoter resulting in β-cell restricted expression. Upon infection with LCMV, normal mice mount an anti LCMV

immune response, which is dominated by the generation of glycoprotein-specific cytotoxic $CD8^+$ T cells that not only clear the virus, but also destroy β cells that express the LCMV glycoprotein, subsequently inducing development of diabetes [41]. We created bone marrow chimeras by transferring WAS KO or wild type C57BL/6 bone marrow into lethally irradiated RIP-GP mice and challenged the mice after a further 50 days with LCMV. Despite the development of insulitis (Fig 2, *A*), characterized by infiltration of $CD4^+$ and $CD8^+$ T cells into the □-cell-containing Islets of Langerhans, and generalized up-regulated expression of MHC class I as a result of inflammatory conditions, mice reconstituted with WAS KO bone marrow did not develop overt diabetes (Fig 2, *B*). Similarly, when RIP-GP mice were crossed with WAS KO mice, the incidence of overt diabetes following LCMV challenge was significantly reduced compared to RIP-GP single transgenic animals (Fig 2, *C*), albeit not as strong as in bone marrow chimeric mice, which is probably due to the additional immunosuppressive effects of irradiation and bone marrow transplantation. To analyze the CD8+ response *in vivo* in more detail, we infected wild type C57BL/6 or WAS KO mice with LCMV and analyzed the virus specific $CD8^+$ T cell response. Six days after infection, the total number of $CD8^+$ T cells and LCMV-specific, GP33-tetramer positive, $CD8^+$ T cells in spleen, liver and blood was similar between C57BL/6 and WAS KO mice (Fig 3, *A*-*C*). However on days 12 and 20 after infection, the numbers of total and virus-specific $CD8^+$ T cells recovered from blood was markedly reduced in WAS KO mice (Fig 3, *C*), while at that time LCMV had been eliminated in C57BL/6 mice (Fig 1, *C*). WAS KO mice also mounted $CD8^+$ T cells specific for the immunodominant epitope of the LCMV nucleoprotein (NP396), but although reduced compared to C57BL/6 mice this did not reach statistical significance (Fig E1). A typical $CD8^+$ T cell response will peak around day eight after infection, after which only a small subset of $CD8^+$ T cells will survive and develop into memory T cells. This subset can be identified by interleukin-7 receptor (IL-7R) expression [124,178,179]. We analyzed the expression of IL-7R on GP33- and NP396-tetramer positive cells at day eight after infection and indeed found fewer $IL\text{-}7R^+$ virus specific $CD8^+$ T cells in WAS KO mice (Fig 3, *D*). We then analyzed the function of virus specific $CD8^+$ T cells in more detail and found that splenic WASP deficient $CD8^+$ T cells, isolated at day six after infection, were impaired in their ability to produce intracellular IFN-γ after re-stimulation *in vitro* with GP33 and

NP396 peptides (Fig 3, *E*). Next, we injected LCMV in the footpad of mice, as footpad swelling is dependent on viral titer, $CD8^+$ T cell infiltration and $CD8^+$ T cell cytotoxicity [180] and found that WAS KO animals exhibited a significantly diminished response (Fig 3, *F*). Finally, we tested the ability of WAS KO $CD8^+$ T cells to specifically lyse target cells *in vitro*. T cells were collected at day six after infection when antigen-specific cell numbers were equivalent between WAS KO and C57BL/6 animals. WAS KO $CD8^+$ T cells showed reduced cytotoxicity to cells presenting the virus specific GP33 and NP396 epitopes (Fig 3, *G*). To investigate whether this was due to intrinsic dysfunction of WAS KO $CD8^+$ T cells, we analyzed the ability of WAS KO $CD8^+$ T cells to lyse allogeneic Balb/c splenocytes and observed that WAS KO $CD8^+$ T cells also showed reduced cytotoxicity in this non-viral setting (Fig 3, *H*). Overall these findings suggest an intrinsic cytotoxic dysfunction of WAS KO $CD8^+$ T cells, but also a more complex disruption to priming and long term survival following antigen challenge.

4.4.3. *Impaired priming of $CD8^+$ T cells*

As T cells require antigen-specific stimulation by DC for optimal priming, we investigated the contribution of defective DC-mediated T cell priming to abnormal CD8+ T cell responses. We adoptively transferred bone marrow-derived WAS KO DC pulsed with ovalbumin into wild type C57BL/6 recipients and analyzed the antigen-specific IFN-γ response. Both in spleen and in the draining lymph nodes, we observed reduced numbers of IFN-γ producing wild type $CD8^+$ T cells in response to secondary challenge with ovalbumin (Fig 4, *A-B*), suggesting that defective priming by dendritic cells at least in part contributes to defective function of WAS KO $CD8^+$ T cells. Priming of virus specific $CD8^+$ T cells is also strongly dependent on IFN-I, acting either directly on the $CD8^+$ T cells or by maturing DC necessary for antiviral T cell immunity [91,92]. Accordingly we analyzed the type I IFN response in WAS KO mice after infection with LCMV. Induction of serum IFN-α was significantly abrogated in WAS KO mice in response to LCMV infection (Fig 5, *A*). Similarly, when we infected mice with vesicular stomatitis virus (VSV) or administered the non-viral, non-replicating IFN-I stimulator TLR3/RIG-I ligand poly(I:C) *in vivo*, WAS KO mice exhibited a markedly diminished IFN-α response (Fig 5, *B-C*). These

findings indicate a general reduction of stimulated IFN-I production *in vivo* in the absence of WASP expression.

4.4.4. *Decreased expression of IFN-I by DC*

To investigate which cells were responsible for the defective production of IFN-I, we made use of the IFN-β reporter-knockin mouse, in which yellow fluorescent protein (YFP) expression is bicistronically linked to expression of IFN-β of the endogenous *ifnb* locus, so that IFN-β producing cells can easily be identified by YFP expression [181]. These IFNβ$^{mob/mob}$ mice were crossed with WAS KO mice and challenged with poly(I:C). As expected, we found that in the absence of WASP IFNβ/YFP expression was reduced in splenocytes and that this was restricted to CD11c$^+$ cells (Fig 6, *A-B*). To verify that this was not caused by an overall reduction in the number of DC in WAS KO mice, we analyzed the proportion of conventional migratory (cDC; CD11c$^+$CD11b$^+$CD8α$^-$B220$^-$), conventional CD8α$^+$ (CD11c$^+$CD11b$^-$ CD8α$^+$B220$^-$) and plasmacytoid (pDC; CD11c$^+$CD11b$^-$B220$^+$ or CD11c$^+$mPDCA1$^+$) DC subsets. As expected from previous reports [155,182], we did not observe significant differences between distinct subsets in spleen or lymph nodes in C57BL/6 or WAS KO mice (Fig 6, *C-D* and Fig E2, *A*). Total splenocyte and lymph node cell numbers in WAS KO and C57BL/6 mice were comparable, as were absolute cell counts of DC subsets (Fig E2, *B-E*). Finally, we tested whether the impaired production of IFN-I observed *in vivo* reflected an intrinsic deficiency of DC in the absence of WASP. Both pDC and cDC showed a reduced IFN-α response when stimulated with poly (I:C), CpG and LPS *in vitro* (Fig 6, *E*). Similarly, when we used *ex vivo* isolated splenic CD11c$^+$ cells a similar deficiency to produce IFN-α in response to poly (I:C), LPS and CpG was observed (Fig E2, *F*). These findings show that WAS KO DC are intrinsically compromised in their ability to secrete IFN-I.

4.5. Discussion

WAS patients suffer from recurrent viral infections [144,145], but relatively little is known about the mechanistic role of WASP in antiviral immunity. We found that WAS KO mice failed to clear LCMV infection and developed exaggerated immunopathology. One possibility is that there was reduced homing of inflammatory cells to the sites of infection [150]. However, we observed a persistent infiltration of

$CD4^+$ and $CD8^+$ T cells in the liver after viral infection, suggesting that reduced viral clearance is not primarily the result of defective $CD8^+$ T cell migration. In chimeric or transgenic RIP-GP/WAS KO mice, we observed T cell infiltration around the islets of Langerhans, which is typically associated with the onset of diabetes. Both in antigen-specific and allogeneic settings, we observed reduced cytotoxic function of WAS KO $CD8^+$ T cells. Overall, these findings indicate that there are intrinsic defects of cytotoxicity in WAS KO $CD8^+$ T cells, and that they play a significant role in the control of viral infection *in vivo*. They are also in line with a recent report showing that cytotoxicity is reduced in human WASP deficient $CD8^+$ T cells and that WASP is required for delivery and polarization of the lytic granules towards the center of the immunological synapse [170]. Similar to cytotoxic T cells, impaired lytic activity of NK cells in WAS patients has also been reported previously [183]. In addition, defective NK cell function can result from impaired DC priming [184], but the role of NK cells in LCMV mediated immunity is expected to be limited as depletion of NK cells improves $CD8^+$ T cell immunity [185]. Impaired immunological synapse formation is likely to contribute to defective $CD8^+$ T cell function [155]. Dependence on WASP for DC-mediated priming has previously also been demonstrated for $CD4^+$ T cells and NK cells, where WASP was shown to be required for formation of an activating immunological synapse [147,154,184]. Perhaps most strikingly, although at early time points the $CD8^+$ T cell response to LCMV appears relatively normal, it is poorly sustained compared to that observed in normal mice with fewer IL-$7R^+$ cells, marking a reduction in survival and memory $CD8^+$ T cell development. It therefore appears that WASP deficiency not only intrinsically impairs function of $CD8^+$ T cells, as shown by reduced cytotoxicity and IFN-γ production, but also results in abrogated survival or expansion. This might help explain the progressive immunodeficiency observed in WAS patients, as a consequence of accelerated exhaustion.

IFN-I are crucial for the control of LCMV replication. In complete absence of IFN-I, no detectable virus-specific $CD8^+$ T cell response is mounted [57]. Ligation of host pattern recognition receptors, such as the cytoplasmic helicase RIG-I family and toll-like receptors (TLR)-3, -7 and -9, triggers activation of the transcription factor IRF7, which translocates to the nucleus where it promotes IFN-I production [176,186]. IFN-I are normally induced at early time points following viral infection and are therefore critical for control of replication and establishment of a definitive

immunological clearance. WAS KO animals demonstrated reduced IFN-I production by DC following LCMV and VSV infections, as well as after non-viral stimulation of TLR-3 and TLR-9. Normal pDC are known for their ability to quickly produce large amounts of IFN-α in response to viral infection or TLR-9 ligation. Depletion of pDC abrogates virus induced IFN-α production and exacerbates virus induced immunopathology, including diminished $CD8^+$ T cell responses [187,188]. Normally, in response to LCMV infection, a rapid expansion of splenic IFN-I producing pDC can be observed [189]. There were no differences in the frequency of pDC in WAS KO mice in steady state, but upon stimulation with virus or TLR ligands WAS KO pDC showed significantly reduced ability to produce IFN-I both *in vitro* and *in vivo*. The expansion of virus specific $CD8^+$ T cells has been shown to be strongly dependent on IFN-I, acting directly on $CD8^+$ T cells to promote survival during antigen-driven proliferation and subsequent establishment of memory [92,174,180,190]. Furthermore, IFN-I plays a key role in enhancing the maturation and activation of DC [91]. It therefore seems likely that a reduced IFN-I response in WAS KO mice contributes to the weakened antiviral $CD8^+$ T cell response by directly affecting $CD8^+$ T cell function, by influencing the activation of DC or by a combination of the both. pDC activation by iNKT cells has been reported to play an important role in control of LCMV infection through stimulation of IFN-I production [191]. WAS patients and WAS KO mice have impaired homeostasis and function of iNKT cells, so it is interesting to speculate that there may be a mechanistic link [192,193]. Further studies will be required to determine whether defective iNKT cell function affects pDC function in WAS KO model systems.

In conclusion we have shown that WASP is required to mount a protective antiviral immune response in an *in vivo* model of persistence prone LCMV infection. In the absence of WASP a markedly diminished $CD8^+$ T cell response is induced, which most likely is the combination of intrinsic dysfunction of WASP deficient $CD8^+$ T cells and impaired priming and maintenance by IFN-I producing DC. This also raises the possibility that IFN-I therapy may be useful for refractory or chronic viral infections in WAS patients.

4.6. Acknowledgements

We would like to thank Alisha Elford, Konstanze Schättel and Patricia Spieker for technical support, Dr. Siobhan Burns for critically reading of the manuscript and the NIH tetramer facility for providing tetramers.

4.7. Figure legends

4.7.1. *Fig 1. Absence of WASP enhances virus induced immunopathology*

Virus induced immunopathology was analyzed as serum ALT activity (A) and bilirubin levels (B) after LCMV infection. Viral clearance was assessed by measuring viral titers in liver (C). The presence of $CD4^+$ and $CD8^+$ T cells in liver was analyzed by immunohistochemistry (D). Data in (A-B) mean ± SEM and peaks (A; C57BL/6, n=6-12; WAS KO, n=8-10) or AUC (B; C57BL/6, n=5-9; WAS KO, n=5-6) compared using Students t-test. Symbols in (C) represent individual mice and images in (D) are representative of data shown in (C).

4.7.2. *Fig 2. Reduced incidence of virus induced diabetes*

C57BL/6 and WAS KO bone marrow was transferred into irradiated RIP-GP mice and after 50 days mice were infected with LCMV. Insulitis was determined by immunohistochemistry (A) and incidence of diabetes analyzed (B), n=4. Transgenic WAS KO/RIP-GP mice were made by crossing RIP-GP mice with WAS KO mice. Mice were infected with LCMV and incidence of diabetes analyzed (C), n=8.

4.7.3. *Fig 3. Impaired CD8+ T cell response in WASP deficiency*

The virus specific $CD8^+$ T cell response was analyzed after LCMV infection as the total number (left panel) or LCMV-specific, GP33-tetramer positive (right panel), $CD8^+$ T cells in spleen (A), liver (B) and blood (C). IL-7R expression was determined on virus specific $CD8^+$ T cells (D). IFN-γ expression was analyzed by FACS after re-stimulation of *in vivo* primed (day 6) virus-specific T cells (E). Swelling of the

footpad after LCMV infection was analyzed over time (F). Cytotoxicity of $CD8^+$ T cells was determined in virus-specific (F) and allogeneic (G) settings. Data is shown as mean ± SEM, (A-C) and represents n=4-8 (C57BL/6 day 6 n=5-6, day 12 n=7-8, day 20 n=4-5; WAS KO day 6 n=6, day 12 n=6, day 20 n=4), (D) n=3, representative of at least two independent experiments, (E) n=5-6, (F) n=6-8, (G) n=6 and (H) is a representative experiment of two independent experiments with a total of n=4.

4.7.4. *Fig 4. Impaired $CD8^+$ T cell priming*

IFN-γ expression of $CD8^+$ T cells isolated from spleen (A) and lymph nodes (B) was determined after in vivo priming by ovalbumin-pulsed DC and subsequent in vitro re-stimulation with ovalbumin peptide. Data is shown as mean ± SEM; day 4, n=3; day 7, n=3; day 11, n=3.

4.7.5. *Fig 5. WASP deficiency leads to a reduced IFN-α response*

Mice were infected with 200 pfu of the LCMV strain WE (A), $2x10^6$ pfu VSV (B) or injected with 200 µg poly (I:C) (C) and IFN-α was measured in the serum at the indicated time points. Data is shown as mean ± SEM, LCMV n=6-11, VSV n=3 and Poly (I:C) n=6, serum taken 3 hours after injection.

4.7.6. *Fig 6. Reduced IFN-I response by dendritic cells*

IFN-β/YFP reporter mice were challenged with poly (I:C) and splenic IFN-β expression analyzed by FACS. Plots in (A) show representative FACS plots of IFN-β expression by $CD11c^+$ DC after gating for live $CD3^-CD19^-$ cells and quantification is shown in (B) as percentage of all splenocytes (left) or as percentage of $CD11c^+$ cells (right). Frequency of DC populations was determined in spleen (C) and lymph nodes (D). $CD8α^+$ DC, cDC and pDC were identified as $CD11c^+CD8α^+CD11b^-B220^-$ cells, $CD11c^+CD8α^-CD11b^+B220^-$ cells and $CD11c^+CD11b^-B220^+$ cells, respectively. IFN-α expression was determined by intracellular FACS of in vitro cultured DC subsets (E). Symbols in (B) represent individual mice and line is the mean. Data in (C-E) is expressed as mean ± SEM of (C-D) n= 4, (E) LPS and CpG, n=7; poly (I:C), n=4.

4.7.7. *Fig E1. Analysis of T cell response for immunodominant epitope of LCMV nucleoprotein*

The virus specific $CD8^+$ T cell response for the immunodominant epitope of the LCMV nucleoprotein was analyzed 12 days after LCMV infection. Data is shown as mean ± SEM, n=3.

4.7.8. *Fig E2. Total number of leukocytes in lymphoid tissue*

The number of splenic $CD11c^+mPDCA1^+$ pDC (A) and total number of leukocytes was determined in spleen (B) and lymph nodes (C). DC subsets were quantified in spleen (D) and lymph node (E). IFN-α expression was determined by intracellular flow cytometry after stimulation of ex vivo isolated DC subsets (F). Symbols in A-C represent individual mice and line indicates the mean. Data in (D-F) is expressed as mean ± SEM of (D-E) n= 4, (F) LPS and CpG, n=7; poly (I:C), n=4.

Fig 1

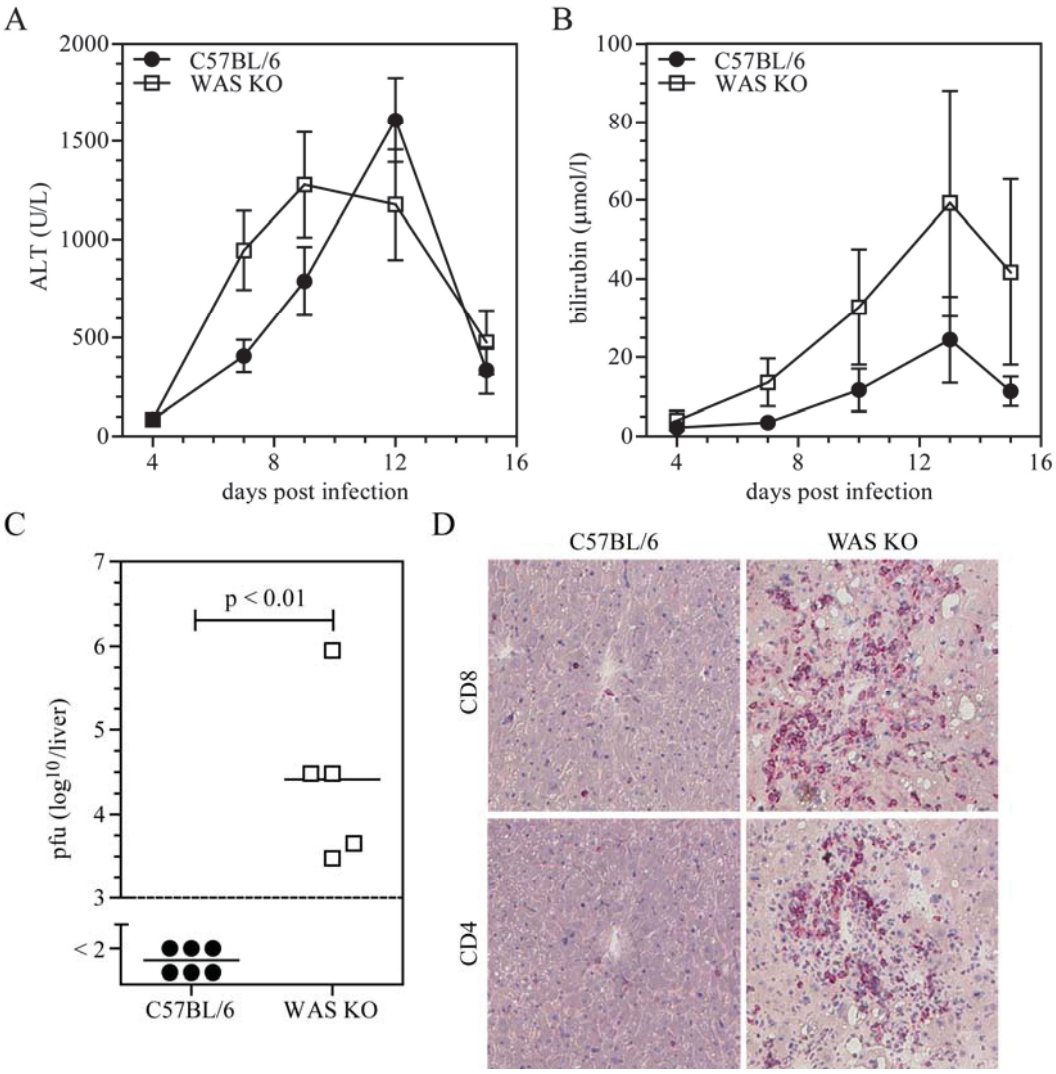

Figure 4-1 Absence of WASP enhances virus induced immunopathology

Fig 2

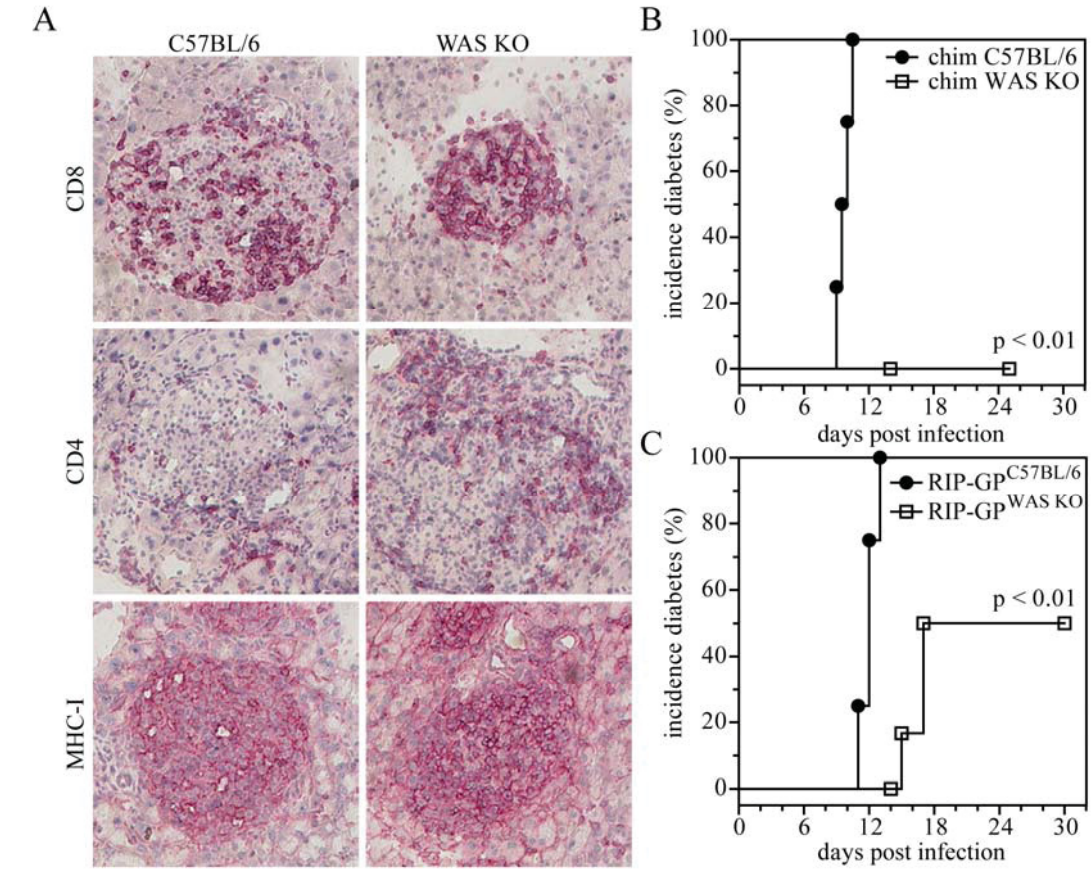

Figure 4-2 Reduced incidence of virus induced diabetes

Fig 3

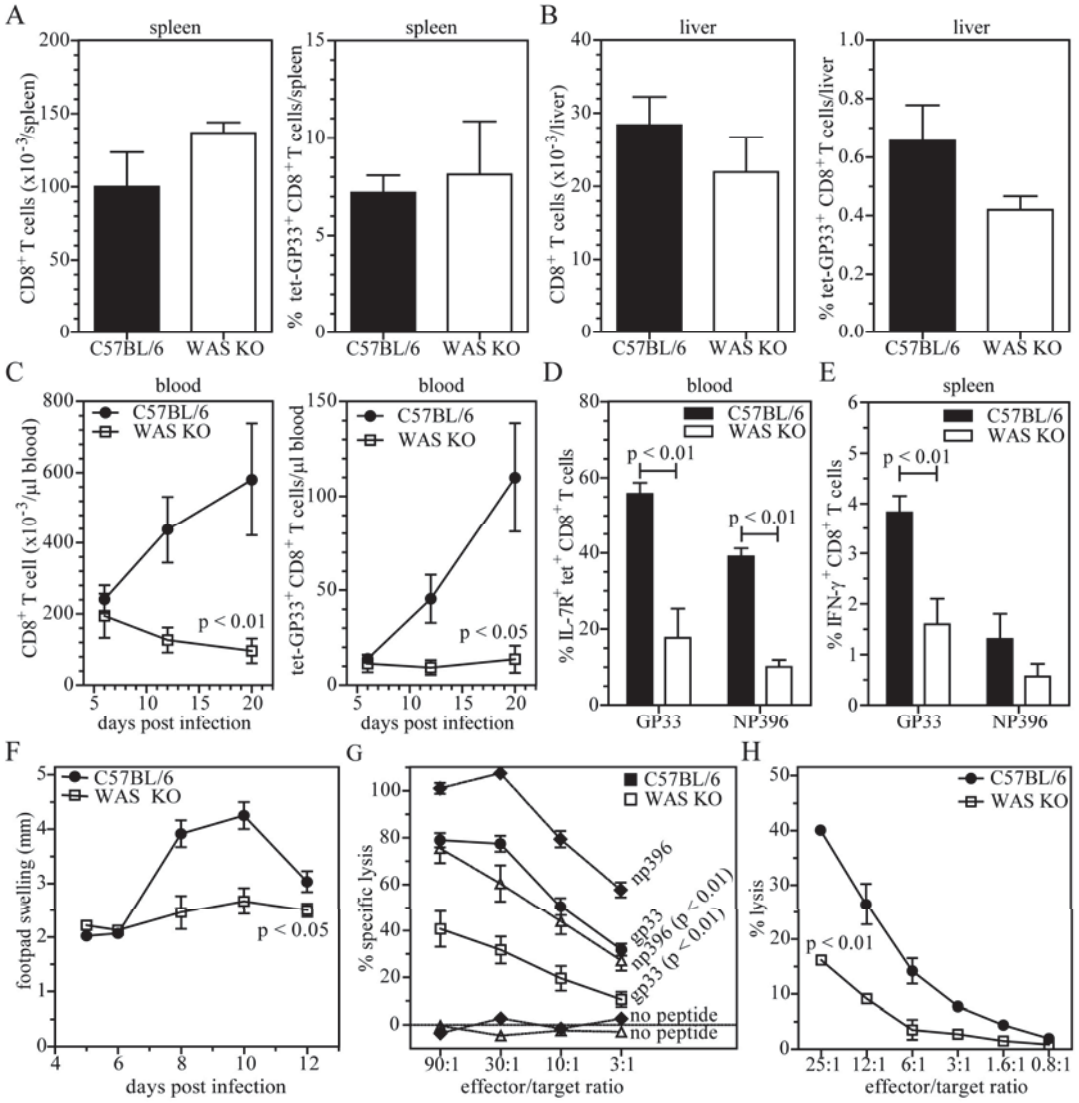

Figure 4-3 Impaired CD8$^+$ T cell response in WASP deficiency

Fig 4

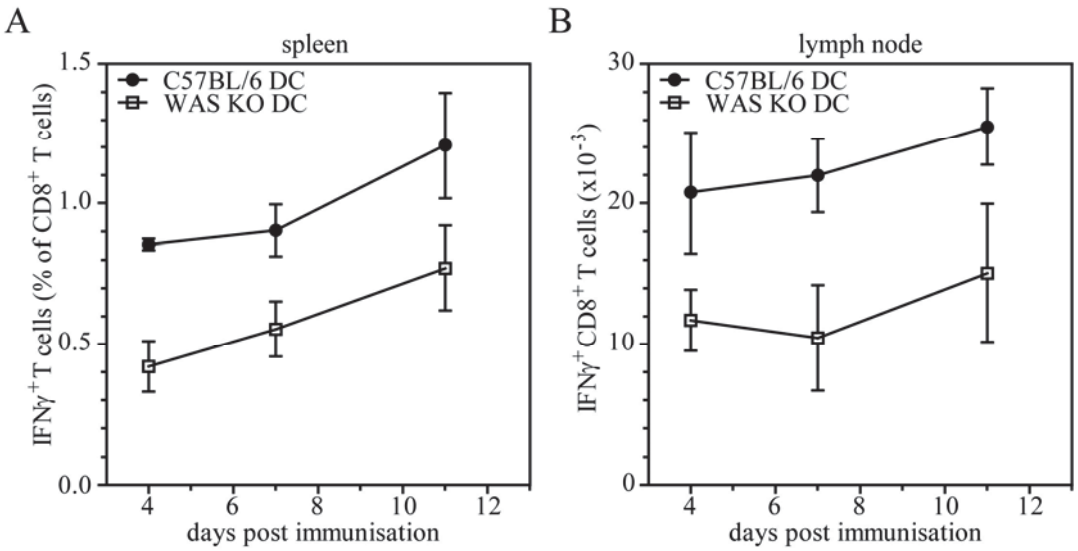

Figure 4-4 Impaired CD8$^+$ T cell priming

Fig 5

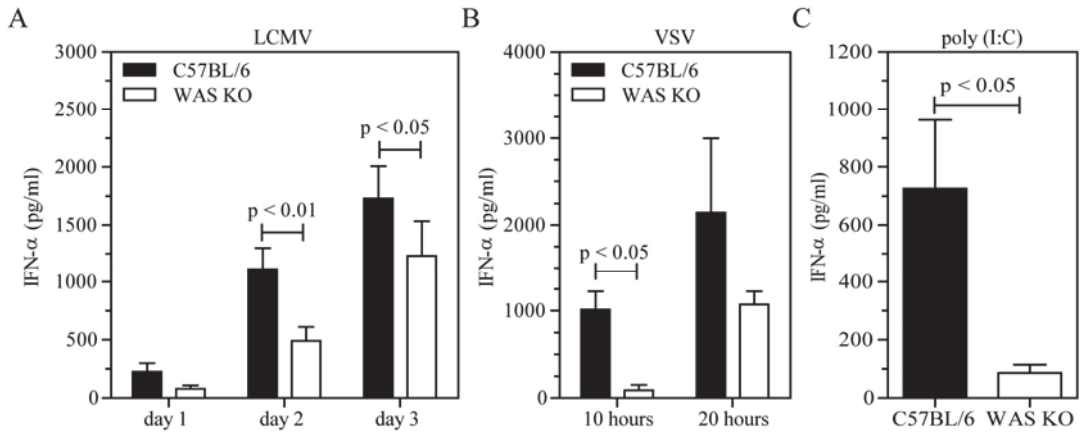

Figure 4-5 WASP deficiency leads to a reduced IFN-α response

Fig 6

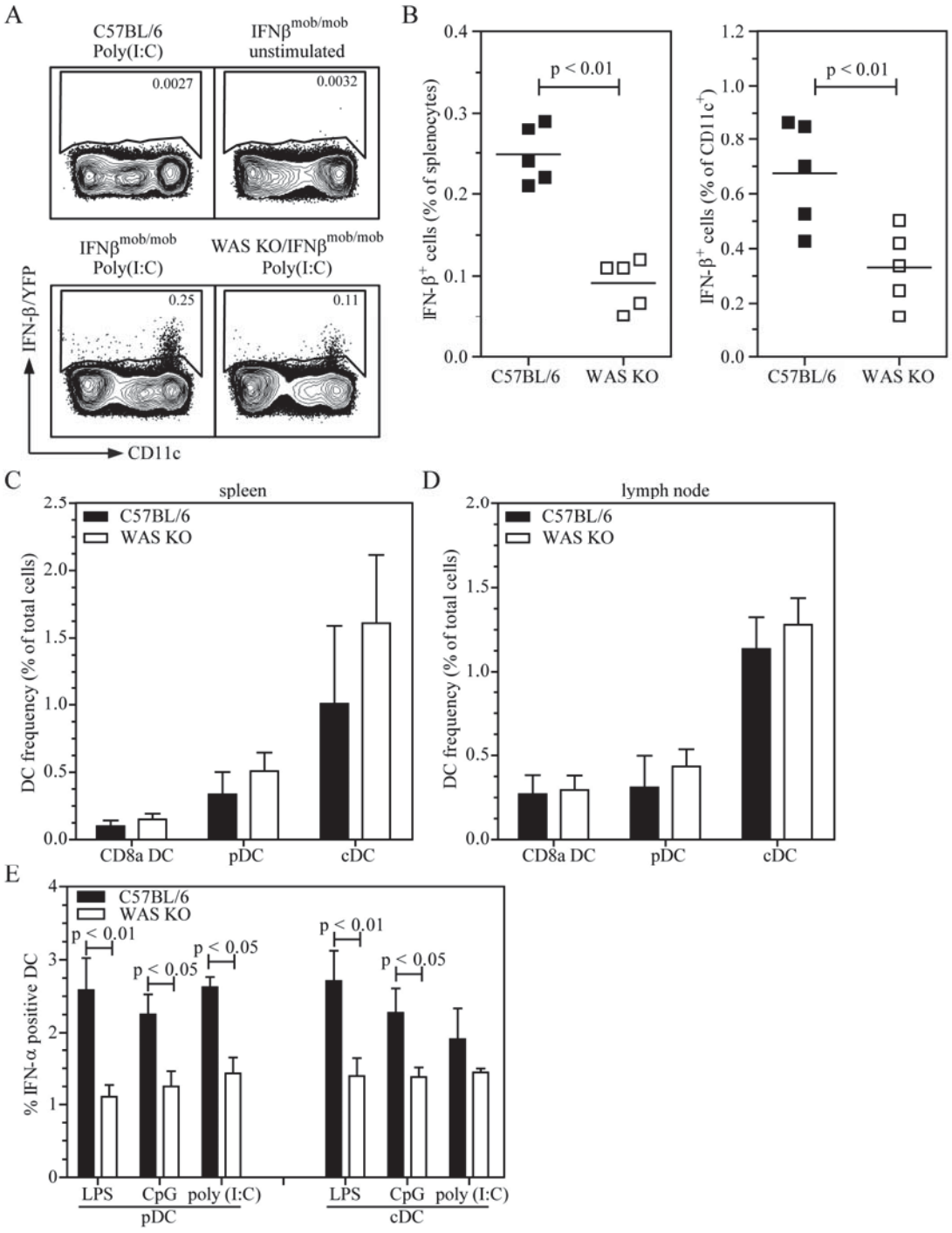

Figure 4-6 Reduced IFN-I response by dendritic cells

Fig E1

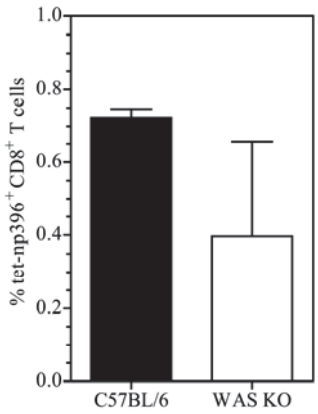

Supplementary Figure 4-1 Analysis of T cell response for immunodominant epitope of LCMV nucleoprotein

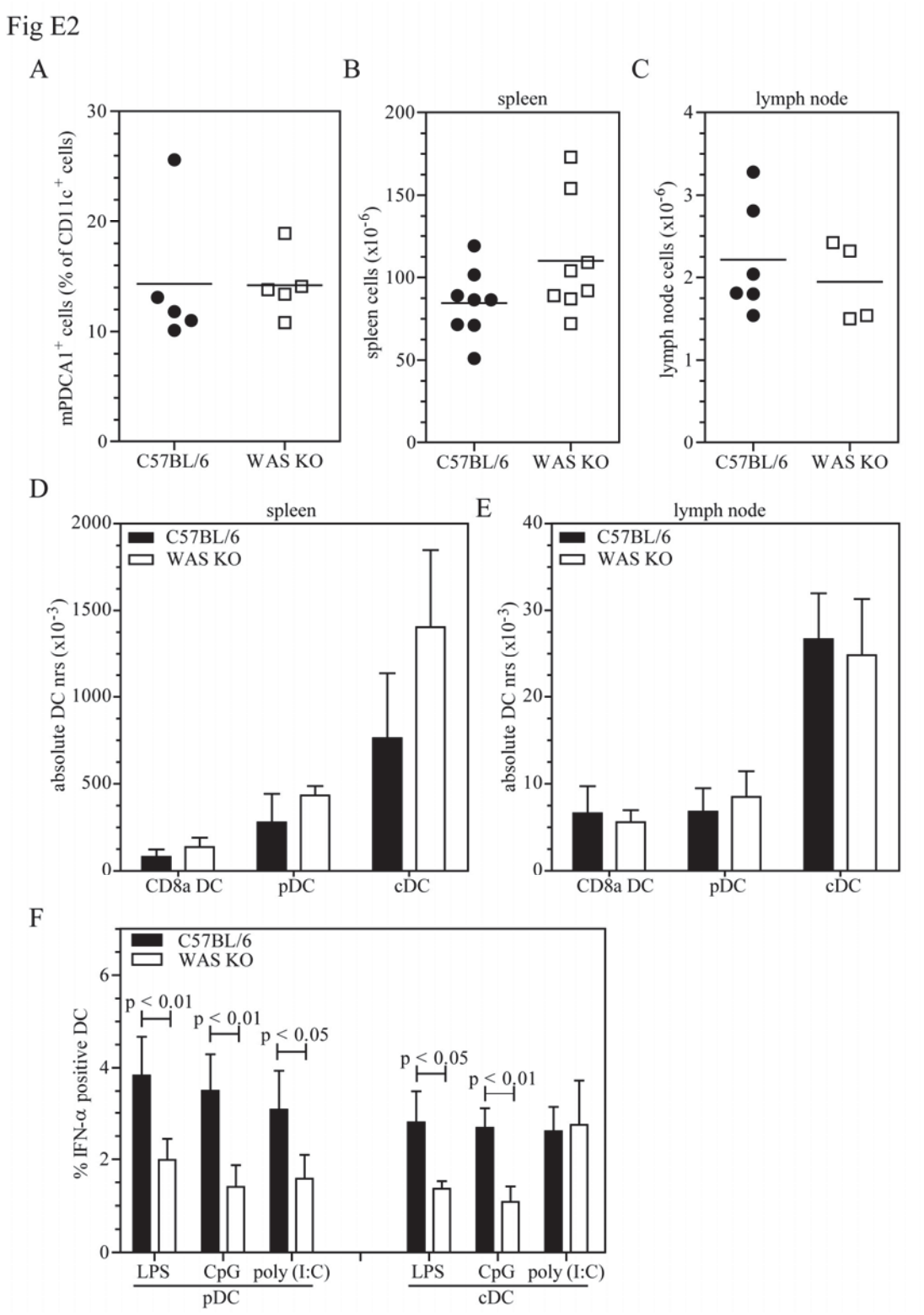

Supplementary Figure 4-2 Total number of leukocytes in lymphoid tissue

Anteilserklärung

3. Publikation:

Lang PA*, **Shaabani N***, Borkens S, Honke N, Scheu S, Booth S, Brenner D, Meryk A, Barthuber C, Recher M, Mak TW, Ohashi PS, Häussinger D, Griffiths GM, Thrasher AJ, Bouma G and Lang KS

Reduced type I interferon production by dendritic cells and weakened antiviral immunity in Wiskott-Aldrich syndrome protein deficiency.

J Allergy Clin Immunol. 2013 Mar;131(3):815-24.

Name des Journals:	*Journal of allergy and clinical immunology*
Impact factor (Stand 2013):	12,047
Anteil an Experimenten in dieser Arbeit (%):	30%
Autor:	Erstautor(* geteilte Erstautorschaft)
Beitrag an dieser Arbeit:	Herr Namir Shaabani war für einen größen Teil der Durchführung und Auswertung der praktischen Experimente sowie für das experimentelle Design verantwortlich.

Namir Shaabani

Prof. Dr. Karl Lang

5. Chapter V: Tunicamycin inhibits diabetes

Namir Shaabani , Nadine Honke, Philipp A. Lang, Boris Görg, Peter Proksch,

Nicole Gailus, Tomomi Gotoh, Dieter Häussinger, Karl S. Lang

5.2. Abstract

Background: Autoimmune diseases are characterized by a breakdown of immunologic tolerance, and this breakdown can lead to life-threatening or lifelong disorders. Moreover; drugs that are used to treat these diseases are few in number and are associated with many serious adverse effects. Methods: We used the rat insulin promoter-glycoprotein mouse model to analyze the role of tunicamycin in the process of autoimmune diabetes; the P14 mouse model to analyze the effect of tunicamycin on $CD8^+$ T cells; *chop* knockout mice to analyze the role of tunicamycin on an endoplasmic reticulum stress model; and fluorescence-activated cell sorting, quantitative real-time polymerase chain reaction, and histologic methods. Results: We found that a single dose of tunicamycin reduced the activation and pancreatic infiltration of $CD8^+$ T cells. This activity delayed the incidence of virus-induced diabetes and improved survival rates. Conclusion: Tunicamycin may offer therapeutic opportunities for T cell–mediated autoimmune diseases such as diabetes.

5.3. Introduction

Diabetes mellitus is an insulin homeostasis disorder characterized by metabolic abnormalities in carbohydrate and lipid metabolism. Type 1 diabetes is primarily immune-mediated. The loss of beta cells is due to a T cell–mediated autoimmune attack, which results in the failure of the pancreas to produce insulin [194-198].

Tunicamycin is produced by the bacterium *Streptomyces lysosuperificus* and is a mixture of homologous nucleoside antibiotics that inhibit the enzyme GlcNAc phosphotransferase (GPT). GPT catalyzes the transfer of N-actelyglucosamine-1-phosphate from UDP-N-acetylglucosamine to dolichol phosphate, which blocks the synthesis of asparagine-linked glycoproteins. Tunicamycin inhibits the synthesis of all N-linked glycoproteins (N-glycans) and causes cell cycle arrest in the G1 phase. In addition, it is used in biology as an experimental tool that induces an unfolded protein response [39,40,199-202].

Here we analyzed the effects of tunicamycin in suppressing the immune response. We found that a single dose of tunicamycin significantly reduces T-cell proliferation and delays the incidence of diabetes in a model of virus-induced type 1 diabetes.

5.4. Materials and methods

5.4.1. Mice treatment, viruses

Lymphocytic choriomeningitis virus (LCMV) strain WE was originally obtained from F. Lehmann-Grube (Heinrich Pette Institute, Hamburg, Germany) and was propagated in L929 cells. Virus titers were measured with a focus-forming assay as described previously [142]. All mice used in this study were maintained on the C57BL/6 genetic background. Rat insulin promoter-glycoprotein (RIP-GP) mice which express the LCMV glycoprotein as a transgene under the rat insulin promoter were used for analysis of autoimmune diabetes [41] . P14 × CD45.1 mice express the LCMV GP33 peptide–specific TCR as a transgene were used for T-cell studies[43]. H25 transgenic mice expressing the heavy chain of the LCMV-neutralizing MAb KL25 produce LCMV-neutralizing immunoglobulin M (IgM) antibodies early after LCMV infection[203]. Mice lacking the Chop gene were maintained on the C57BL6 background [204]. Animals were kept in single ventilated cages. Animal experiments were carried out with the authorization of the Veterinäramt of Nordrhein Westfalen, Germany, and in accordance with the German law for animal protection, the institutional guidelines of the Ontario Cancer Institute, or both. Mice developing symptoms of sickness or showing serious weight loss during LCMV infection were killed and considered as dead. Tunicamycin was purchased from Sigma-Aldrich (St. Louis, MO) and solved in DMSO for intravenously animal treatment.

5.4.2. Diabetes measurement

Blood glucose concentrations were measured with an Elite Meter (Bayer, Tarrytown, NY). Mice were considered to be diabetic if this concentration was higher than 14 mM for 2 consecutive days.

5.4.3. Histology

In virus infection experiments, histological analyses were performed on snap-frozen tissue [142]. Sections of pancreas were stained with the rat monoclonal antibodies anti-CD8 (BD Pharmingen, San Diego, CA), anti-major histocompatibility complex I (MHC-I) (eBioscience, San Diego, CA) and with guinea pig anti-insulin (Dako, Carpinteria, CA).

5.4.4. *Fluorescence-activated cell sorting analysis*

Tetramer staining, surface staining and intracellular fluorescence-activated cell sorting (FACS) staining were performed as described previously [142]. Briefly, splenocytes or peripheral blood lymphocytes were stained with allophycocyanin (APC)-labeled GP33 MHC class I tetramers (GP33/H-2Db) for 15 minutes at 37°C. Afterwards, they were stained with anti-CD8 peridinin chlorophyll protein complex (PerCP; BD Biosciences, Franklin Lakes, NJ) for 30 minutes at 4°C. Tetramers were provided by the National Institutes of Health (NIH) Tetramer Facility.

5.4.5. *Lymphocyte transfer*

Splenocytes from P14×CD45.1 mice were labeled with carboxyfluorescein succinimidyl ester (CFSE) and injected intravenously into 4 groups of mice. On the next day, 2 groups were infected with 2×10^4 PFU LCMV-WE. After 12 hours, one group of the unifected and the infected mice was given 20 nmol of tunicamycin intravenously; the other mice served as a control group and were left untreated.

5.4.6. *In vitro T cell proliferation*

The proliferation of $CD8^+$ T cells in vitro without antigen was performed as described [205]. Briefly, T cells were sorted with MACS using Pan T Cell Biotin Antibody Cocktail (130-090-861, Miltenyi Biotec), and then labeled with CFSE. T-cell activation was achieved using 24 well plate coated with anti-CD3 (5µg/ml; 14-0031-85, eBioscience) with or without soluble anti-CD28 (2µg/ml; 553294, BD Pharmingen).

5.4.7. *RT-PCR*

Total RNA was extracted from splenocytes by using the RNeasy Mini Kit (Qiagen, Hilden, Germany) according to the manufacturer's instructions. RNA was quantified with a NanoDrop ND-1000 spectrophotometer (Thermo Fisher Scientific, Peqlab Biotechnologie GmbH, Erlangen, Germany). The RNA was reverse-transcribed into cDNA by using the Quantitect Reverse Transcription kit (Qiagen, Hilden, Germany). Gene expression analysis was performed with assays from Applied Biosystems, Carlsbad, CA (glyceraldehyde-3-phosphate dehydrogenase [GAPDH, 4352339E-0806018], Chop [Mm00492097_m1], IFN-γ [Mm99999071_m1]), and interleukin-2 [IL-2] [Mm99999222-m1]). Gene expression values were then calculated by using the ddCt method; the mean of the control group was used as a

calibrator to which all other samples were compared. Relative quantities (RQs) were determined with the equation RQ = 2–ddCt.

5.4.8. *In vivo killer assay*

C57BL/6 mice were infected with 200 PFU of LCMV-WE. On day 7, CD45.1$^+$ splenocytes were labeled either with GP33 peptide or with CFSE and transferred to the infected mice in ratio 1:1. After 30 minutes, the presence of GP33 labeled splenocytes was compared to CFSE labeld.peptide negative splenocytes.

5.4.9. *Statistical analysis*

Data are expressed as means ± S.E.M. Statistically significant differences between two groups were analyzed with Student's t-test. Statistical significance was set at $P < 0.05$.

5.5. Results

5.5.1. *Tunicamycin inhibits LCMV-induced diabetes*

To analyze the role of tunicamycin in diabetes we used RIP-GP mice, which express a viral antigen (LCMV glycoprotein) under the rat insulin promoter. Priming of CD8$^+$ T cells with LCMV-WE induces the proliferation of β-islet epitope–specific CD8$^+$ T cells; these cells subsequently destroy pancreatic β-islet cells, leading to diabetes [41]. To test the effect of tunicamycin in diabetes, we infected RIP-GP mice with 200 PFU LCMV-WE (day 0), and then treated one group of mice additionally with 20 nmol tunicamycin on day 4. Treatment with tunicamycin significantly delayed the onset of diabetes; mice treated with tunicamycin did not show any obvious sign of disease until day 15. In contrast, diabetic mice that were not given tunicamycin exhibited high glucose concentrations beginning on day 10 and died within 40 days (Fig. 1 A, B).

5.5.2. *Tunicamycin reduces the infiltration of CD8+ T cells to the pancreas*

To investigate the effect of tunicamycin on the infiltration of CD8$^+$ T cells to the pancreas, we used 2 groups of RIP-GP mice that had been infected with LCMV-WE. One group was treated intravenously with 20 nmol tunicamycin on day 4, and the other group was left untreated. After 6 days of infection, mice were euthanized. Pancreas slices were stained with fluorescence antibodies against beta islet cells,

$CD8^+$ T cells, and MHC-I. Treatment with tunicamycin reduced the infiltration of T cells and the expression of MHC-I (Fig. 2).

5.5.3. *Tunicamycin induces rapid apoptosis in proliferating T cells*

To investigate whether tunicamycin specifically reduces $CD8^+$ T cells or its suppressive activity also affects other immune cells, we infected mice with 200 PFU of LCMV and administered 20 nmol of tunicamycin on day 6. On day 8, mice were euthanized and immune cell counts were determined. We found that the administration of tunicamycin primarily reduced the number of $CD8^+$ T cells (Fig. 3 A). The main reduction was in NP396 and GP33-specific T cells (Fig. 3 B). Moreover, we analyzed the effect of tunicamycin on the proliferation of specific B cells. We used B cells from the spleens of KL25 mice, which are specific for LCMV-GP. The B cells were labeled with CFSE and incubated with LCMV with or without 10µM tunicamycin. We found a slight effect of tunicamcin on the proliferation of the specific B cells (Fig. 3 C).

5.5.4. *Tunicamycin acts directly on T cells*

To determine whether the reduction of $CD8^+$ T cells is direct, we transferred CFSE-labeled splenocytes from P14×CD45.1 mice into 4 groups of C57BL/6 mice. One group was infected with 2×10^4 PFU of LCMV-WE; the second group was also infected (2×104 PFU) and additionally treated with 20 nmol of tunicamycin on day 1; the third group was not infected but was only treated with 20 nmol of tunicamycin; and the fourth group served as a control group. The mice were sacrificed on day 3, and the proliferation of the labeled splenocytes was followed by the reduction of CFSE dye by FACS. Addition of tunicamycin in the absence of T cell activation had only a mild influence on $CD8^+$ T cell survival. T cell activation in the absence of tunicamycin led to rapid CFSE dilution and expansion of $CD8^+$ T cells. In the presence of tunicamycin, number of $CD8^+$ T cells decrease rapidly even below the original cell count (Fig. 4 A, B). This finding suggests that activated T cells, but hardly non-activated T cell are sensitive to tunicamycin treatment.

To eliminate the effect of tunicamycin on the expression of MHC-I, we cultured CFSE-labeled $CD8^+$ T cells in anti-CD3 coated 24 well plate and was stimulated with or without CD28, one group of each was treated with tunicamycin on day 0. After 3 days, the absolute number of $CD8^+$ T cells and the CFSE content was measured with FACS (Fig. 4 C, D). Surprisingly, tunicamycin inhibited the proliferation of the $CD8^+$ T cells directly, excluding the effect of tunicamycin on the antigen presenting pathway.

In order to restrict the effect of tunicamycin on MHC-I, we treated C57BL/6 mice with tunicamycin 12 hours prior of the transferring of CFSE-labeled splenocytes from P14×CD45.1. After 48 hours, the proliferation of $CD8^+$ transferred T cells was measured with FACS. We found that $CD8^+$ T cells proliferate normally (Fig. 4 E).

5.5.5. *Tunicamycin increases the expression of the Chop gene in T cells*

Tunicamycin has a strong effect on endoplasmic reticulum (ER) stress and precisely on the Chop gene; under circumstances of stress this effect can lead to apoptosis [206-208]. Therefore, we next measured the expression of Chop mRNA in T cells. We stimulated splenocytes from P14 mice with GP33 and incubated the cells with 10 µM tunicamycin for 48 hours. Tunicamycin increased the expression of Chop (Fig. 5 A). To determine whether this enhanced Chop expression was the reason for the reduced proliferation of T cells, we injected $Chop^{-/-}$ mice with 2×10^6 PFU LCMV-WE, with or without 20 nmol of tunicamycin. We found that also $Chop^{-/-}$ mice were sensitive to Tunicamycin suggesting that other factors than Chop contributed to fast death of $CD8^+$ T cells (Fig. 5 B).

5.5.6. *Tunicamycin inhibits the production of cytokines by proliferated T cells*

T cells begin to produce cytokines after activation. This enhances proliferation (IL-2) and is beneficial for controlling the virus (IFN-γ) [209,210]. We used quantitative real time polymerase chain reaction (qRT-PCR) to measure mRNA expression of IL-2 and IFN-γ in T cells. Splenocytes from P14 mice were stimulated with GP33 peptide and treated with 10 µM tunicamycin for 48 hours, or were left untreated. Tunicamycin reduced gene expression (Fig. 6 A, B) which suggests that also cytokine production was effected by tunicamycin.

Next, we measured the cytotoxic activity of $CD8^+$ T cells after tunicamycin treatment. The cytolytic activity of $CD8^+$ T cells was reduced significantly if mice were treated with tunicamycin (Fig. 6 C).

Next we compared immunosuppressive effects of tunicamycin to a standard immunosuppressive therapy (Dexamethasone). First, we analyzed virus control of both regimes. Both treatments led to the persistence of LCMV, (Fig. 7 A). Toxicity study showed that once dose was increased, tunicamycin lead to death, (Fig. 7 B). This suggests that its therapeutic window is narrow.

5.6. Discussion

In this study we found that tunicamycin can prevent type I diabetes by reducing the proliferation of T cells. The main target cells were active antigen specific $CD8^+$ T cells. This strong effect of tunicamycin could also be important for treating other types of diseases that are related to autoimmune responses. However, due to its narrow application window, specific cell toxicity has probably to be achieved The results of this study may also suggest a new approach to the treatment of diabetes in humans, once the therapeutic dose, the proper route of administration and the accompanying adverse effects have been determined.

5.7. Acknowledgments

We thank K. Schättel for technical support. The authors also acknowledge the NIH Tetramer Facility for providing the tetramers used in the study. This study was supported by the Sonderforschungsbereich SFB575, Experimentelle Hepatologie (Sprecher: Prof. Dieter Häussinger). K.S.L. was funded with the Sofja Kovalevskaja Award from the Alexander von Humboldt Foundation. In addition, this study was funded by the Deutsche Forschungsgemeinschaft (DFG LA 1419/3-1). This work was also supported by the MOI Manchot Graduate school (Jürgen Manchot Foundation).

K.S.L studied and wrote manuscript; N.S. performed most of the experiments and prepared the initial manuscript; N.H. performed many experiments; B.G and N.G, performed experiments; P.A.L, P.P. and D.H. analyzed data; T.M. provided Chop knockout mice.

5.8. *Figure legends*

5.8.1. *Fig. 1. Tunicamycin inhibits lymphocytic choriomeningitis virus–induced diabetes*

A: Rat insulin promoter-glycoprotein (RIP-GP) mice, expressing the lymphocytic choriomeningitis virus (LCMV) glycoprotein under the rat insulin promoter, were infected with 200 plaque-forming units (PFU) LCMV-WE. One group of mice was treated with 20 nmol tunicamycin on day 4 after infection. Induction of diabetes was monitored (n = 6).B: Survival of mice was analyzed (n = 6).

5.8.2. *Fig. 2. Tunicamycin reduces the infiltration of CD8+ T cells to the pancreas*

Rat insulin promoter-glycoprotein (RIP-GP) mice were infected with 200 PFU LCMV-WE. One group of mice was treated with 20 nmol tunicamycin on day 4 after infection. On day 6, mice were killed, and beta-islet cells were stained with immune fluorescence antibodies (n = 3). Scale bar, 100 µm.

5.8.3. *Fig. 3. Tunicamycin primarily kills CD8+ T cells*

A-B: C57BL/6 mice were infected with 200 PFU LCMV-WE. On day 6 after infection, one group of mice was treated with 20 nmol tunicamycin. On day 8, mice were killed, and numbers of subsets of cells in the spleen (A) (n = 3) and of LCMV-specific $CD8^+$ T cells in the blood (B) were counted (n = 3). One of two similar experiments is shown. C: Two million KL25 splenocytes were labeled with carboxyfluorescein succinimidyl ester (CFSE) and activated with LCMV-WE in the presence or absence of 10 µM tunicamycin. After 48 h, B-cell proliferation was measured by fluorescence-activated cell sorting (FACS) (n = 4).

5.8.4. *Fig. 4. Tunicamycin acts directly on T cells*

A-B: P14/CD45.1 splenocytes were labeled with CFSE and transferred to C57BL/6 mice. Mice were then infected with LCMV-WE or left uninfected in the presence or absence of 20 µmol tunicamycin. The proliferation capability (A) and the number (B) of T cells were determined by FACS (n = 3). C-D: MACS-sorted T cells were labeled with CFSE and stimulated with anti-CD3 and with or without anti-CD28, in the presence or absence of 10µM tunicamycin. After 3 days, the CFSE content (C) and the absolute number of CD8+ T cells (D) determined by FACS (n = 6). E: C57BL/6 mice were treated with 20 µmol tunicamycin or left untreated. P14/CD45.1

splenocytes were labeled with CFSE and transferred to the mice with or without LCMV-WE infection. The proliferation of T cells was determined by FACS (n = 4).

5.8.5. *Fig. 5. Tunicamycin induces the expression of chop in T cells*

A: P14 splenocytes were activated with GP33 peptide in the presence or absence of 10 μM tunicamycin. After 48 hours, chop gene expression was measured (n = 6). B: Chop knockout mice and C57BL/6 mice were infected with 2×106 PFU LCMV-WE. On day 4, mice were treated with 20 nmol of tunicamycin. CD8+ T cells in the blood were counted on day 8 (n = 3).

5.8.6. *Fig. 6. Tunicamycin reduces the expression of interleukin 2 and interferon γ*

A-B: After being cultured in a 24-well plate, 4×106 P14 splenocytes were activated with GP33 peptide in the presence or absence of 10 μM tunicamycin. After 24 hours, RNA was isolated, and the expression of interleukin-2 (IL-2, A) and interferon gamma (IFN-γ, B) mRNA was measured by real-time polymerase chain reaction (RT-PCR) (n = 6). C: C57BL/6 mice were infected with 200 PFU of LCMV-WE strain. On day four, mice were treated with 20 nmol of tunicamycin intravenously. On day 8 after infection, the cytotoxic capability of CD8+ T cells was determined with an in vivo killer assay (n = 4).

5.8.7. *Fig. 7. The comparison of tunicamycin to dexamethasone*

A: C57BL/6 mice were infected with 2×106 PFU LCMV-WE. On day 4, mice were treated once with 20 nmol of tunicamycin intravenously, or daily with 20 μg of dexamethasone intraperitoneally. Viral titers were analyzed on day 11 after infection (n = 4-6). B: C57BL/6 mice were injected with 10, 20, or 40 nmol tunicamycin or with 10, 20, or 40 μg of dexamethasone. Survival was monitored.

Figure 1

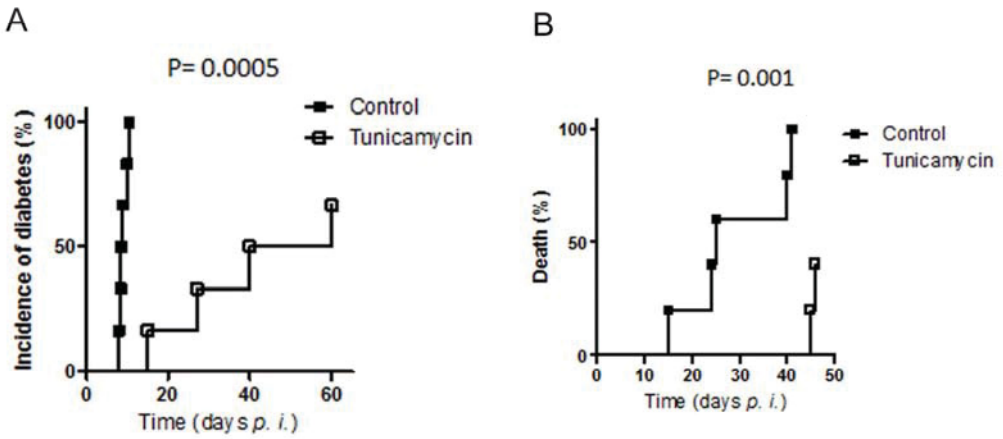

Figure 5-1 Tunicamycininhibits lymphocytic choriomeningitis virus-induced diabtets

Figure 2

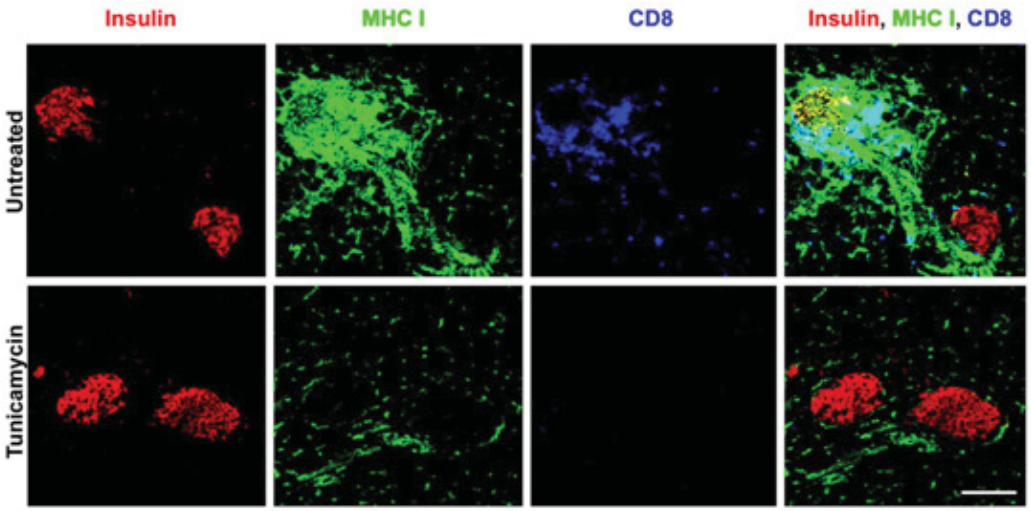

Figure 5-2 Tunicamycin reduces the infiltration of $CD8^+$ T cells to the panreas

Figure 3

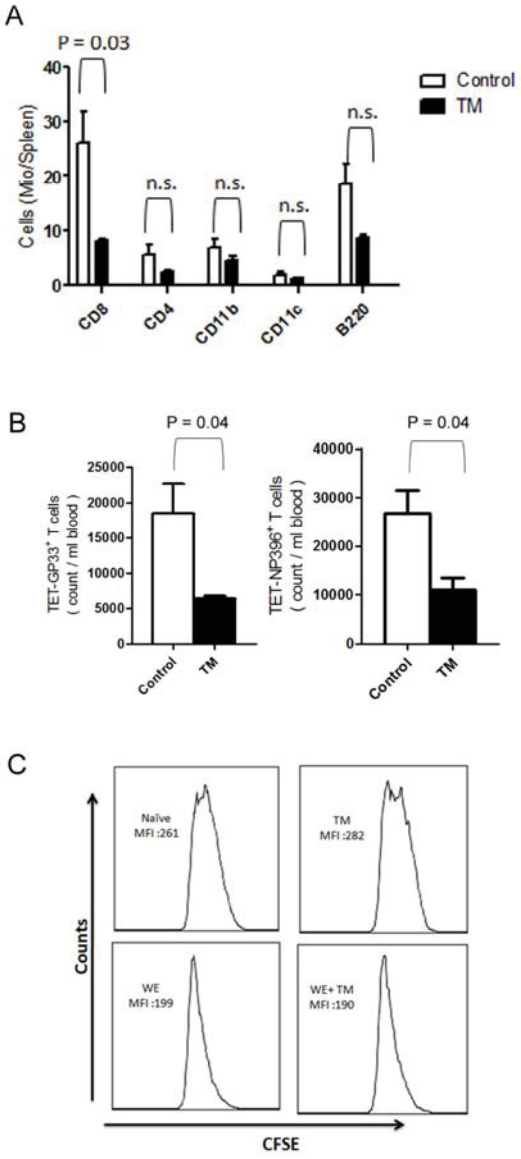

Figure 5-3 Tunicamycin primarily kills CD8$^+$ T cells

Figure 4

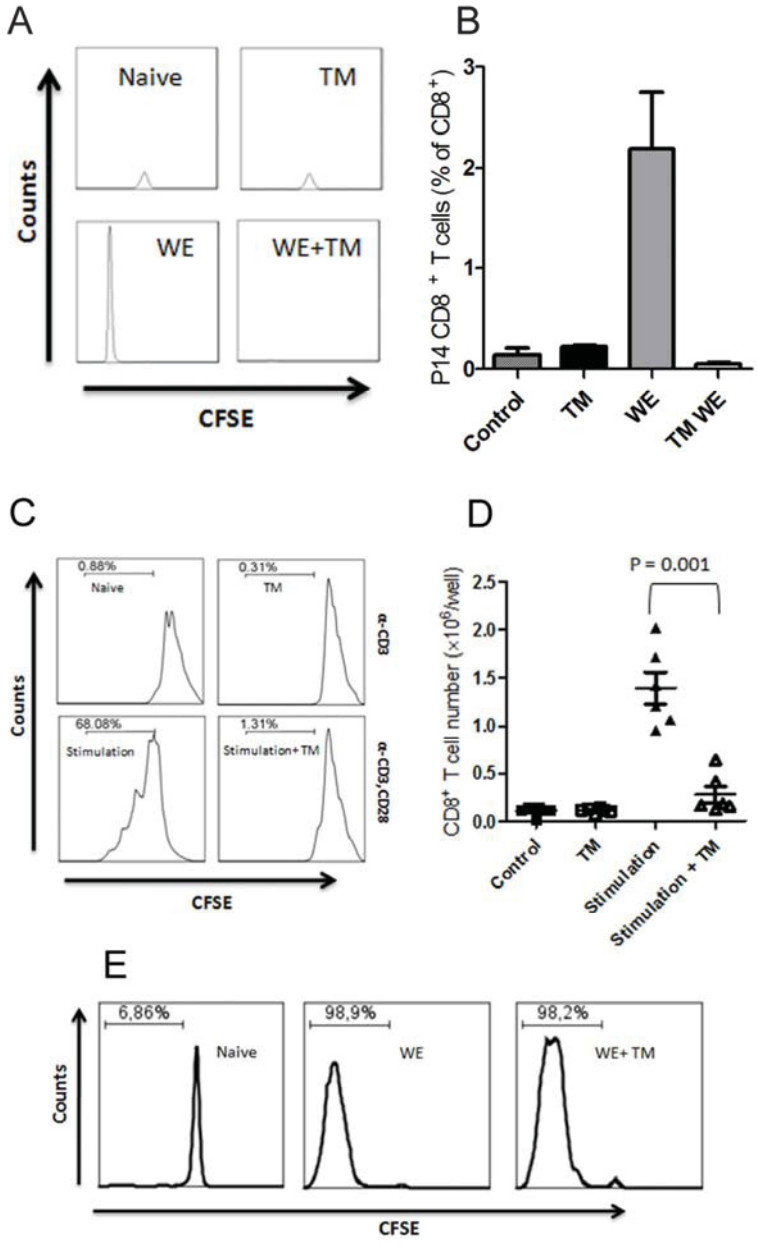

Figure 5-4 Tunicamycin acts directly on T cells

Figure 5

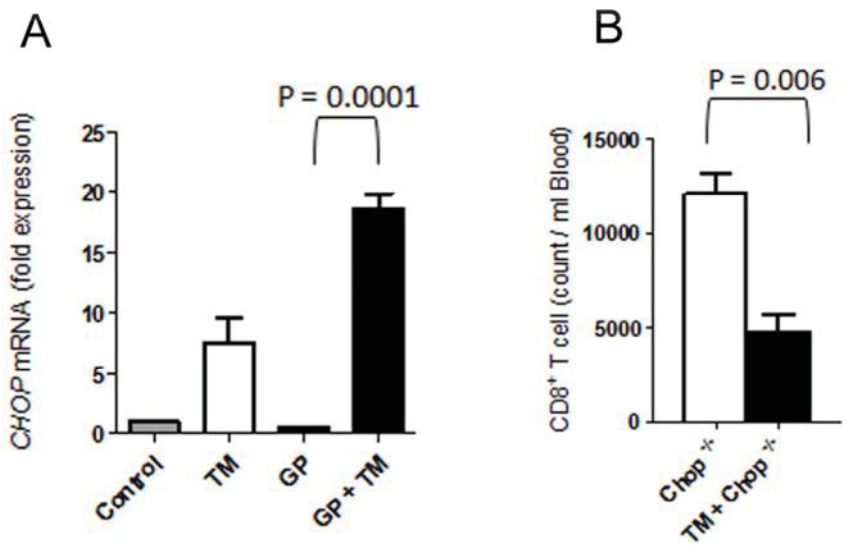

Figure 5-5 Tunicamycin induces the expression of *chop* in T cells

Figure 6

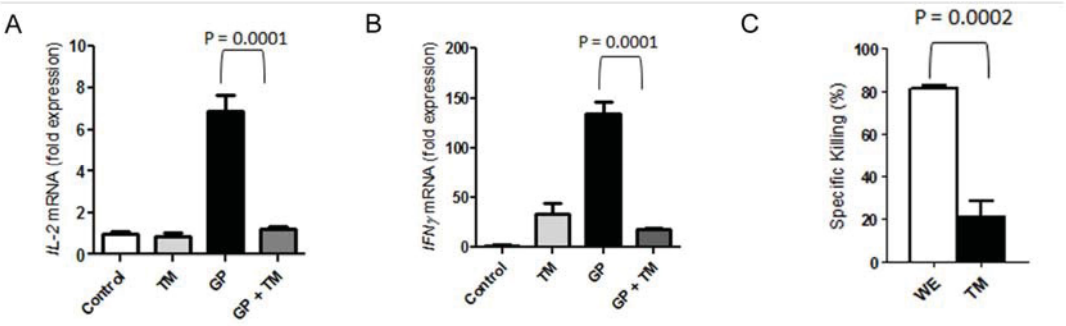

Figure 5-6 Tunicamycin reduces the expression of interleukin 2 and interferon γ

Figure 7

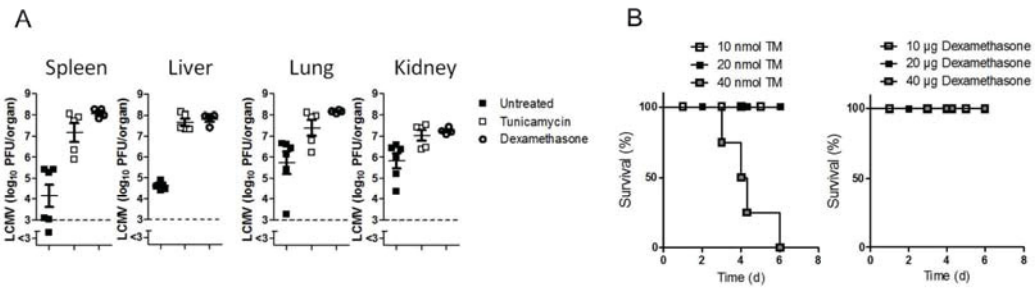

Figure 5-7 The comparsion of tunicamycin to dexamethasone

Anteilserklärung

4. Publikation:

Shaabani N, Honke N, Lang PA, Görg B, Proksch P, Gailus N, Gotoh T, Häussinger D, Lang KS

Tunicamycin inhibits diabetes.

Cell Physiol Biochem 2012; 29(3-4):595-602

Name des Journals:	*Cellular Physiology and Biochemistry*
Impact factor (Stand 2013):	3,415
Anteil an Experimenten in dieser Arbeit (%):	80%
Autor:	Erstautor
Beitrag an dieser Arbeit:	Herr Namir Shaabani war für den größten Teil der Durchführung und Auswertung der praktischen Experimente sowie für das experimentelle Design verantwortlich. Er war außerdem an der Manuskripterstellung beteiligt.

_____ _____

Namir Shaabani Prof. Dr. Karl Lang

6. Chapter VI: Oxidized ATP inhibits T-cell-mediated autoimmunity

Philipp A Lang , Doron Merkler, Pauline Funkner , Namir Shaabani , Andreas Meryk , Caroline Krings , Carmen Barthuber , Micke Recher, Brück W, Dieter Häussinger,Pamela S Ohashi ,Karl S Lang

6.1. Abstract:

T cells directed against self antigens play an important role in several autoimmune diseases. The available immunosuppressive compounds used to treat autoimmune diseases are limited, and often they have side effects which limit their application. T cells express ATP receptors, which could be new target molecules to treat autoimmune disease. Here we analyzed the effect of oxidized ATP (oxATP), an inhibitor of the ATP receptor P2rx7, in different murine models of T cell-mediated autoimmune diseases. Treatment with oxATP inhibited proliferation and effector function of T cells. The systems we used, oxATP did not obviously interfere with the innate immune response, but strongly reduced antigen-specific T cell responses. This treatment ameliorated T cell mediated autoimmune type I diabetes and autoimmune encephalitis in mice. In conclusion, oxATP was found to strongly inhibit activated T cells and could thus be used to target T cell-mediated autoimmune disease.

6.2. Introduction

T cells are crucially involved in various autoimmune diseases. Autoimmune diseases such as type I diabetes, multiple sclerosis, severe rheumatoid arthritis or systemic lupus erythematosus can lead to life threatening complications, or lifelong disability, respectively. Therefore effective, early and specific interference with ongoing self-destructive inflammation could contribute to a better prognosis. Several compounds have so far been tested for their ability to suppress immune reactions. Glucocorticoids, tacrolimus or cyclosporine have a strong T cell suppressive effect, but show severe side effects [196,211-214]. A new generation of so called “biological” compounds include antibodies which are directed against molecules that are important in T cell activation. How these novel therapeutic approaches will influence disease and which side effects may develop after long term antibody treatment is being explored [215-218].

Oxidized ATP (oxATP) was recently discovered as an antagonist of the ATP receptor P2rx7 [219] which is also expressed on activated T cells [220-223]. ATP sensitive cation channels have been shown to be important in T cell activation [220] . Activation of P2rx7 leads to ion channel activity which can depolarize the cell. This can lead to activation of several signaling cascades including Protein Kinase C (PKC) as well as the MAPK pathway [224-227]. Those processes can influence T cell activation and

maintenance [228-236]. Evidence also suggested that oxATP may inhibit ATP dependent pathways [237], which are probably crucial in highly activated cells.

Here we analyzed the immunosuppressive activity of oxATP in a prototypic virus-induced autoimmune diabetes model in mice. We found that oxATP had limited effects on viral replication and on the innate immune system, but it caused a strong suppression of T cell activity. In addition, a single dose of oxATP was sufficient to block T cell dependent induction of autoimmune diabetes and to delay the onset of experimental autoimmune encephalitis (EAE).

6.3. Results and discussion

6.3.1. *OxATP inhibits LCMV-induced diabetes and T cell expansion*

To analyze whether oxATP influences onset of type I diabetes we used a model of $CD8^+$ T cell mediated autoimmune diabetes [41,238]. In this model a viral antigen (the LCMV-glycoprotein) is expressed under the rat insulin promoter and thus expression restricted to pancreatic islets. Priming of $CD8^+$ T cells with LCMV-WE will induce β-islet-specific $CD8^+$ T cells, which then will destroy pancreatic β-islet cells leading to diabetes. To test the effect of oxATP in diabetes we infected RIP-GP mice with LCMV-WE and then treated one group of mice with 1mg oxATP on day 4. Treatment with oxATP suppressed the induction of diabetes in 75% of the treated mice (Fig. 1A).

In addition to the adaptive immune system, diabetes onset in this model needs activation of the innate immunity [101,102,174,239]. Therefore we analyzed induction of type I interferon and virus distribution after treatment with oxATP. We treated C57BL/6 mice with 1mg oxATP and infected them with LCMV-WE. Mice were then further monitored for production of IFN-α. We did not find any significant difference in IFN-α production between oxATP treated and control mice (Fig. 1B). Accordingly, there was no significant difference in early virus replication in mice treated with oxATP (Fig. 1C). Next we analyzed if the distribution of splenocyte subsets was affected by oxATP. We injected naïve non-infected or LCMV-WE infected mice with 1mg oxATP or 1mg ATP. An additional group was left untreated. One day after injection we analyzed total amount of cells in the spleen. In mice which were not infected with LCMV, neither oxATP nor ATP changed the total numbers of

splenocytes (Fig. 1D). In contrast injection of LCMV infected mice with oxATP decreased significantly the numbers of $CD4^+$ and $CD8^+$ T cells and $CD11b^+$ cells (Fig. 1E). There was no statistically difference in B cell numbers and $CD11c^+$ cells between oxATP treated and untreated mice (Fig. 1E). Activated CD8+ T cells showed the strongest sensitivity to oxATP (3.2 ± 0.5 fold change to untreated mice). CD4+ T cells were reduced by 2.1 ± 0.39 fold and $CD11b^+$ cells were reduced by 2.1 ± 0.27 fold. From those data we concluded that oxATP affected T cell proliferation. In addition oxATP might slightly influence innate immune cells. Because the induction of diabetes in the RIP-GP model is strongly dependent on CD8 T cells, we concluded that the reason for reduced diabetes in oxATP treated mice was very likely due to oxATP dependent depletion of activated CD8+ T cells. Because we have not seen any effect of oxATP in naïve mice, we suggested that only activated CD8+ T cells were sensitive to oxATP. In line with this, virus-specific T cells were significantly reduced upon treatment with oxATP (Fig. 1F). This reduction in frequency correlated with a reduced cytotoxic function (Fig. 1G). Immunohistology showed that β-islets in control mice were infiltrated by CD8 T cells (Fig. 1G). Some islets did not stain for Insulin, suggesting that cells in this β-islet have lost their function (Fig. 1G). RIP-GP mice which were treated with oxATP did hardly show any CD8 T cells within the pancreas (Fig. 1G). In conclusion we found that oxATP reduced the frequency and function of $CD8^+$ T cells, which led to reduced infiltration of pancreatic β-islets and protection form diabetes.

6.3.2. *OxATP inhibited IFN-γ production and induced apoptosis in T cells*

We found that oxATP specifically reduced T cell responses during LCMV infection. Infection with LCMV usually induces a robust $CD8^+$ T cell response in mice, which is hardly affected by several known immune regulatory molecules [240-242]. Therefore we considered the effect of oxATP potent and underwent further analysis. To analyze the effect of oxATP on activated T cells, we infected mice with LCMV to induce virus-specific T cells. Eight to ten days after infection, virus-specific $CD8^+$ T cells were challenged in vitro with different concentrations of oxATP.

According to our in vivo data we found that oxATP inhibited cytotoxic T cell activity in vitro (Fig. 2A). OxATP directly acted on T cells as pre-treatment of target cells with oxATP did not affect cytotoxicity of effector T cells (Fig. 2A). Next we

measured intracellular IFN-γ after restimulation. OxATP inhibited IFN-γ production with an IC50 of about 50µM (Fig. 2B). OxATP did not inhibit TCR signaling upstream of Proteinkinase C and intracellular Ca^{2+} influx. This could be seen by activation of T cells with the Proteinkinase C activator PMA together with the ionophore ionomycin which was similarly blocked by oxATP (Fig. 2B).

Next we analyzed the effect of oxATP on memory versus naïve T cells. Therefore we stimulated naïve or memory GP33-TCR transgenic T cells with GP33 peptide with different concentrations of oxATP. In this assay we stimulated naïve and memory T cells for 16 hours with antigen to guarantee IFN-γ production in naïve T cells. In parallel we analyzed induction of apoptosis by oxATP. We found that oxATP inhibited IFN-γ production in both memory and naïve T cells (Fig. 2C). Only at higher concentrations of oxATP increased apoptosis was observed (Fig. 2C). In line with these results, 100µM oxATP blunted the production of IL-2 (Fig. 2D). Concentrations above 100µM in addition induced cell death in $CD8^+$ T cells (Fig. 2C&D). oxATP dose-dependently inhibited expansion of $CD8^+$ T cells in vitro (Fig. 2E).

In conclusion we found that T cell mediated cytokine secretion was blunted by oxATP. Increasing concentrations of oxATP in addition led to apoptosis. Form this results we would suggest that oxATP causes cell stress in activated T cells.

6.3.3. *T-cell suppression of oxATP is independent from P2X7, but is not due to general toxicity*

In previous studies it was shown that T cells express the receptor P2rx7 which indeed influences T cell activation [220,222,223,243-245]. We found that P2rx7 is expressed on naïve $CD8^+$ T cells (Supplementary Fig. 1). Upon activation it is down-regulated but still expressed about background level (Supplementary Fig. 1). Analyzing the *P2rx7*$^{-/-}$ mice showed a normal $CD8^+$ T cell response against LCMV when compared to wildtype mice (Supplementary Fig. 1). In vitro treatment with oxATP showed that the effect of oxATP was not dependent on P2rx7. Thus, oxATP may be effective through mechanisms distinct from P2X7 signaling [237,246]. Finally, we analyzed the in vivo toxicity of oxATP. We did not find any toxic effects when treating mice with 1mg oxATP (Supplementary Figure 2). Survival and vital organ functions of kidney

and liver were not affected. Only higher doses of oxATP (2mg) was associated with mortality and signs of organ pathology (Supplementary Fig. 2).

6.3.4. *OxATP inhibits onset of $CD4^+$ T cell dependent experimental allergic encephalitis (EAE)*

We found that oxATP can strongly inhibit activation of $CD8^+$ T cells and onset of $CD8^+$ T cell mediated disease. To further evaluate the role of oxATP in T cell-mediated disease we applied the experimental autoimmune encephalomyelitis (EAE) model, a widely used animal model for the human disease of multiple sclerosis [247]. The induction of disease in this model is strongly dependent on the activation of $CD4^+$ T cells reactive against the myelin-derived MOG peptide (MOG_{35-55}). We found that a single dose of 1mg oxATP, given shortly before onset of disease could significantly ameliorate the course of the disease (Fig. 3A). In addition, histology of the spinal cord revealed a significant reduction of demyelinization in oxATP treated animals (Fig. 3B). In conclusion we found that oxATP inhibited onset of T cell dependent autoimmune diseases.

6.4. Concluding remarks

OxATP inhibited intracellular IFN-γ production and reduced frequencies of activated T cells in vivo. In vitro this correlated with lack of proliferation, IFN-γ production and at higher concentrations with induction of apoptosis. In a model of T cell mediated disease we found prevention or amelioration of disease upon a single application of oxATP. As those models have similarities with human disease [238,247] the questions raises if there is some implications of oxATP for treatment in humans. Due to the narrow therapeutic index, OxATP may not qualify for chronic maintenance treatment of autoimmune diseases. However, due to the striking in vivo effect of single doses, it might be used in life threatening flares in autoimmune diseases where other immunesuppressive agents act to slowly. In conclusion, we have shown that oxATP is a strong and very fast acting immunosuppressive drug, which can inhibit T cell mediated autoimmune-disease in vivo.

6.5. Materials and methods

6.5.1. Mice treatment, viruses

LCMV strain WE was originally obtained from F. Lehmann-Grube (Heinrich Pette Institute, Hamburg, Germany) and was propagated in L929 cells. Virus titers were measured using a focus forming assay as described [142]. Mice were infected with 200 plaque forming units (PFU) LCMV-WE. All mice used in this study were maintained on the C57BL/6 genetic background. For analysis of autoimmune diabetes RIP-GP mice were used [41]. RIP-GP express the LCMV Glycoprotein as a transgen under the rat insulin promoter [43]. For T cell studies P14 mice were used. P14 mice express the LCMV GP33-peptide-specific TCR as a transgen [43]. All experiments were performed in single ventilated cages. Animal experiments were carried out with authorization of the Veterinäramt of the Kanton Zurich and in accordance with the Swiss law for animal protection or in accordance with the Ontario Cancer Institute guidelines. Oxidized ATP was purchased by Sigma-Aldrich (Oakville) and solved in PBS for animal treatment.

6.5.2. Diabetes

Measurement of blood sugar was done using Elite sensor (Bayer). Mice were considered to be diabetic if blood sugar was above 14mM for two consecutive days.

6.5.3. Induction and Clinical Evaluation of EAE

For EAE induction, female 8- to 9-week-old mice from each group were immunized subcutaneously with 200 mg of $MOG_{35–55}$ peptide emulsified in CFA containing 1 mg of Mycobacterium tuberculosis (H37RA; Difco Laboratories, Detroit, MI). The mice received intraperitonal injections with 250 ng pertussis toxin (Sigma-Aldrich, Deisenhofen, Germany) at the time of immunization and 48 hr later. Mice were scored daily as follows: 0, no detectable signs of EAE; 0.5, distal limb tail; 1.0, complete limb tail; 1.5, limb tail and hind-limb weakness; 2, unilateral partial hind-limb paralysis; 2.5, bilateral partial hind-limb paralysis; 3, complete bilateral hind-limb paralysis; 3.5, complete hind-limb paralysis and unilateral forelimb paralysis; 4, total paralysis of forelimbs and hind limbs; and 5, death.

6.5.4. Histology

Histological analysis of virus infection experiments were performed on snap frozen or formaline fixed tissue as described [142]. Sections were stained with rat

monoclonal antibodies anti-CD8. Histological analysis of EAE was performed on paraffin embedded tissue. LFB/PAS stainings were performed to evaluated extend of demyelination. For this purpose, surface area of demyelinated was measured of 8-10 spinal cord sections per animal comprising the cervical to lumbal spinal cord level. Extent of demyelination was then calculated and expressed in % of analyzed spinal cord white matter.

6.5.5. *FACS analysis*

Tetramer staining, surface and intracellular FACS staining was performed as described previously [142]. Briefly, splenocytes or peripheral blood lymphocytes were stained using PE-labeled or APC-labeled gp33 MHC class I tetramers (gp33/H-2D^b) for 15 minutes at 37°C, followed by staining with anti-CD8-PerCP (BD Biosciences, USA) for 30 minutes at 4°C. Tetramers were house- made or provided by the NIH Tetramer facility. For intracellular IFN-γ staining cells were fixed with formalin and then permeabilized using saponin.

6.5.6. *Cytotoxicity assay*

^{51}Cr release assays were performed as previously described [248] and supernatants analyzed after 8 hours. Release of chromium is given in percent of chemically lysed cells. Splenocytes were titrated and ratio of splenocytes to target cells is shown on the x-axis.

6.5.7. *In vitro activation*

T Cells were purified using MACS beads (untouched) according to the manufactures protocol. 500000cells/well (24 well plate) were plated and activated with GP33 (1µg/ml).

6.5.8. *IL-2 ELISA*

was purchased from eBiosciences and performed according to the manufacturer's protocol.

6.5.9. *MTT assay*

5 x10^6 cells were cultured in 24 wells plate with and without oxATP 200µM, 100µM or gp33 peptide (1µg/ml). Cells were incubated overnight (37°C, 5% CO_2). MTT (Sigma, M2128) was added for 3h (37°C, 5% CO_2) and its purple formazan substrate was quantified in a spectrophotometer by 560nm.

6.5.10. *Statistical analysis*

Data are expressed as mean ± S.E.M. Statistical significant differences between two different groups were analyzed using students t test. For MTT Assay paired students t test was performed. Analysis including several groups were tested with one-way ANOVA with additional Bonferoni or Dunnett test. Statistically significant differences between treatment groups in experiments involving more than one analysis timepoint were calculated using two-way ANOVA (repeated measurements). p values < 0.05 were considered as statistically significant.

6.6. Acknowledgments

We would like to thank Alisha Elford for technical support. The authors would also like to acknowledge the NIH tetramer facility for providing tetramers. This study was supported by the Sonderforschungsbereich SFB575, Experimentelle Hepatologie (Sprecher: Prof. Dieter Häussinger). Karl Lang was funded with the Sofja Kovalevskaja Award by the Alexander von Humboldt foundation. In addition this study was funded by the Manchot Graduiertenschule. This work was also supported by CIHR grant FRN 79434 to PSO. PSO holds a Canada Research Chair in Autoimmunity and Tumor Immunity. Doron Merkler and Wolfgang Brück are supported by the Sonderforschungsbereich SFB/TR43.

6.7. Figure legends

6.7.1. *Figure 1: oxATP inhibits LCMV-induced diabetes, but does not affect innate immunity*

A: RIP-GP mice were infected with 200 pfu LCMV-WE. One group of mice was treated with 1mg oxATP on day 4 after infection. Induction of diabetes was monitored ($n = 7 – 10$, $p = 0.0015$). Data were pooled from three independent experiments. B: C57BL/6 mice were treated with 1mg oxATP intravenously. After 1 hour mice were infected with 200 pfu of LCMV-WE. At days 1 and 3 after infection, IFN-α was measured in the serum ($n = 3$). One of two similar experiments is shown. C: C57BL/6 mice were treated with 1mg oxATP intravenously. After 1 hour mice were infected with 2x106 pfu of LCMV-WE. Viral titers were analyzed on day 3 after infection ($n = 3$). One of two similar experiments is shown. D: C57BL/6 mice were treated with 1 mg oxATP, 1 mg ATP or were left untreated. Subset of cells in the spleen were

analyzed after one day (n = 6). Data were pooled from two independent experiments. E: C57BL/6 mice were infected with 200 pfu LCMV-WE. On day 6 mice were treated with 1mg oxATP, 1mg ATP or were left untreated. Subset of cells in the spleen were analyzed on day 7 (n = 6). Data were pooled from two independent experiments. F: C57BL/6 mice were infected with 200pfu LCMV-WE. On day 6 mice were treated with 1mg oxATP intravenously. On day 7 LCMV-specific $CD8^+$ T cells were measured in the blood (n = 3). One of three similar experiments is shown. G: C57BL/6 mice were infected with 200pfu LCMV-WE. On day 6 mice were treated with 1mg oxATP intravenously. Direct ex vivo cytotoxic activity of LCMV-specific splenic $CD8^+$ T cells were analyzed on day6, with and without 24 hour treatment with oxATP (day7, day7 oxATP, n = 3). One of two similar experiments is shown. H: RIP-GP mice, expressing the glycoprotein of LCMV under the rat insulin promoter were infected with 200pfu LCMV-WE. One group of mice was treated with 1mg oxATP on day 4 after infection. On day 6 pancreas was stained for anti-insulin (green) and anti-CD8. Two representative islets from untreated mice, and one representative islet of oxATP treated mice is shown. Immunohistology was performed from 5 mice/group out of two independent experiments. Scale bars indicate 50µm.

6.7.2. *Figure 2: oxATP inhibits T-cell function in vivo following virus infection*

A: Splenocytes obtained from mice 8-10 days following LCMV-WE infection were analyzed in a direct ex vivo cytotoxicity assay with or without addition of titrated doses of oxATP. As a control, target cells were pretreated with oxATP for 2 hours and then used in the cytotoxicity assay. One of two similar experiments is shown. B: Splenocytes obtained from mice 8-10 days following LCMV-WE infection were removed and re-stimulated in vitro with the immuno-dominant LCMV-derived peptide GP33-41 in the presence of titrated concentrations of oxATP. PMA/Ionomycin was used as an alternative T-cell-activating compound. After 6 hours of in vitro re-stimulation, intracellular production of IFN-γ in T cells was analyzed by FACS analysis. One of two similar experiments is shown. C: Naïve or memory (day 100 after 200pfu LCMV-WE) splenocytes of p14 mice (about 90% of all $CD8^+$ T cells are specific for the GP33 epitope, see the Methods and methods section) were stimulated with GP33-41 peptide at titrated oxATP concentrations. After 16 hours intracellular cytokine accumulation was analyzed. In parallel,

expression of annexin V was measured (n = 6). Data were pooled from two independent experiments. D: P14 Splenocytes were restimulated with GP33 with and without oxATP. After 24 hours IL-2 was measured in the supernatant. Apoptotic T cells were analyzed using Annexin V (n = 4). One of two similar experiments is shown. E: P14 Splenocytes were activated with GP33 peptide in presence or absence of oxATP. After 24 hours, cell expansion and viability was analyzed using MTT Assay (n = 3-4). Data are pooled from two experiments.

6.7.3. *Figure 3: oxATP inhibits onset of $CD4^+$ T-cell-dependent experimental allergic encephalitis (EAE)*

C57BL/6 mice were immunized with the MOG-peptide (200mg s.c.). Ten days after immunization animals were once either treated with 1mg of oxATP (n = 13) or PBS (n = 15). Data were pooled from two independent experiments. A: Mice were monitored using the EAE score. B: Representative LFB/PAS stained spinal cord sections of PBS-treated or oxATP-treated animals. Arrowheads indicate demyelinated area. Quantification of demyelinated areas (right panel) showed in average a reduction of demyelinated areas in oxATP-treated animals.

6.7.4. *Supplementary Figure 1: $P2rx7^{-/-}$ cells are influenced by oxATP*

A: P14 T cells were FACS-sorted and in vitro restimulated with GP33 peptide. Expression of *P2rx7* mRNA was analyzed using RT-PCR on days 0, 1 and 2 (n = 4). B: $P2rx7^{-/-}$ mice were infected with 200PFU of LCMV-WE. Nine days after infection IFN-gamma production was analyzed after in-vitro restimulation of virus-specific T cells by the indicated LCMV-specific peptides (n = 3). C: Splenocytes from $P2rx7^{-/-}$ mice and control mice were restimulated in vitro with different concentrations of oxATP. Intracellular IFN-gamma was analyzed (n = 6).

6.7.5. *Supplementary Figure 2: Toxicity of oxATP*

C57BL/6 mice were treated with 1mg or 2mg oxATP or were left untreated. A: Survival was analyzed (n = 4). B: ALT levels were analyzed on days 1 and 2 (n = 3 - 4). C: Urea was analyzed on days 1 and 2 (n = 3 - 4). D: Creatinin was analyzed on days 1 and 2 (n = 3 - 4).

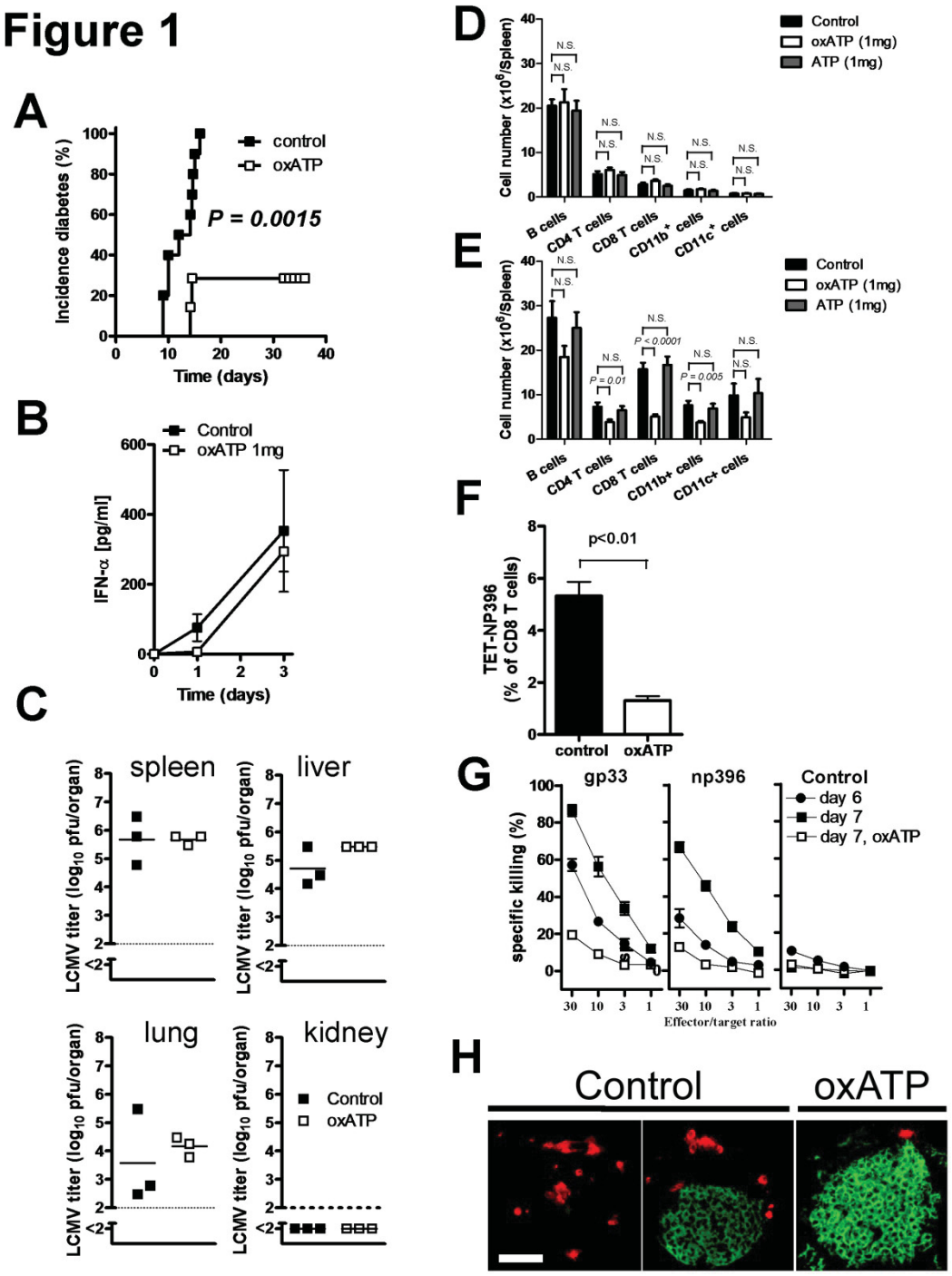

Figure 6-1 oxATP inhibits LCMV-induced diabetes, but does not affect innate immunity

Figure 2

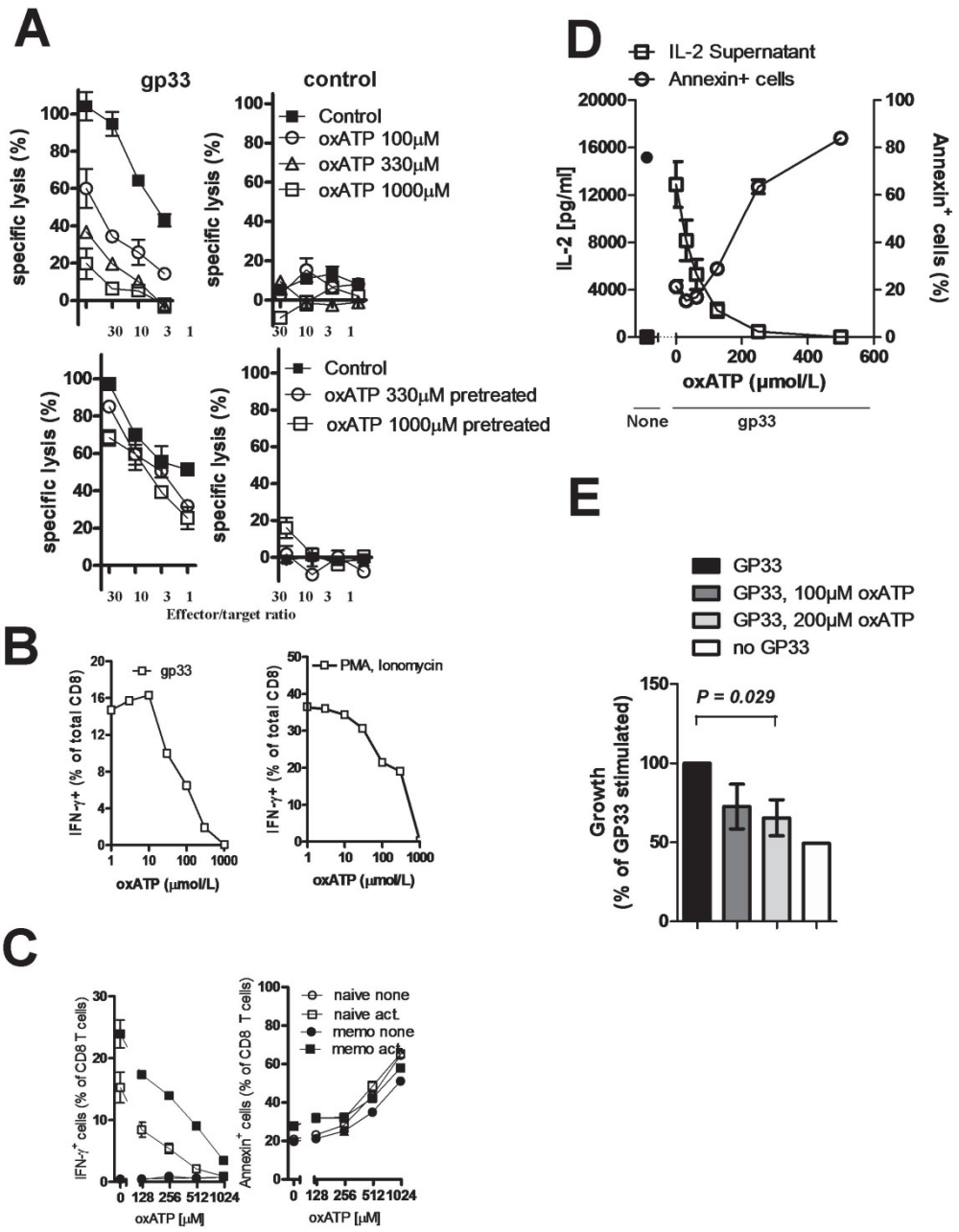

Figure 6-2 oxATP inhibits T-cell function in vivo following virus infection

Figure 3

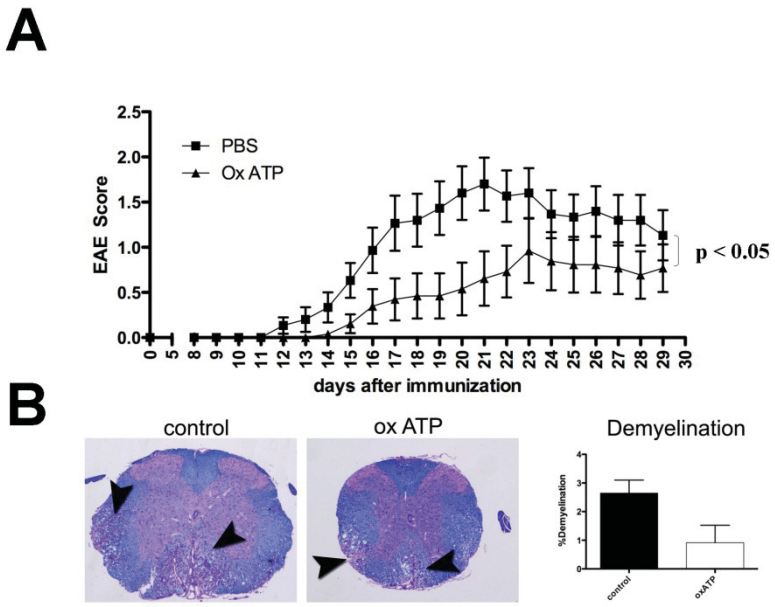

Figure 6-3 oxATP inhibits onset of $CD4^+$ T-cell-dependent experimental allergic encephalitis (EAE)

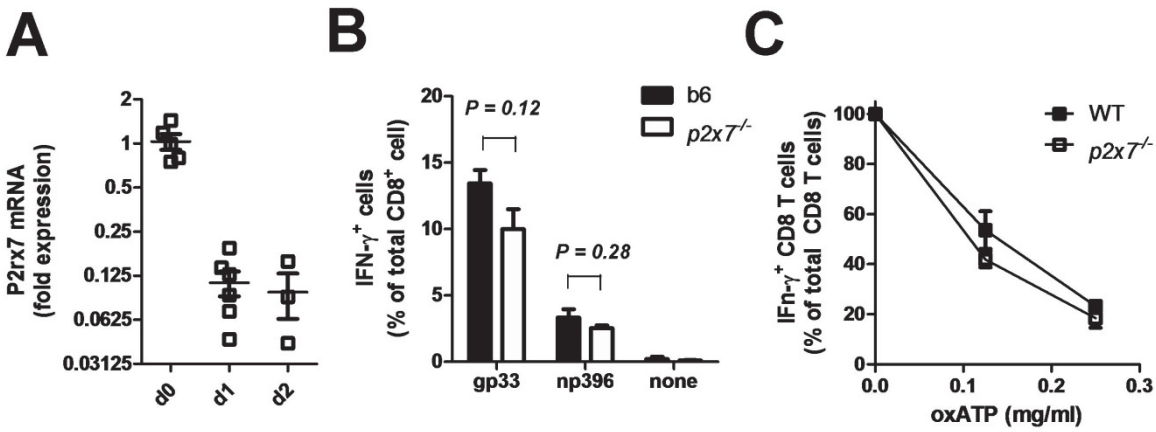

Supplementary Figure 6-1 P2rx7$^{-/-}$ cells are influenced by oxATP

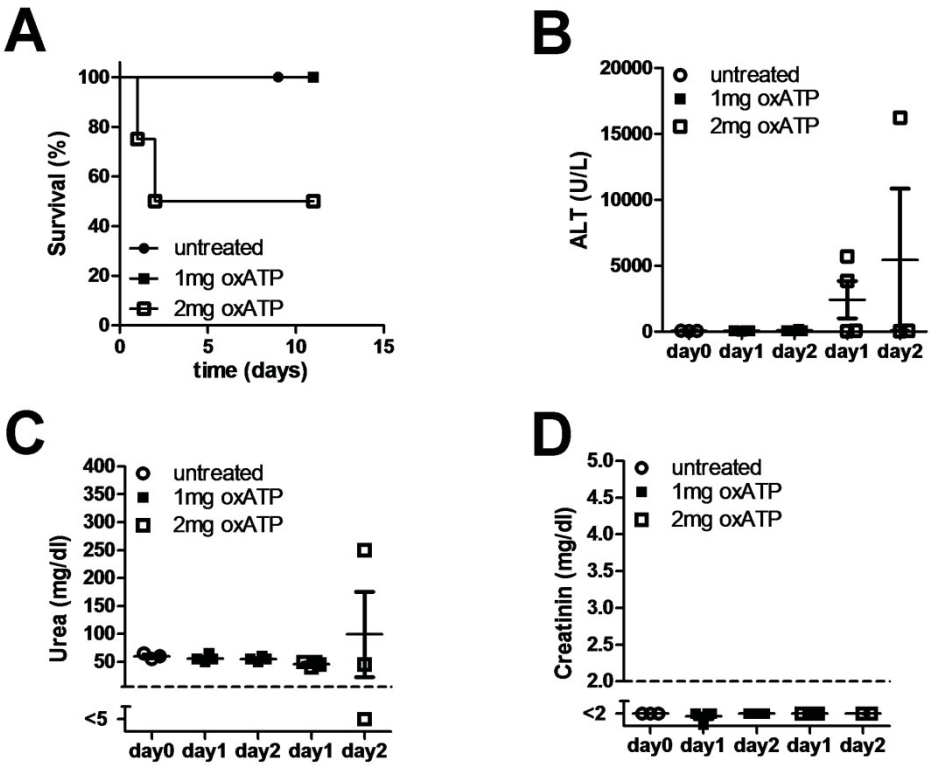

Supplementary Figure 6-2 Toxicity of oxATP

Anteilserklärung

5. Publikation:

Lang PA, Merkler D, Funkner P, Shaabani N, Meryk A, Krings C, Barthuber C, Recher M, Brück W, Häussinger D, Ohashi PS, Lang KS

Oxidized ATP inhibits T-cell-mediated autoimmunity

Eur J Immunol. 2010 Sep;40(9):2401-8.

Name des Journals:	*European journal of immunology*
Impact factor (Stand 2013):	4,97
Anteil an Experimenten in dieser Arbeit (%):	22%
Autor:	Co-Autor
Beitrag an dieser Arbeit:	Herr Namir Shaabani war für ein Teil der Durchführung und Auswertung der praktischen Experimente verantwortlich.

Namir Shaabani

Prof. Dr. Karl Lang

7. Chapter VII: General discussion

In these studies, we have provided novel insights into understanding type I diabetes, by trying to clarify the mechanism of the incidence of the disease, we may have uncovered potential novel treatment strategies. Currently, autoimmune disease treatment strategy can be classified into four categories according to their mechanism of action

1) Mono and polyclonal antibodies: which are prepared either by immunization of rabbits or horses with human lymphoid cells or by hybridoma technology. These antibodies are directed against some clusters of differentiation which are expressed on T cells such as anti-CD3 Muromonab or interleukin 2 receptor antagonists (Basiliximab) [249] , or they can also be directed against B cells receptors like anti-CD20 (Rituximab) [250].
2) Selective inhibitors of cytokine production or function: the most popular medicine is cyclosporine [251], it binds to cyclophillin (also called immunophillin) which then binds to calcineurin and inhibits the production of interleukin-2. Similarly, there are also tacrolimus [252] and sirolimus [253] which bind to alternative immunophillins.
3) Immunosuppressive antimetabolites: including Azathioprine and mycophenolate mofetil.
4) Corticosteroids: which are considered the first line therapy as immunosuppressive but their mechanism of action is not clear yet.

In this study we found that tunicamycin and oxATP could be a good candidate as new potential medicines. Tunicamycin and oxATP can be categorized under the immunosuppressive drugs as selective inhibitors of cytokine and immunosuppressive antimetabolites.

We found that oxATP had a strong inhibitory effect on the IFN-γ production of T cells *in vitro* and *in vivo*. In RIP-GP mouse model, oxATP suppressed activation of T cell responses and inhibited the activation of T cell mediated autoimmune diabetes and autoimmune encephalitis [254].

We showed that tunicamycin can prevent type I diabetes by reducing the proliferation of T cells, primarily active antigen-specific $CD8^+$ T cells [255]. This strong effect of tunicamycin could also be important for treating other types of diseases that are related to autoimmune responses like graft-versus-host (GVH). However, due to

the narrow application window of tunicamycin, specific cell toxicity will probably be demand. The results of study may be a one step further in the way to understand and design treatment for type I diabetes in humans, of course after the determination of safty factors, including the therapeutic dose, the proper route of administration, and the accompanying adverse effects.

In this study, we found also that antigen presenting cells allow the replication of the virus in order to prime the adaptive immune system. In case of viral infection, red pulp macrophages and kupffer cells track down the virus and suppress its replication in a type I interferon-dependent manner. In contrast, $CD169^{+}$ macrophages allow the viral replication by inhibiting the interferon signaling through upregulation of *Usp18* expression. In case of depletion of $CD169^{+}$ macrophages or the deficiency of *Usp18*, the adaptive immune system was not promoted and viral infection was not controlled [126].

The architectural shape of the situated cells in the spleen are designed to achieve the optimal striving to the infection, $CD169^{+}$ macrophages are connected to fibroblastic reticular cells conduits, which can transport antigen to DC's in T cell zone and/or presenting the antigen to B cells.

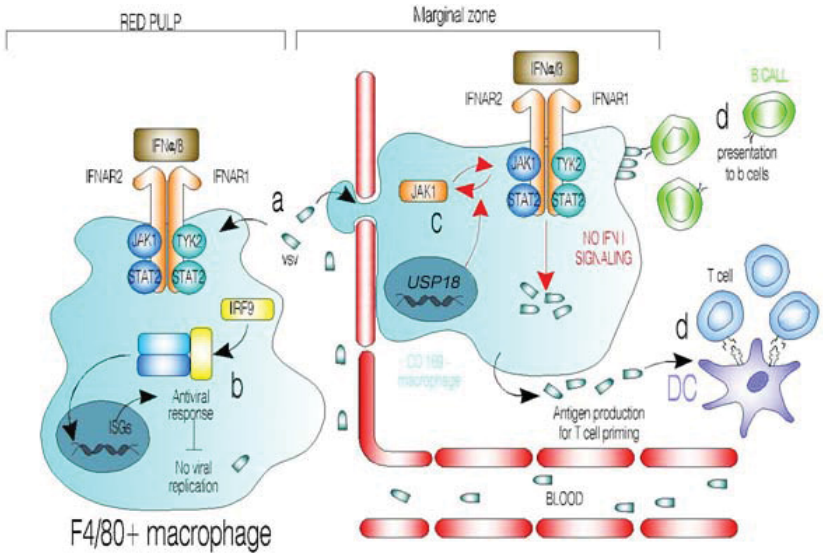

Figure 7-1 CD169+ macrophages take up the bullet

Burkhard Ludewig & Luisa Cervantes-Barragan (Nature Immunology 2012) (modified)

UBP43 as an inhibitor of type I interferon response not only allows virus replication by reducing the antiviral actions of IFN-I but also impairs IFN-I driven

proteasomal degradation [135], cross-priming [90,136] and co-stimulatory molecules on APCs [256]. While the inhibition of the latter would generally favor adaptive immune responses, impaired IFN-I signaling in $CD11c^+$ cells was still of overall benefit for effective autoantigen-specific $CD8^+$ T cell priming. Thus, our results indicate that treatment of humans with inhibitors of IFN-I, which are used in clinical studies for systemic lupus erythematosus [257], might in some cases contribute to the autoimmune disease, especially in the presence of a virus infection.

On the other hand, the enhancement of the amount of foreign viral antigen through enforced viral replication can lead to breaking of the immunological ignorance and activation of the immune system. Using the RIP-GP mice model, we investigated why replicating self-antigen is much more efficient in breaking autoimmune tolerance than the presence of non-replicating self-antigen. Antigen presenting cells, mainly $CD169^+$ macrophages and $CD11c^+$ dendritic cells, were responsible for the replication of autoantigen in a type I interferon dependent manner, leading to onset of autoimmune diabetes [258].

Since *Usp18* expressing APCs are only slightly responsive to the antiviral actions of type I interferons, they act as endogenous "replicators" of auto-antigen. We hypothesize that enforced viral replication is also of importance in dendritic cells for initiating innate and adaptive immune response against LCMV. We found that DC's have high expression of *Usp18* contrary to macrophages or fibroblasts, which could explain the long-known phenomenon, those DCs can be easily infected with several viruses. The presence of non-replicating auto-antigen could not activate the adaptive immune system which demonstrate the important role of enforced viral replication in helping the adaptive immune system to distinguish between foreign and self antigen.

We would like to emphasize that the autoimmune disease model studied here is a model of organ-specific autoimmunity induced by $CD8^+$ T cells and the results cannot be extended to autoimmune diseases in general at this stage. Further studies are needed to evaluate whether the mechanisms described here are of importance for other organ-specific or systemic autoimmune diseases.

Histological staining showed the replication of LCMV mainly in the $CD169^+$ macrophages and $CD11c^+$ cells. By using CD11c-DTR mice and depleting $CD11c^+$ cells, the early replication of LCMV was completely blunted in the spleen. On the

other hand, depletion of $CD169^+$ macrophages by using CD169-DTR mice showed minor effect on the viral replication.

Several previous studies proposed that viral infection may be involved in different autoimmune diseases including autoimmune diabetes. By using various knockout mouse models, we explained in this study how viruses can induce inflammatory status in beta islets cells in a type I IFN and *Usp18* dependent manner. However, an earlier study showed that enhanced activity of *Usp18* in beta islet cells can limit the type I interferon signaling in these cells and could prevent diabetes during presence of IFN-I [140]. In other words, it still remains to be investigated whether the expression of interferon inhibitors such as *Usp18* in certain cell types contributes to the risk of human diabetes.

Furthermore, we described a new mechanism, where the immune tolerance is broken, and this demonstrate the response of $CD8^+$ T cells to the pancreatic islet autoantigen and its correlation with the induction of $CD8^+$ T cell-driven type I diabetes in a mouse model. The onset of autoimmune diabetes requires active autoantigen replication in specialized antigen-presenting cells that express *Usp18*. After infection with LCMV, *Usp18* is highly upregulated due to non-responsiveness to the antiviral actions of type I interferons. $Usp18^+$ antigen-presenting cells act as an endogenous “replicators” of autoantigen and lead to the production of high amount of autoantigen. This is enough to induce sustained expansion of pancreatic islet-specific $CD8^+$ T cells and subsequent induction of autoimmune diabetes. Non-replicating autoantigens were not able to energize T cells even in the presence of an inflammatory environment induced by poly I:C, only a prolonged antigen exposure with increasing antigen amounts was able to induce a sustained $CD8^+$ T cell response. This is in keeping with the fact that high and sustained amounts of autoantigen were essential to break immunological ignorance in RIP-GP mice.

Previously, Reis e Sousa suggested in his perspectives that dendritic cells can either on or off with T cell differentiation and this rely on the antigen capturing and processing [259], if this processing and maturation is related to upregulation of *Usp18* need to be studied

It is still questionable how the bacteria that carry cross reactive autoantigen, failed to induce diabetes, despite their ability to replicate. As we showed, using recombinant

LCMV-GP33 expressing facultative intracellular *Listeria monocytogenes* did not induce diabetes in RIP-GP mice. This hints that amplification of viral antigen was more efficient to break immunological tolerance. It remains to be studied why the bacterial antigen amplification failed to break the tolerance.

In this thesis we also investigated another protein (WASP) which can play an important role in autoimmune diabetes, as mentioned above, WASP is expressed by all haematopoiteic cell lineages and precursor cells[33], here we focused in this thesis on the role of WASP on dendritic cells and their ability to produce type I interferon and the influence of WASP in dendritic cells in priming cytotoxic $CD8^+$ T cells. We found that WASP play essential role in priming functional $CD8^+$ T cells and consequently break the tolerance in RIP-GP mouse model [260].

In conclusion prevention of diabetes is dependent on two strategies. First strategy is mechanistically, through reduction of the antigen amounts by inhibition of enforced viral replication, either by depletion of dendritic cells, genetic deletion of *Usp18*, pharmacological inhibition of viral replication which blunted the expansion of autoreactive $CD8^+$ T cells and prevented diabetes, or through influencing $CD8^+$ T cell priming by genetic deletion of WASP from dendritic cells.

Second strategy is therapeutically, through prevention of T cell proliferation by inhibition of interleukin-2 production and cell metabolism.

8. References

1. Vesely, M.D., Kershaw, M.H., Schreiber, R.D. & Smyth, M.J. Natural innate and adaptive immunity to cancer. *Annu Rev Immunol* **29**, 235-271.
2. Mak, T.M. & Saunders, M.E. *The immune response*, (Elsevier, 2004).
3. Doan, T., Melvold, R., Viselli, S. & Waltenbaugh, C. *immunology*, (Lippincott wiliams & wilkins, 2008).
4. Abbas, A.K. & Lichtman, A.H. *Basic immunology*, (Elsevier, 2004).
5. Steinman, R.M. & Cohn, Z.A. Identification of a novel cell type in peripheral lymphoid organs of mice. I. Morphology, quantitation, tissue distribution. *J Exp Med* **137**, 1142-1162 (1973).
6. Colonna, M., Trinchieri, G. & Liu, Y.J. Plasmacytoid dendritic cells in immunity. *Nat Immunol* **5**, 1219-1226 (2004).
7. Liu, Y.J. IPC: professional type 1 interferon-producing cells and plasmacytoid dendritic cell precursors. *Annu Rev Immunol* **23**, 275-306 (2005).
8. El Shikh, M.E., El Sayed, R.M., Sukumar, S., Szakal, A.K. & Tew, J.G. Activation of B cells by antigens on follicular dendritic cells. *Trends Immunol* **31**, 205-211 (2010).
9. Keir, M.E. & Sharpe, A.H. The B7/CD28 costimulatory family in autoimmunity. *Immunol Rev* **204**, 128-143 (2005).
10. Larsen, C.P., Ritchie, S.C., Pearson, T.C., Linsley, P.S. & Lowry, R.P. Functional expression of the costimulatory molecule, B7/BB1, on murine dendritic cell populations. *J Exp Med* **176**, 1215-1220 (1992).
11. Inaba, K.*, et al.* The tissue distribution of the B7-2 costimulator in mice: abundant expression on dendritic cells in situ and during maturation in vitro. *J Exp Med* **180**, 1849-1860 (1994).
12. Russell, D.G., Vanderven, B.C., Glennie, S., Mwandumba, H. & Heyderman, R.S. The macrophage marches on its phagosome: dynamic assays of phagosome function. *Nat Rev Immunol* **9**, 594-600 (2009).
13. Hume, D.A., Halpin, D., Charlton, H. & Gordon, S. The mononuclear phagocyte system of the mouse defined by immunohistochemical localization of antigen F4/80: macrophages of endocrine organs. *Proc Natl Acad Sci U S A* **81**, 4174-4177 (1984).
14. Backer, R.*, et al.* Effective collaboration between marginal metallophilic macrophages and CD8+ dendritic cells in the generation of cytotoxic T cells. *Proc Natl Acad Sci U S A* **107**, 216-221.
15. Andrews, D.M., Andoniou, C.E., Granucci, F., Ricciardi-Castagnoli, P. & Degli-Esposti, M.A. Infection of dendritic cells by murine cytomegalovirus induces functional paralysis. *Nat Immunol* **2**, 1077-1084 (2001).
16. Kurts, C., Robinson, B.W. & Knolle, P.A. Cross-priming in health and disease. *Nat Rev Immunol* **10**, 403-414.
17. Joffre, O.P., Segura, E., Savina, A. & Amigorena, S. Cross-presentation by dendritic cells. *Nat Rev Immunol* **12**, 557-569.
18. Lindenmann, J., Burke, D.C. & Isaacs, A. Studies on the production, mode of action and properties of interferon. *Br J Exp Pathol* **38**, 551-562 (1957).
19. Killestein, J. & Polman, C.H. Determinants of interferon beta efficacy in patients with multiple sclerosis. *Nat Rev Neurol* **7**, 221-228.
20. NIH Consensus Statement on Management of Hepatitis C: 2002. *NIH Consens State Sci Statements* **19**, 1-46 (2002).
21. Silvennoinen, O., Ihle, J.N., Schlessinger, J. & Levy, D.E. Interferon-induced nuclear signalling by Jak protein tyrosine kinases. *Nature* **366**, 583-585 (1993).
22. Platanias, L.C. Mechanisms of type-I- and type-II-interferon-mediated signalling. *Nat Rev Immunol* **5**, 375-386 (2005).

23. Ahmad, S., Alsayed, Y.M., Druker, B.J. & Platanias, L.C. The type I interferon receptor mediates tyrosine phosphorylation of the CrkL adaptor protein. *J Biol Chem* **272**, 29991-29994 (1997).
24. Farrell, P.J., Broeze, R.J. & Lengyel, P. Accumulation of an mRNA and protein in interferon-treated Ehrlich ascites tumour cells. *Nature* **279**, 523-525 (1979).
25. D'Cunha, J., Knight, E., Jr., Haas, A.L., Truitt, R.L. & Borden, E.C. Immunoregulatory properties of ISG15, an interferon-induced cytokine. *Proc Natl Acad Sci U S A* **93**, 211-215 (1996).
26. Hsiang, T.Y., Zhao, C. & Krug, R.M. Interferon-induced ISG15 conjugation inhibits influenza A virus gene expression and replication in human cells. *J Virol* **83**, 5971-5977 (2009).
27. Lenschow, D.J.*, et al.* IFN-stimulated gene 15 functions as a critical antiviral molecule against influenza, herpes, and Sindbis viruses. *Proc Natl Acad Sci U S A* **104**, 1371-1376 (2007).
28. Osiak, A., Utermohlen, O., Niendorf, S., Horak, I. & Knobeloch, K.P. ISG15, an interferon-stimulated ubiquitin-like protein, is not essential for STAT1 signaling and responses against vesicular stomatitis and lymphocytic choriomeningitis virus. *Mol Cell Biol* **25**, 6338-6345 (2005).
29. Knobeloch, K.P., Utermohlen, O., Kisser, A., Prinz, M. & Horak, I. Reexamination of the role of ubiquitin-like modifier ISG15 in the phenotype of UBP43-deficient mice. *Mol Cell Biol* **25**, 11030-11034 (2005).
30. Ritchie, K.J.*, et al.* Role of ISG15 protease UBP43 (USP18) in innate immunity to viral infection. *Nat Med* **10**, 1374-1378 (2004).
31. Malakhova, O.A.*, et al.* UBP43 is a novel regulator of interferon signaling independent of its ISG15 isopeptidase activity. *EMBO J* **25**, 2358-2367 (2006).
32. Recher, M.*, et al.* B cell-intrinsic deficiency of the Wiskott-Aldrich syndrome protein (WASp) causes severe abnormalities of the peripheral B-cell compartment in mice. *Blood* **119**, 2819-2828 (2012).
33. Thrasher, A.J. & Burns, S.O. WASP: a key immunological multitasker. *Nat Rev Immunol* **10**, 182-192 (2010).
34. Mueller, D.L. & Jenkins, M.K. Autoimmunity: when self-tolerance breaks down. *Curr Biol* **7**, R255-257 (1997).
35. Mueller, D.L. Mechanisms maintaining peripheral tolerance. *Nat Immunol* **11**, 21-27.
36. Hogquist, K.A., Baldwin, T.A. & Jameson, S.C. Central tolerance: learning self-control in the thymus. *Nat Rev Immunol* **5**, 772-782 (2005).
37. Gregersen, P.K. & Behrens, T.W. Genetics of autoimmune diseases--disorders of immune homeostasis. *Nat Rev Genet* **7**, 917-928 (2006).
38. Salsali, A. & Nathan, M. A review of types 1 and 2 diabetes mellitus and their treatment with insulin. *Am J Ther* **13**, 349-361 (2006).
39. Noda, I.*, et al.* Inhibition of N-linked glycosylation by tunicamycin enhances sensitivity to cisplatin in human head-and-neck carcinoma cells. *Int J Cancer* **80**, 279-284 (1999).
40. Martinez, J.A.*, et al.* Tunicamycin inhibits capillary endothelial cell proliferation by inducing apoptosis. Targeting dolichol-pathway for generation of new anti-angiogenic therapeutics. *Adv Exp Med Biol* **476**, 197-208 (2000).
41. Ohashi, P.S.*, et al.* Ablation of "tolerance" and induction of diabetes by virus infection in viral antigen transgenic mice. *Cell* **65**, 305-317 (1991).
42. von Herrath, M.G., Dockter, J. & Oldstone, M.B. How virus induces a rapid or slow onset insulin-dependent diabetes mellitus in a transgenic model. *Immunity* **1**, 231-242 (1994).

43. Pircher, H., Burki, K., Lang, R., Hengartner, H. & Zinkernagel, R.M. Tolerance induction in double specific T-cell receptor transgenic mice varies with antigen. *Nature* **342**, 559-561 (1989).
44. Lang, K.S*., et al.* Toll-like receptor engagement converts T-cell autoreactivity into overt autoimmune disease. *Nature medicine* **11**, 138-145 (2005).
45. Ritchie, K.J*., et al.* Dysregulation of protein modification by ISG15 results in brain cell injury. *Genes Dev* **16**, 2207-2212 (2002).
46. Jung, S*., et al.* In vivo depletion of CD11c+ dendritic cells abrogates priming of CD8+ T cells by exogenous cell-associated antigens. *Immunity* **17**, 211-220 (2002).
47. Miyawaki, S*., et al.* A new mutation, aly, that induces a generalized lack of lymph nodes accompanied by immunodeficiency in mice. *Eur J Immunol* **24**, 429-434 (1994).
48. Hunziker, L*., et al.* Hypergammaglobulinemia and autoantibody induction mechanisms in viral infections. *Nat Immunol* **4**, 343-349 (2003).
49. Zinszner, H*., et al.* CHOP is implicated in programmed cell death in response to impaired function of the endoplasmic reticulum. *Genes Dev* **12**, 982-995 (1998).
50. Ahmed, R. & Oldstone, M.B. Organ-specific selection of viral variants during chronic infection. *J Exp Med* **167**, 1719-1724 (1988).
51. Zinkernagel, R.M*., et al.* T cell-mediated hepatitis in mice infected with lymphocytic choriomeningitis virus. Liver cell destruction by H-2 class I-restricted virus-specific cytotoxic T cells as a physiological correlate of the 51Cr-release assay? *J Exp Med* **164**, 1075-1092 (1986).
52. Lang, P.A., Recher, M., Haussinger, D. & Lang, K.S. Genes determining the course of virus persistence in the liver: lessons from murine infection with lymphocytic choriomeningitis virus. *Cell Physiol Biochem* **26**, 263-272.
53. Hangartner, L., Zinkernagel, R.M. & Hengartner, H. Antiviral antibody responses: the two extremes of a wide spectrum. *Nat Rev Immunol* **6**, 231-243 (2006).
54. Seiler, P*., et al.* Additive effect of neutralizing antibody and antiviral drug treatment in preventing virus escape and persistence. *J Virol* **74**, 5896-5901 (2000).
55. Yan, Z*., et al.* Efficacy and safety of low-dose peginterferon alpha-2a plus ribavirin on chronic hepatitis C. *Gastroenterol Res Pract* **2012**, 302093.
56. Druyts, E*., et al.* Efficacy and safety of peg-interferon alpha-2a or alpha-2b plus ribavirin for the treatment of chronic hepatitis C in children and adolescents: a systematic review and meta-analysis. *Clin Infect Dis*.
57. Muller, U*., et al.* Functional role of type I and type II interferons in antiviral defense. *Science* **264**, 1918-1921 (1994).
58. Sadler, A.J. & Williams, B.R. Interferon-inducible antiviral effectors. *Nat Rev Immunol* **8**, 559-568 (2008).
59. Aichele, P*., et al.* Macrophages of the splenic marginal zone are essential for trapping of blood-borne particulate antigen but dispensable for induction of specific T cell responses. *J Immunol* **171**, 1148-1155 (2003).
60. Cervantes-Barragan, L*., et al.* Type I IFN-mediated protection of macrophages and dendritic cells secures control of murine coronavirus infection. *Journal of immunology* **182**, 1099-1106 (2009).
61. Lang, P.A*., et al.* Tissue macrophages suppress viral replication and prevent severe immunopathology in an interferon-I-dependent manner in mice. *Hepatology* **52**, 25-32 (2010).
62. Seiler, P*., et al.* Crucial role of marginal zone macrophages and marginal zone metallophils in the clearance of lymphocytic choriomeningitis virus infection. *Eur J Immunol* **27**, 2626-2633 (1997).

63. Steiniger, B. & Barth, P. Microanatomy and function of the spleen. *Adv Anat Embryol Cell Biol* **151**, III-IX, 1-101 (2000).
64. Wardle, E.N. Kupffer cells and their function. *Liver* **7**, 63-75 (1987).
65. Kraal, G., Ter Hart, H., Meelhuizen, C., Venneker, G. & Claassen, E. Marginal zone macrophages and their role in the immune response against T-independent type 2 antigens: modulation of the cells with specific antibody. *European journal of immunology* **19**, 675-680 (1989).
66. Der, S.D., Zhou, A., Williams, B.R. & Silverman, R.H. Identification of genes differentially regulated by interferon alpha, beta, or gamma using oligonucleotide arrays. *Proceedings of the National Academy of Sciences of the United States of America* **95**, 15623-15628 (1998).
67. Junt, T., Scandella, E. & Ludewig, B. Form follows function: lymphoid tissue microarchitecture in antimicrobial immune defence. *Nat Rev Immunol* **8**, 764-775 (2008).
68. Oetke, C., Kraal, G. & Crocker, P.R. The antigen recognized by MOMA-I is sialoadhesin. *Immunol Lett* **106**, 96-98 (2006).
69. Junt, T*., et al.* Subcapsular sinus macrophages in lymph nodes clear lymph-borne viruses and present them to antiviral B cells. *Nature* **450**, 110-114 (2007).
70. Gretz, J.E., Anderson, A.O. & Shaw, S. Cords, channels, corridors and conduits: critical architectural elements facilitating cell interactions in the lymph node cortex. *Immunol Rev* **156**, 11-24 (1997).
71. Sixt, M*., et al.* The conduit system transports soluble antigens from the afferent lymph to resident dendritic cells in the T cell area of the lymph node. *Immunity* **22**, 19-29 (2005).
72. Aichele, P., Brduscha-Riem, K., Zinkernagel, R.M., Hengartner, H. & Pircher, H. T cell priming versus T cell tolerance induced by synthetic peptides. *J Exp Med* **182**, 261-266 (1995).
73. Iezzi, G., Karjalainen, K. & Lanzavecchia, A. The duration of antigenic stimulation determines the fate of naive and effector T cells. *Immunity* **8**, 89-95 (1998).
74. Lanzavecchia, A. & Sallusto, F. Antigen decoding by T lymphocytes: from synapses to fate determination. *Nat Immunol* **2**, 487-492 (2001).
75. Zinkernagel, R.M. Localization dose and time of antigens determine immune reactivity. *Semin Immunol* **12**, 163-171; discussion 257-344 (2000).
76. Zinkernagel, R.M*., et al.* Antigen localisation regulates immune responses in a dose- and time-dependent fashion: a geographical view of immune reactivity. *Immunol Rev* **156**, 199-209 (1997).
77. Irvine, D.J., Purbhoo, M.A., Krogsgaard, M. & Davis, M.M. Direct observation of ligand recognition by T cells. *Nature* **419**, 845-849 (2002).
78. Henrickson, S.E*., et al.* T cell sensing of antigen dose governs interactive behavior with dendritic cells and sets a threshold for T cell activation. *Nat Immunol* **9**, 282-291 (2008).
79. Holler, P.D. & Kranz, D.M. Quantitative analysis of the contribution of TCR/pepMHC affinity and CD8 to T cell activation. *Immunity* **18**, 255-264 (2003).
80. Bachmann, M.F., Bast, C., Hengartner, H. & Zinkernagel, R.M. Immunogenicity of a viral model vaccine after different inactivation procedures. *Med Microbiol Immunol* **183**, 95-104 (1994).
81. Miyake, Y*., et al.* Critical role of macrophages in the marginal zone in the suppression of immune responses to apoptotic cell-associated antigens. *J Clin Invest* **117**, 2268-2278 (2007).

82. Bachmann, M.F., Kundig, T.M., Kalberer, C.P., Hengartner, H. & Zinkernagel, R.M. Formalin inactivation of vesicular stomatitis virus impairs T-cell- but not T-help-independent B-cell responses. *J Virol* **67**, 3917-3922 (1993).
83. Freer, G.*, et al.* Role of T helper cell precursor frequency on vesicular stomatitis virus neutralizing antibody responses in a T cell receptor beta chain transgenic mouse. *Eur J Immunol* **25**, 1410-1416 (1995).
84. Nonacs, R., Humborg, C., Tam, J.P. & Steinman, R.M. Mechanisms of mouse spleen dendritic cell function in the generation of influenza-specific, cytolytic T lymphocytes. *J Exp Med* **176**, 519-529 (1992).
85. Brundler, M.A.*, et al.* Immunity to viruses in B cell-deficient mice: influence of antibodies on virus persistence and on T cell memory. *Eur J Immunol* **26**, 2257-2262 (1996).
86. Plakhov, I.V., Arlund, E.E., Aoki, C. & Reiss, C.S. The earliest events in vesicular stomatitis virus infection of the murine olfactory neuroepithelium and entry of the central nervous system. *Virology* **209**, 257-262 (1995).
87. Junt, T.*, et al.* Expression of lymphotoxin beta governs immunity at two distinct levels. *Eur J Immunol* **36**, 2061-2075 (2006).
88. Ware, C.F. Targeting lymphocyte activation through the lymphotoxin and LIGHT pathways. *Immunol Rev* **223**, 186-201 (2008).
89. Seifert, U.*, et al.* Immunoproteasomes preserve protein homeostasis upon interferon-induced oxidative stress. *Cell* **142**, 613-624.
90. Le Bon, A.*, et al.* Cross-priming of CD8+ T cells stimulated by virus-induced type I interferon. *Nat Immunol* **4**, 1009-1015 (2003).
91. Longhi, M.P.*, et al.* Dendritic cells require a systemic type I interferon response to mature and induce CD4+ Th1 immunity with poly IC as adjuvant. *J Exp Med* **206**, 1589-1602 (2009).
92. Kolumam, G.A., Thomas, S., Thompson, L.J., Sprent, J. & Murali-Krishna, K. Type I interferons act directly on CD8 T cells to allow clonal expansion and memory formation in response to viral infection. *J Exp Med* **202**, 637-650 (2005).
93. Fink, K.*, et al.* Early type I interferon-mediated signals on B cells specifically enhance antiviral humoral responses. *European journal of immunology* **36**, 2094-2105 (2006).
94. Iannacone, M.*, et al.* Subcapsular sinus macrophages prevent CNS invasion on peripheral infection with a neurotropic virus. *Nature* **465**, 1079-1083 (2010).
95. Yoshimura, A. Negative regulation of cytokine signaling. *Clin Rev Allergy Immunol* **28**, 205-220 (2005).
96. Battegay, M.*, et al.* Antiviral immune responses of mice lacking MHC class II or its associated invariant chain. *Cell Immunol* **167**, 115-121 (1996).
97. Ogra, P.L., Karzon, D.T., Righthand, F. & MacGillivray, M. Immunoglobulin response in serum and secretions after immunization with live and inactivated poliovaccine and natural infection. *N Engl J Med* **279**, 893-900 (1968).
98. Ogra, P.L., Kerr-Grant, D., Umana, G., Dzierba, J. & Weintraub, D. Antibody response in serum and nasopharynx after naturally acquired and vaccine-induced infection with rubella virus. *N Engl J Med* **285**, 1333-1339 (1971).
99. Ida-Hosonuma, M.*, et al.* The alpha/beta interferon response controls tissue tropism and pathogenicity of poliovirus. *J Virol* **79**, 4460-4469 (2005).
100. Ohashi, P.S.*, et al.* Induction of diabetes is influenced by the infectious virus and local expression of MHC class I and tumor necrosis factor-alpha. *J Immunol* **150**, 5185-5194 (1993).
101. Lang, K.S.*, et al.* Toll-like receptor engagement converts T-cell autoreactivity into overt autoimmune disease. *Nat Med* **11**, 138-145 (2005).

102. Millar, D.G.*, et al.* Hsp70 promotes antigen-presenting cell function and converts T-cell tolerance to autoimmunity in vivo. *Nat Med* **9**, 1469-1476 (2003).
103. Lehuen, A., Diana, J., Zaccone, P. & Cooke, A. Immune cell crosstalk in type 1 diabetes. *Nature reviews. Immunology* **10**, 501-513 (2010).
104. Hyoty, H. & Taylor, K.W. The role of viruses in human diabetes. *Diabetologia* **45**, 1353-1361 (2002).
105. Roep, B.O.*, et al.* Molecular mimicry in type 1 diabetes: immune cross-reactivity between islet autoantigen and human cytomegalovirus but not Coxsackie virus. *Ann N Y Acad Sci* **958**, 163-165 (2002).
106. Schloot, N.C.*, et al.* Molecular mimicry in type 1 diabetes mellitus revisited: T-cell clones to GAD65 peptides with sequence homology to Coxsackie or proinsulin peptides do not crossreact with homologous counterpart. *Hum Immunol* **62**, 299-309 (2001).
107. Yoon, J.W., Austin, M., Onodera, T. & Notkins, A.L. Isolation of a virus from the pancreas of a child with diabetic ketoacidosis. *The New England journal of medicine* **300**, 1173-1179 (1979).
108. Ramondetti, F.*, et al.* Type 1 diabetes and measles, mumps and rubella childhood infections within the Italian Insulin-dependent Diabetes Registry. *Diabet Med* **29**, 761-766 (2012).
109. Stene, L.C.*, et al.* Enterovirus infection and progression from islet autoimmunity to type 1 diabetes: the Diabetes and Autoimmunity Study in the Young (DAISY). *Diabetes* **59**, 3174-3180 (2010).
110. Foxman, E.F. & Iwasaki, A. Genome-virome interactions: examining the role of common viral infections in complex disease. *Nat Rev Microbiol* **9**, 254-264 (2011).
111. Smyth, D.J.*, et al.* A genome-wide association study of nonsynonymous SNPs identifies a type 1 diabetes locus in the interferon-induced helicase (IFIH1) region. *Nat Genet* **38**, 617-619 (2006).
112. von Herrath, M. Diabetes: A virus-gene collaboration. *Nature* **459**, 518-519 (2009).
113. Pietropaolo, M.*, et al.* Islet cell autoantigen 69 kD (ICA69). Molecular cloning and characterization of a novel diabetes-associated autoantigen. *J Clin Invest* **92**, 359-371 (1993).
114. Karjalainen, J.*, et al.* A bovine albumin peptide as a possible trigger of insulin-dependent diabetes mellitus. *The New England journal of medicine* **327**, 302-307 (1992).
115. Cavallo, M.G., Fava, D., Monetini, L., Barone, F. & Pozzilli, P. Cell-mediated immune response to beta casein in recent-onset insulin-dependent diabetes: implications for disease pathogenesis. *Lancet* **348**, 926-928 (1996).
116. Atkinson, M.A.*, et al.* Lack of immune responsiveness to bovine serum albumin in insulin-dependent diabetes. *The New England journal of medicine* **329**, 1853-1858 (1993).
117. Vaarala, O.*, et al.* Cellular immune response to cow's milk beta-lactoglobulin in patients with newly diagnosed IDDM. *Diabetes* **45**, 178-182 (1996).
118. Judkowski, V.A., Allicotti, G.M., Sarvetnick, N. & Pinilla, C. Peptides from common viral and bacterial pathogens can efficiently activate diabetogenic T-cells. *Diabetes* **53**, 2301-2309 (2004).
119. Masala, S.*, et al.* Antibodies recognizing Mycobacterium avium paratuberculosis epitopes cross-react with the beta-cell antigen ZnT8 in Sardinian type 1 diabetic patients. *PLoS One* **6**, e26931 (2011).
120. Lammi, N., Karvonen, M. & Tuomilehto, J. Do microbes have a causal role in type 1 diabetes? *Med Sci Monit* **11**, RA63-69 (2005).

121. Turley, S.J., Fletcher, A.L. & Elpek, K.G. The stromal and haematopoietic antigen-presenting cells that reside in secondary lymphoid organs. *Nature reviews. Immunology* **10**, 813-825 (2010).
122. George, T.C., Bilsborough, J., Viney, J.L. & Norment, A.M. High antigen dose and activated dendritic cells enable Th cells to escape regulatory T cell-mediated suppression in vitro. *European journal of immunology* **33**, 502-511 (2003).
123. Kang, H.K., Liu, M. & Datta, S.K. Low-dose peptide tolerance therapy of lupus generates plasmacytoid dendritic cells that cause expansion of autoantigen-specific regulatory T cells and contraction of inflammatory Th17 cells. *Journal of immunology* **178**, 7849-7858 (2007).
124. Lang, K.S*., et al.* Inverse correlation between IL-7 receptor expression and CD8 T cell exhaustion during persistent antigen stimulation. *Eur J Immunol* **35**, 738-745 (2005).
125. Aichele, P., Brduscha-Riem, K., Zinkernagel, R.M., Hengartner, H. & Pircher, H. T cell priming versus T cell tolerance induced by synthetic peptides. *The Journal of experimental medicine* **182**, 261-266 (1995).
126. Honke, N*., et al.* Enforced viral replication activates adaptive immunity and is essential for the control of a cytopathic virus. *Nature immunology* **13**, 51-57 (2012).
127. Recher, M*., et al.* Extralymphatic virus sanctuaries as a consequence of potent T-cell activation. *Nature medicine* **13**, 1316-1323 (2007).
128. Lang, P.A*., et al.* Aggravation of viral hepatitis by platelet-derived serotonin. *Nature medicine* **14**, 756-761 (2008).
129. Gessner, A. & Lother, H. Homologous interference of lymphocytic choriomeningitis virus involves a ribavirin-susceptible block in virus replication. *Journal of virology* **63**, 1827-1832 (1989).
130. Lenzen, S. The mechanisms of alloxan- and streptozotocin-induced diabetes. *Diabetologia* **51**, 216-226 (2008).
131. Hunziker, L*., et al.* Hypergammaglobulinemia and autoantibody induction mechanisms in viral infections. *Nature immunology* **4**, 343-349 (2003).
132. Coppieters, K.T., Wiberg, A. & von Herrath, M.G. Viral infections and molecular mimicry in type 1 diabetes. *Apmis* **120**, 941-949 (2012).
133. Christen, S*., et al.* Blockade but not overexpression of the junctional adhesion molecule C influences virus-induced type 1 diabetes in mice. *PLoS One* **8**, e54675 (2013).
134. Freigang, S., Probst, H.C. & van den Broek, M. DC infection promotes antiviral CTL priming: the 'Winkelried' strategy. *Trends in immunology* **26**, 13-18 (2005).
135. Cong, X.L*., et al.* Usp18 promotes conventional CD11b+ dendritic cell development. *Journal of immunology* **188**, 4776-4781 (2012).
136. Seifert, U*., et al.* Immunoproteasomes preserve protein homeostasis upon interferon-induced oxidative stress. *Cell* **142**, 613-624 (2010).
137. Millar, D.G*., et al.* Hsp70 promotes antigen-presenting cell function and converts T-cell tolerance to autoimmunity in vivo. *Nature medicine* **9**, 1469-1476 (2003).
138. Nejentsev, S., Walker, N., Riches, D., Egholm, M. & Todd, J.A. Rare variants of IFIH1, a gene implicated in antiviral responses, protect against type 1 diabetes. *Science* **324**, 387-389 (2009).
139. Heinig, M*., et al.* A trans-acting locus regulates an anti-viral expression network and type 1 diabetes risk. *Nature* **467**, 460-464 (2010).
140. Santin, I*., et al.* USP18 is a key regulator of the interferon-driven gene network modulating pancreatic beta cell inflammation and apoptosis. *Cell Death Dis* **3**, e419 (2012).

141. Eschli, B.*, et al.* Early antibodies specific for the neutralizing epitope on the receptor binding subunit of the lymphocytic choriomeningitis virus glycoprotein fail to neutralize the virus. *Journal of virology* **81**, 11650-11657 (2007).
142. Lang, K.S.*, et al.* Immunoprivileged status of the liver is controlled by Toll-like receptor 3 signaling. *J Clin Invest* **116**, 2456-2463 (2006).
143. Bouma, G., Burns, S.O. & Thrasher, A.J. Wiskott-Aldrich Syndrome: Immunodeficiency resulting from defective cell migration and impaired immunostimulatory activation. *Immunobiology* **214**, 778-790 (2009).
144. Sullivan, K.E., Mullen, C.A., Blaese, R.M. & Winkelstein, J.A. A multiinstitutional survey of the Wiskott-Aldrich syndrome. *J Pediatr* **125**, 876-885 (1994).
145. Imai, K.*, et al.* Clinical course of patients with WASP gene mutations. *Blood* **103**, 456-464 (2004).
146. Derry, J.M., Ochs, H.D. & Francke, U. Isolation of a novel gene mutated in Wiskott-Aldrich syndrome. *Cell* **79**, following 922 (1994).
147. Bouma, G., Burns, S. & Thrasher, A.J. Impaired T-cell priming in vivo resulting from dysfunction of WASp-deficient dendritic cells. *Blood* **110**, 4278-4284 (2007).
148. de Noronha, S.*, et al.* Impaired dendritic-cell homing in vivo in the absence of Wiskott-Aldrich syndrome protein. *Blood* **105**, 1590-1597 (2005).
149. Gallego, M.D.*, et al.* WIP and WASP play complementary roles in T cell homing and chemotaxis to SDF-1alpha. *Int Immunol* **18**, 221-232 (2006).
150. Snapper, S.B.*, et al.* WASP deficiency leads to global defects of directed leukocyte migration in vitro and in vivo. *J Leukoc Biol* **77**, 993-998 (2005).
151. Westerberg, L.*, et al.* Wiskott-Aldrich syndrome protein deficiency leads to reduced B-cell adhesion, migration, and homing, and a delayed humoral immune response. *Blood* **105**, 1144-1152 (2005).
152. Leverrier, Y.*, et al.* Cutting edge: the Wiskott-Aldrich syndrome protein is required for efficient phagocytosis of apoptotic cells. *J Immunol* **166**, 4831-4834 (2001).
153. Lorenzi, R., Brickell, P.M., Katz, D.R., Kinnon, C. & Thrasher, A.J. Wiskott-Aldrich syndrome protein is necessary for efficient IgG-mediated phagocytosis. *Blood* **95**, 2943-2946 (2000).
154. Bouma, G.*, et al.* Cytoskeletal remodeling mediated by WASp in dendritic cells is necessary for normal immune synapse formation and T-cell priming. *Blood* **118**, 2492-2501 (2011).
155. Pulecio, J.*, et al.* Expression of Wiskott-Aldrich syndrome protein in dendritic cells regulates synapse formation and activation of naive CD8+ T cells. *J Immunol* **181**, 1135-1142 (2008).
156. Burns, S., Thrasher, A.J., Blundell, M.P., Machesky, L. & Jones, G.E. Configuration of human dendritic cell cytoskeleton by Rho GTPases, the WAS protein, and differentiation. *Blood* **98**, 1142-1149 (2001).
157. Gallego, M.D., Santamaria, M., Pena, J. & Molina, I.J. Defective actin reorganization and polymerization of Wiskott-Aldrich T cells in response to CD3-mediated stimulation. *Blood* **90**, 3089-3097 (1997).
158. Snapper, S.B.*, et al.* Wiskott-Aldrich syndrome protein-deficient mice reveal a role for WASP in T but not B cell activation. *Immunity* **9**, 81-91 (1998).
159. Zhang, J.*, et al.* Antigen receptor-induced activation and cytoskeletal rearrangement are impaired in Wiskott-Aldrich syndrome protein-deficient lymphocytes. *J Exp Med* **190**, 1329-1342 (1999).
160. Henriquez, N.V., Rijkers, G.T. & Zegers, B.J. Antigen receptor-mediated transmembrane signaling in Wiskott-Aldrich syndrome. *J Immunol* **153**, 395-399 (1994).

161. Molina, I.J., Sancho, J., Terhorst, C., Rosen, F.S. & Remold-O'Donnell, E. T cells of patients with the Wiskott-Aldrich syndrome have a restricted defect in proliferative responses. *J Immunol* **151**, 4383-4390 (1993).
162. Meyer-Bahlburg, A.*, et al.* Wiskott-Aldrich syndrome protein deficiency in B cells results in impaired peripheral homeostasis. *Blood* **112**, 4158-4169 (2008).
163. Westerberg, L.S.*, et al.* WASP confers selective advantage for specific hematopoietic cell populations and serves a unique role in marginal zone B-cell homeostasis and function. *Blood* **112**, 4139-4147 (2008).
164. Marangoni, F.*, et al.* WASP regulates suppressor activity of human and murine CD4(+)CD25(+)FOXP3(+) natural regulatory T cells. *J Exp Med* **204**, 369-380 (2007).
165. Maillard, M.H.*, et al.* The Wiskott-Aldrich syndrome protein is required for the function of CD4(+)CD25(+)Foxp3(+) regulatory T cells. *J Exp Med* **204**, 381-391 (2007).
166. Humblet-Baron, S.*, et al.* Wiskott-Aldrich syndrome protein is required for regulatory T cell homeostasis. *J Clin Invest* **117**, 407-418 (2007).
167. Adriani, M.*, et al.* Impaired in vitro regulatory T cell function associated with Wiskott-Aldrich syndrome. *Clin Immunol* **124**, 41-48 (2007).
168. Strom, T.S.*, et al.* Defects in T-cell-mediated immunity to influenza virus in murine Wiskott-Aldrich syndrome are corrected by oncoretroviral vector-mediated gene transfer into repopulating hematopoietic cells. *Blood* **102**, 3108-3116 (2003).
169. Andreansky, S.*, et al.* WASP- mice exhibit defective immune responses to influenza A virus, Streptococcus pneumoniae, and Mycobacterium bovis BCG. *Exp Hematol* **33**, 443-451 (2005).
170. De Meester, J., Calvez, R., Valitutti, S. & Dupre, L. The Wiskott-Aldrich syndrome protein regulates CTL cytotoxicity and is required for efficient killing of B cell lymphoma targets. *J Leukoc Biol* **88**, 1031-1040 (2010).
171. Rehermann, B. Hepatitis C virus versus innate and adaptive immune responses: a tale of coevolution and coexistence. *J Clin Invest* **119**, 1745-1754 (2009).
172. Rehermann, B. & Nascimbeni, M. Immunology of hepatitis B virus and hepatitis C virus infection. *Nat Rev Immunol* **5**, 215-229 (2005).
173. Guidotti, L.G. & Chisari, F.V. Immunobiology and pathogenesis of viral hepatitis. *Annu Rev Pathol* **1**, 23-61 (2006).
174. Lang, P.A.*, et al.* Hematopoietic cell-derived interferon controls viral replication and virus-induced disease. *Blood* **113**, 1045-1052 (2009).
175. Lang, P.A.*, et al.* Aggravation of viral hepatitis by platelet-derived serotonin. *Nat Med* **14**, 756-761 (2008).
176. Honda, K.*, et al.* IRF-7 is the master regulator of type-I interferon-dependent immune responses. *Nature* **434**, 772-777 (2005).
177. Recher, M.*, et al.* Deliberate removal of T cell help improves virus-neutralizing antibody production. *Nat Immunol* **5**, 934-942 (2004).
178. Wherry, E.J., Barber, D.L., Kaech, S.M., Blattman, J.N. & Ahmed, R. Antigen-independent memory CD8 T cells do not develop during chronic viral infection. *Proc Natl Acad Sci U S A* **101**, 16004-16009 (2004).
179. Kaech, S.M.*, et al.* Selective expression of the interleukin 7 receptor identifies effector CD8 T cells that give rise to long-lived memory cells. *Nat Immunol* **4**, 1191-1198 (2003).
180. Zinkernagel, R.M., Leist, T., Hengartner, H. & Althage, A. Susceptibility to lymphocytic choriomeningitis virus isolates correlates directly with early and high cytotoxic T cell activity, as well as with footpad swelling reaction, and all three are regulated by H-2D. *J Exp Med* **162**, 2125-2141 (1985).

181. Scheu, S., Dresing, P. & Locksley, R.M. Visualization of IFNbeta production by plasmacytoid versus conventional dendritic cells under specific stimulation conditions in vivo. *Proc Natl Acad Sci U S A* **105**, 20416-20421 (2008).
182. Catucci, M.*, et al.* Dendritic cell functional improvement in a preclinical model of lentiviral-mediated gene therapy for Wiskott-Aldrich syndrome. *Gene Ther* **19**, 1150-1158 (2011).
183. Orange, J.S.*, et al.* Wiskott-Aldrich syndrome protein is required for NK cell cytotoxicity and colocalizes with actin to NK cell-activating immunologic synapses. *Proc Natl Acad Sci U S A* **99**, 11351-11356 (2002).
184. Borg, C.*, et al.* NK cell activation by dendritic cells (DCs) requires the formation of a synapse leading to IL-12 polarization in DCs. *Blood* **104**, 3267-3275 (2004).
185. Lang, P.A.*, et al.* Natural killer cell activation enhances immune pathology and promotes chronic infection by limiting CD8+ T-cell immunity. *Proc Natl Acad Sci U S A* **109**, 1210-1215 (2012).
186. Honda, K. & Taniguchi, T. IRFs: master regulators of signalling by Toll-like receptors and cytosolic pattern-recognition receptors. *Nat Rev Immunol* **6**, 644-658 (2006).
187. Asselin-Paturel, C.*, et al.* Mouse type I IFN-producing cells are immature APCs with plasmacytoid morphology. *Nat Immunol* **2**, 1144-1150 (2001).
188. Smit, J.J.*, et al.* The balance between plasmacytoid DC versus conventional DC determines pulmonary immunity to virus infections. *PLoS One* **3**, e1720 (2008).
189. Montoya, M., Edwards, M.J., Reid, D.M. & Borrow, P. Rapid activation of spleen dendritic cell subsets following lymphocytic choriomeningitis virus infection of mice: analysis of the involvement of type 1 IFN. *J Immunol* **174**, 1851-1861 (2005).
190. Ferrantini, M.*, et al.* IFN-alpha 1 gene expression into a metastatic murine adenocarcinoma (TS/A) results in CD8+ T cell-mediated tumor rejection and development of antitumor immunity. Comparative studies with IFN-gamma-producing TS/A cells. *J Immunol* **153**, 4604-4615 (1994).
191. Diana, J.*, et al.* NKT cell-plasmacytoid dendritic cell cooperation via OX40 controls viral infection in a tissue-specific manner. *Immunity* **30**, 289-299 (2009).
192. Locci, M.*, et al.* The Wiskott-Aldrich syndrome protein is required for iNKT cell maturation and function. *J Exp Med* **206**, 735-742 (2009).
193. Astrakhan, A., Ochs, H.D. & Rawlings, D.J. Wiskott-Aldrich syndrome protein is required for homeostasis and function of invariant NKT cells. *J Immunol* **182**, 7370-7380 (2009).
194. Van den Driessche, A., Eenkhoorn, V., Van Gaal, L. & De Block, C. Type 1 diabetes and autoimmune polyglandular syndrome: a clinical review. *Neth J Med* **67**, 376-387 (2009).
195. Pozzilli, P. & Di Mario, U. Autoimmune diabetes not requiring insulin at diagnosis (latent autoimmune diabetes of the adult): definition, characterization, and potential prevention. *Diabetes Care* **24**, 1460-1467 (2001).
196. Pinschewer, D.D.*, et al.* FTY720 immunosuppression impairs effector T cell peripheral homing without affecting induction, expansion, and memory. *J Immunol* **164**, 5761-5770 (2000).
197. Lang, P.A.*, et al.* Oxidized ATP inhibits T-cell-mediated autoimmunity. *Eur J Immunol* **40**, 2401-2408.
198. Fairweather, D. & Rose, N.R. Type 1 diabetes: virus infection or autoimmune disease? *Nat Immunol* **3**, 338-340 (2002).
199. Olden, K., Pratt, R.M. & Yamada, K.M. Selective cytotoxicity of tunicamycin for transformed cells. *Int J Cancer* **24**, 60-66 (1979).

200. Prives, J. & Bar-Sagi, D. Effect of tunicamycin, an inhibitor of protein glycosylation, on the biological properties of acetylcholine receptor in cultured muscle cells. *J Biol Chem* **258**, 1775-1780 (1983).
201. Watson, A. & Bach, F.H. The role of gp70 in the target antigen recognized by murine leukemia virus immune cytotoxic T-lymphocytes. *Int J Cancer* **26**, 483-494 (1980).
202. Tordai, A., Brass, L.F. & Gelfand, E.W. Tunicamycin inhibits the expression of functional thrombin receptors on human T-lymphoblastoid cells. *Biochem Biophys Res Commun* **206**, 857-862 (1995).
203. Hangartner, L.*, et al.* Antiviral immune responses in gene-targeted mice expressing the immunoglobulin heavy chain of virus-neutralizing antibodies. *Proceedings of the National Academy of Sciences of the United States of America* **100**, 12883-12888 (2003).
204. Gotoh, T., Terada, K., Oyadomari, S. & Mori, M. hsp70-DnaJ chaperone pair prevents nitric oxide- and CHOP-induced apoptosis by inhibiting translocation of Bax to mitochondria. *Cell Death Differ* **11**, 390-402 (2004).
205. Blais, M.-E.*, et al.* Do thymically and strictly extrathymically developing T cells generate similar immune responses? *Blood* **103**, 3102-3110 (2004).
206. Song, B., Scheuner, D., Ron, D., Pennathur, S. & Kaufman, R.J. Chop deletion reduces oxidative stress, improves beta cell function, and promotes cell survival in multiple mouse models of diabetes. *J Clin Invest* **118**, 3378-3389 (2008).
207. Chen, G.*, et al.* Brain-derived neurotrophic factor suppresses tunicamycin-induced upregulation of CHOP in neurons. *J Neurosci Res* **85**, 1674-1684 (2007).
208. Vanderford, N.L. Defining the regulation of IL-1beta- and CHOP-mediated beta-cell apoptosis. *Islets* **2**, 334-336.
209. Ohteki, T.*, et al.* Negative regulation of T cell proliferation and interleukin 2 production by the serine threonine kinase GSK-3. *J Exp Med* **192**, 99-104 (2000).
210. Schwiebert, E.M. Underlying purinergic signaling contributes to T lymphocyte activation in tissue repair. Focus on "shockwaves increase the T-cell proliferation and IL-2 expression through ATP release, P2X7 receptors, and FAK activation". *Am J Physiol Cell Physiol* **298**, C446-447.
211. Tedesco-Silva, H.*, et al.* FTY720 versus mycophenolate mofetil in de novo renal transplantation: six-month results of a double-blind study. *Transplantation* **84**, 885-892 (2007).
212. Kronke, M.*, et al.* Cyclosporin A inhibits T-cell growth factor gene expression at the level of mRNA transcription. *Proc Natl Acad Sci U S A* **81**, 5214-5218 (1984).
213. Lemster, B.*, et al.* Influence of FK 506 (tacrolimus) on circulating CD4+ T cells expressing CD25 and CD45RA antigens in 19 patients with chronic progressive multiple sclerosis participating in an open label drug safety trial. *Autoimmunity* **19**, 89-98 (1994).
214. Fairbanks, L.D., Bofill, M., Ruckemann, K. & Simmonds, H.A. Importance of ribonucleotide availability to proliferating T-lymphocytes from healthy humans. Disproportionate expansion of pyrimidine pools and contrasting effects of de novo synthesis inhibitors. *J Biol Chem* **270**, 29682-29689 (1995).
215. Moreland, L.W.*, et al.* Interleukin-2 diphtheria fusion protein (DAB486IL-2) in refractory rheumatoid arthritis. A double-blind, placebo-controlled trial with open-label extension. *Arthritis Rheum* **38**, 1177-1186 (1995).
216. Sewell, K.L.*, et al.* DAB486IL-2 fusion toxin in refractory rheumatoid arthritis. *Arthritis Rheum* **36**, 1223-1233 (1993).
217. Weinblatt, M.E.*, et al.* CAMPATH-1H, a humanized monoclonal antibody, in refractory rheumatoid arthritis. An intravenous dose-escalation study. *Arthritis Rheum* **38**, 1589-1594 (1995).

218. Moreland, L.W*., et al.* Double-blind, placebo-controlled multicenter trial using chimeric monoclonal anti-CD4 antibody, cM-T412, in rheumatoid arthritis patients receiving concomitant methotrexate. *Arthritis Rheum* **38**, 1581-1588 (1995).
219. Murgia, M., Hanau, S., Pizzo, P., Rippa, M. & Di Virgilio, F. Oxidized ATP. An irreversible inhibitor of the macrophage purinergic P2Z receptor. *J Biol Chem* **268**, 8199-8203 (1993).
220. Baricordi, O.R*., et al.* An ATP-activated channel is involved in mitogenic stimulation of human T lymphocytes. *Blood* **87**, 682-690 (1996).
221. Budagian, V*., et al.* Signaling through P2X7 receptor in human T cells involves p56lck, MAP kinases, and transcription factors AP-1 and NF-kappa B. *J Biol Chem* **278**, 1549-1560 (2003).
222. Moon, H., Na, H.Y., Chong, K.H. & Kim, T.J. P2X7 receptor-dependent ATP-induced shedding of CD27 in mouse lymphocytes. *Immunol Lett* **102**, 98-105 (2006).
223. Chused, T.M., Apasov, S. & Sitkovsky, M. Murine T lymphocytes modulate activity of an ATP-activated P2Z-type purinoceptor during differentiation. *J Immunol* **157**, 1371-1380 (1996).
224. Dubyak, G.R. Go it alone no more--P2X7 joins the society of heteromeric ATP-gated receptor channels. *Mol Pharmacol* **72**, 1402-1405 (2007).
225. Suadicani, S.O., Brosnan, C.F. & Scemes, E. P2X7 receptors mediate ATP release and amplification of astrocytic intercellular Ca2+ signaling. *J Neurosci* **26**, 1378-1385 (2006).
226. Sun, Z*., et al.* PKC-theta is required for TCR-induced NF-kappaB activation in mature but not immature T lymphocytes. *Nature* **404**, 402-407 (2000).
227. Bauer, B., Jenny, M., Fresser, F., Uberall, F. & Baier, G. AKT1/PKBalpha is recruited to lipid rafts and activated downstream of PKC isotypes in CD3-induced T cell signaling. *FEBS Lett* **541**, 155-162 (2003).
228. Pfeifhofer, C*., et al.* Protein kinase C theta affects Ca2+ mobilization and NFAT cell activation in primary mouse T cells. *J Exp Med* **197**, 1525-1535 (2003).
229. Berg-Brown, N.N*., et al.* PKCtheta signals activation versus tolerance in vivo. *J Exp Med* **199**, 743-752 (2004).
230. Hermann-Kleiter, N*., et al.* PKCtheta and PKA are antagonistic partners in the NF-AT transactivation pathway of primary mouse CD3+ T lymphocytes. *Blood* **107**, 4841-4848 (2006).
231. Isakov, N. & Altman, A. Protein kinase C(theta) in T cell activation. *Annu Rev Immunol* **20**, 761-794 (2002).
232. Liu, J.O. The yins of T cell activation. *Sci STKE* **2005**, re1 (2005).
233. Smith-Garvin, J.E., Koretzky, G.A. & Jordan, M.S. T cell activation. *Annu Rev Immunol* **27**, 591-619 (2009).
234. Marsland, B.J. & Kopf, M. T-cell fate and function: PKC-theta and beyond. *Trends Immunol* **29**, 179-185 (2008).
235. Marsland, B.J*., et al.* Innate signals compensate for the absence of PKC-{theta} during in vivo CD8(+) T cell effector and memory responses. *Proc Natl Acad Sci U S A* **102**, 14374-14379 (2005).
236. Marsland, B.J., Soos, T.J., Spath, G., Littman, D.R. & Kopf, M. Protein kinase C theta is critical for the development of in vivo T helper (Th)2 cell but not Th1 cell responses. *J Exp Med* **200**, 181-189 (2004).
237. Moayeri, M., Wickliffe, K.E., Wiggins, J.F. & Leppla, S.H. Oxidized ATP protection against anthrax lethal toxin. *Infect Immun* **74**, 3707-3714 (2006).
238. von Herrath, M. & Nepom, G.T. Remodeling rodent models to mimic human type 1 diabetes. *Eur J Immunol* **39**, 2049-2054 (2009).

239. Garza, K.M.*, et al.* Role of antigen-presenting cells in mediating tolerance and autoimmunity. *J Exp Med* **191**, 2021-2027 (2000).
240. Kundig, T.M.*, et al.* Immune responses in interleukin-2-deficient mice. *Science* **262**, 1059-1061 (1993).
241. Shahinian, A.*, et al.* Differential T cell costimulatory requirements in CD28-deficient mice. *Science* **261**, 609-612 (1993).
242. Calzascia, T.*, et al.* TNF-alpha is critical for antitumor but not antiviral T cell immunity in mice. *J Clin Invest* **117**, 3833-3845 (2007).
243. Shigemoto-Mogami, Y.*, et al.* Mechanisms underlying extracellular ATP-evoked interleukin-6 release in mouse microglial cell line, MG-5. *J Neurochem* **78**, 1339-1349 (2001).
244. Chiao, C.W., Tostes, R.C. & Webb, R.C. P2X7 receptor activation amplifies lipopolysaccharide-induced vascular hyporeactivity via interleukin-1 beta release. *J Pharmacol Exp Ther* **326**, 864-870 (2008).
245. Taylor, S.R., Alexander, D.R., Cooper, J.C., Higgins, C.F. & Elliott, J.I. Regulatory T cells are resistant to apoptosis via TCR but not P2X7. *J Immunol* **178**, 3474-3482 (2007).
246. North, R.A. Molecular physiology of P2X receptors. *Physiol Rev* **82**, 1013-1067 (2002).
247. Hohlfeld, R. Multiple sclerosis: human model for EAE? *Eur J Immunol* **39**, 2036-2039 (2009).
248. Recher, M.*, et al.* Extralymphatic virus sanctuaries as a consequence of potent T-cell activation. *Nat Med* **13**, 1316-1323 (2007).
249. Kovarik, J.*, et al.* Disposition of basiliximab, an interleukin-2 receptor monoclonal antibody, in recipients of mismatched cadaver renal allografts. *Transplantation* **64**, 1701-1705 (1997).
250. Tsai, D.*, et al.* Rituximab (anti-CD20 monoclonal antibody) therapy for progressive intermediate-grade non-Hodgkin's lymphoma after high-dose therapy and autologous peripheral stem cell transplantation. *Bone Marrow Transplant* **24**, 521-526 (1999).
251. Traeger, J., Dubernard, J.M., Ruitton, A.M., Malik, M.C. & Touraine, J.L. Clinical experience with renal and neoprene-injected segmental pancreatic allografts in man. *Kidney Int Suppl* **11**, S46-49 (1982).
252. Jegasothy, B.V.*, et al.* Tacrolimus (FK 506)--a new therapeutic agent for severe recalcitrant psoriasis. *Arch Dermatol* **128**, 781-785 (1992).
253. Chen, Y.*, et al.* A putative sirolimus (rapamycin) effector protein. *Biochem Biophys Res Commun* **203**, 1-7 (1994).
254. Lang, P.A.*, et al.* Oxidized ATP inhibits T-cell-mediated autoimmunity. *Eur J Immunol* **40**, 2401-2408 (2010).
255. Shaabani, N.*, et al.* Tunicamycin inhibits diabetes. *Cell Physiol Biochem* **29**, 595-602 (2012).
256. Marckmann, S.*, et al.* Interferon-beta up-regulates the expression of co-stimulatory molecules CD80, CD86 and CD40 on monocytes: significance for treatment of multiple sclerosis. *Clin Exp Immunol* **138**, 499-506 (2004).
257. Crow, M.K. Interferon-alpha: a therapeutic target in systemic lupus erythematosus. *Rheum Dis Clin North Am* **36**, 173-186, x.
258. Honke, N.*, et al.* Usp18 driven enforced viral replication in dendritic cells contributes to break of immunological tolerance in autoimmune diabetes. *PLoS Pathog* **9**, e1003650 (2013).
259. Reis e Sousa, C. Dendritic cells in a mature age. *Nat Rev Immunol* **6**, 476-483 (2006).

260. Lang, P.A.*, et al.* Reduced type I interferon production by dendritic cells and weakened antiviral immunity in patients with Wiskott-Aldrich syndrome protein deficiency. *J Allergy Clin Immunol* **131**, 815-824 (2012).

9. Eidesstattliche Erklärung

Hiermit versichere ich an Eides Statt, dass die vorliegende Dissertation mit dem Titel „Mechanistical and therapeutical aspects of preventing diabetes“ selbstständig und ohne unzulässige fremde Hilfe unter Beachtung der „Grundsätze zur Sicherung guter wissenschaftlicher Praxis an der Heinrich-Heine-Universität Düsseldorf“ erstellt worden ist.

Düsseldorf, den _____ _____

(Namir Shaabani)

10. Acknowledgments

There is no languages on this earth can help me to form my grateful feelings to two persons, who were the reason of my existence and support me every day to be the best human being in this world, thanks to my mother and my father.

To my two wings in this life, with them I can fly to reach the sun, and my eyes to see every beautiful thing, my two brothers Besher and Mohamad Wassim.

To the one who gived meaning to my life, my wife.

To the one who was my Boss, my teacher, my brother and my hope to be like him in the future, to Karl Sebastian Lang who took care of me scientifically and emotionally, and tried hard to make everything easy for me, who believes in me more than I do.

To my supervisor Prof. Dr. Peter Proksch, who was always supporting me.

To the angel Nadine Honke, my ‘’Fels in der Brandung’’ who protected me when all the other didn’t and we spend together best time doing the most exciting experiments and we still going on till we achieve our dream together.

To my friends in Düsseldorf, to Boris Görg, who is always keep telling me that I can, to best friend ever Konstanze Schättel, to Ute, Claudia, Katrin Weissenberger , Jule, Andreas Kulawik, Lina Spomer.

To my friends in Essen, to Patricia Spieker, Vishal Khairner, Katja Merches, Asmae Gassa, Vikas Duhan, Alexandra Pandyra, Halime Kalkavan, Piyush Sharma and Britta Kraczyk.

For all of you

Thank you